PHYSICAL STABILITY OF PHARMACEUTICAL SALTS AND COCRYSTALS IN DRUG PRODUCT ENVIRONMENT

A DISSERTATION

SUBMITTED TO THE FACULTY OF THE

UNIVERSITY OF MINNESOTA

BY

SAMPADA ANIL KORANNE

IN PARTIAL FULFILLMENT OF THE REQUIREMENTS

FOR THE DEGREE OF

DOCTOR OF PHILOSOPHY

RAJ SURYANARAYANAN (ADVISER)

APRIL 2018

Acknowledgements

I gratefully acknowledge the invaluable contributions of several people who have supported, guided, and inspired me during my graduate studies at the University of Minnesota.

I express my deepest gratitude towards my thesis advisor Dr. Raj Suryanarayanan, who has been a tremendous source of inspiration and has contributed immensely in my professional and personal growth. I am grateful to him for his mentorship, encouragement, and unwavering support through all these years in the doctoral program. He has taught me the nuances of pharmaceutical materials science and has instilled a lifelong intellectual curiosity in me. I have learnt the importance of meticulous planning, diligence, patience and perseverance through this journey. This experience has enriched me academically, professionally, and as a person and I hope to continue with this association beyond this thesis.

I would like to thank Dr. Ron Siegel, Dr. Calvin Sun, and Dr. Andreas Stein for serving on my doctoral committee, and for critically examining my thesis. I am grateful to my collaborators Dr. Ramprakash Govindarajan (University of Iowa), Dr. Seema Thakral (University of Minnesota) and Dr. Kapildev Arora (Pfizer Inc, Connecticut) for their valuable inputs, helpful suggestions, and countless research discussions on the different projects. My gratitude also extends to Dr. Wenqian Xu and Dr. Andrey Yakovenko for help with my synchrotron XRD experiments at the Advanced Photon Source (APS) at Argonne National Laboratory (beamline 17 BM). I have greatly enjoyed pulling all-nighters for science at APS during our scheduled beamtime and would like to thank APS for proving top-notch user facilities. The Characterization Facility at the University of Minnesota is

acknowledged for providing excellent XRD and microscopy facilities. Financial support from the 3M Science and Technology Fellowship is gratefully acknowledged.

I would like to thank past and present members of the Sury lab for making the last five years an enjoyable experience. Special thanks to Dr. Naveen Thakral, Dr. Vishard Ragoonanan, and Dr. Sarat Mohapatra for the research discussions and for their guidance during my initial years in the lab. A special thank you note also goes to all the faculty in the Department of Pharmaceutics, staff and fellow graduate students. I would like to thank my friends Avani Gosalia, Nidhi Sharda, Mehak Mehta, Davin Rautiola, Kweku Konadu, Shruthi Vaidyanathan, Drishti Sehgal, Meera Shete for their friendship and wonderful camaraderie.

I am extremely grateful to my husband, Dr. Abhishek Telang, who has been a constant source of inspiration, support, and strength throughout my doctoral journey. As a Materials Scientist himself, he has helped in several of my projects through scientific discussions and always motivated me to publish. I thank him for helping me believe in my abilities, bringing out the best in me and loving me unconditionally.

My family deserves special mention for standing by me and supporting me in all my pursuits. I would like to thank my parents, Vandana and Anil Koranne, who nurtured my dream of pursuing higher education and supported me in all my endeavors. I am grateful to my parents-in-law, Sangeeta and Mohan Telang, for their love and support. Thank you to my brother, Dr. Ameya and sister-in-law Renuka, for always being there for me. To the newest member in my family, my darling niece, Amyra, thank you for your big smiles and reminding me of what it means to “take one step at a time” as you learnt to crawl, while I was writing this thesis.

Dedicated to my parents and late grandparents

Abstract

A developmental risk associated with pharmaceutical salt and cocrystal forms is their propensity to undergo unintended disproportionation, resulting in reversion to the corresponding free drug and counter-ion (as in a salt) or coformer (as in a cocrystal). This can negate the solubility, stability and bioavailability advantages conferred by salt (or cocrystal) formation. The central goal of this thesis work was to gain a comprehensive mechanistic understanding of the influence of formulation components (specifically excipients) and processing conditions (including storage) on solid-state stability of salts and cocrystals. Disproportionation of pioglitazone HCl in tablets and indomethacin sodium in lyophilized formulations were investigated. In tablets, the disproportionation reaction, mediated by water, was attributed to the microenvironmental acidity "experienced" by the salt. The nature and concentration of the formulation excipients influenced the microenvironmental acidity. The *in situ* tablet mapping experiments, by synchrotron X-ray diffractometry (SXRD), revealed that the disproportionation reaction was initiated at the tablet surface and progressed towards the tablet core. In lyophilized formulations, disproportionation of a soluble salt (indomethacin sodium) to an insoluble free acid occurred because of selective crystallization of a buffer component and the consequent pH shift during freeze-drying. A complex interplay of the indomethacin sodium and buffer concentrations dictated the salt stability in the final lyophile. The second part of the thesis focused on excipient-induced dissociation of theophylline cocrystals in tablet formulations. In prototype tablets of theophylline-glutaric acid cocrystal, water mediated dissociation reaction occurred rapidly and the theophylline concentration (the dissociation product), monitored by SXRD, was strongly influenced by the formulation composition. Investigation of binary compacts of theophylline-glutaric acid cocrystal with each excipient, revealed the influence of excipient properties (hydrophilicity, ionizability) on cocrystal stability, thereby providing mechanistic insights into the dissociation reaction. Finally, the role of coformer properties on solid-state stability of theophylline cocrystals highlighted the risk of excipient-induced dissociation in cocrystals comprising of acidic and basic coformers. Furthermore, relative solubilities of the cocrystal and its constituents were important determinants of solid-state cocrystal stability.

Table of Contents

List of Tables

List of Figures

Chapter 1 : Introduction

1.1 Introduction

Recent advancements in drug discovery based on high-throughput screening and combinatorial chemistry have led to the development of compounds that are lipophilic and exhibit poor aqueous solubility.[1,2] Effective oral delivery of these poorly water-soluble compounds poses a major challenge. Following oral administration, for a drug to be absorbed into the systemic circulation, it must dissolve in the gastrointestinal (GI) fluid and exist as a solution.[3,4] Once in solution, the drug then has to permeate across the GI membrane, to enter the systemic circulation.[5] Thus, the aqueous solubility and permeability of a drug are important biopharmaceutical attributes that determine the success of oral drug delivery. The Biopharmaceutical Classification System (BCS), categorizes drugs into four classes based on their solubility and permeability.[6] BCS class II includes drugs exhibiting low aqueous solubility as the major oral absorption barrier. The BCS class II drugs are further sub-classified into IIa (dissolution rate limited) and IIb (solubility limited).[7] The potential success and effectiveness of these compounds hinges on our ability to render these compounds soluble in the GI fluid.

Salt formation and more recently, cocrystallization are two important strategies that have been used to improve the aqueous solubility and dissolution rate of poorly soluble drugs. Salts are formed by ionic interactions between the charged form of an active pharmaceutical ingredient (API) and a suitable counter-ion. In general, strong acids are needed to form salts of weakly basic API and strong bases for weakly acidic drugs. On the other hand, cocrystallization with a second compound, is a useful strategy for solubility

enhancement when the API does not contain readily ionizable functional groups and salts are not a viable option. A pharmaceutical cocrystal is a multicomponent crystalline solid, comprising of API and coformer, held together in a crystal lattice, predominantly by hydrogen bonding interactions. A continuum exists linking salts and cocrystals based on the extent of proton transfer between the components.[8] In general, proton transfer from acid to base is complete for salts while for cocrystals proton transfer is absent.[8–10]

A potential risk in the use of pharmaceutical salt and cocrystal forms is their propensity to undergo unintended disproportionation or dissociation, resulting in reversion to the corresponding free API and counter-ion (as in a salt) or coformer (as in a cocrystal). This can negate the solubility, stability and bioavailability advantages conferred by salt (or cocrystal) formation. The central goal of this thesis work is to gain a comprehensive mechanistic understanding of the influence of formulation components (specifically excipients) and processing conditions (including storage) on solid-state stability of salts and cocrystals. These studies can provide a scientific basis for the development of strategies to mitigate the risk of unintended disproportionation and thereby ensure robust drug products.

1.2 Pharmaceutical Salts

About two-thirds of all existing drugs are ionizable compounds, that are either weakly acidic or weakly basic.[11] Salt formation provides an avenue to improve the aqueous solubility and dissolution rate of poorly soluble ionizable compounds. Solubility enhancement of up to 100-fold has been described for a series of amine salts of diclofenac,[12] and up to four orders of magnitude has been described for salts of ibuprofen.[13] A similar trend is also evident with weakly basic drugs. Enalapril, a poorly soluble (~0.21

mg/ml) weak base, formed salts with a range of aliphatic or aromatic carboxylic acids with solubilities ranging from 22 mg/ml up to 350 mg/ml.[14] The higher solubility of salts compared to the corresponding free acid or base can translate into an increase in dissolution rate. Improvement in solubility and dissolution rate can, in turn, enhance (oral) bioavailability. In addition, properties such as stability, melting point, hygroscopicity and crystallinity, can be optimized by using salt forms.[11,15–18]

The choice of salt-forming agents is restricted to compounds with FDA (Food and Drug Administration) GRAS (generally regarded as safe) status. The other considerations include nature and type of counter-ion, physicochemical properties which would influence its physical and chemical stability (common-ion effect), processability, dissolution rate, and bioavailability. The selection of a counter-ion is based on the acidity or basicity of the ionizable functional group on the drug molecule. In general, to form stable salts, a pK_a difference between the counter-ion and that of ionizable group of free form should be 3 or more units (known as the "rule of 3").[11,19]

1.2.1 Salt Disproportionation

If a salt reverts to the corresponding free acid (or base), a disproportionation reaction is said to take place. Salt disproportionation in a solid formulation (for example, tablets) can have an impact on numerous properties of the API including chemical stability, and therefore the product shelf life. Disproportionation can also occur *in vivo*, due to the physiological pH variations in the gastrointestinal tract. For example, salts of weak acids undergo disproportionation to unionized species during dissolution in the stomach due to the low gastric pH. The formation of the less soluble unionized species, can influence the rate and extent of absorption and in turn affect the bioavailability. Many examples of the

detrimental effects of disproportionation have been reported in the literature and have been recently reviewed.[20–22] An example is the case of delavirdine mesylate, where a decrease in dissolution rate was reported which was correlated to the formation of free base.[23] Another study showed that a basic experimental drug vaporized upon disproportionation of the maleate salt to the free base during stability testing, which led to a loss in potency.[24] In a recent case, the platelet inhibitor drug, prasugrel, converted from the hydrochloride salt to the free base within the tablet, raising regulatory concerns about lower bioavailability in certain patient populations with raised gastric pH.[25] Increase in tablet hardness and disintegration times were noted for tablets subjected to accelerated stability testing, coinciding with formation of the amorphous free base form of a crystalline hydrochloride salt.[26] Disproportionation in parenteral formulations can cause incomplete dissolution of the lyophile upon reconstitution, or the reconstitution time may become unacceptably long. If the drug is formulated for intravenous administration, the consequences can be serious. Given the potential impact on the pharmaceutical product performance, developing a better understanding of disproportionation and the factors that impact solid-state disproportionation have received recent attention in the literature.[21,27]

The mechanism underlying salt disproportionation is not well understood. In a formulation, the microenvironmental acidity "experienced" by the salt is believed to have a significant impact on its stability and pH alterations are implicated in disproportionation reactions. The microenvironmental acidity refers to the "pH" in a microscopic layer of sorbed water present on a solid surface, in which the solid has dissolved and formed a saturated solution.[27,28] Theoretically, a critical parameter, pH_{max}, serves as a reference

value to assess the disproportionation tendency. The phenomenon of disproportionation can be understood by considering the pH solubility profile and the concept of pH_{max}.

1.2.2 pH-Solubility Profile and the Concept of pH_{max}

For weak acids and bases, the degree of ionization is pH dependent and therefore the total solubility of an ionizable compound can change significantly as a function of pH. The classical pH-solubility profile of a weakly basic compound is presented in Figure 1.1.

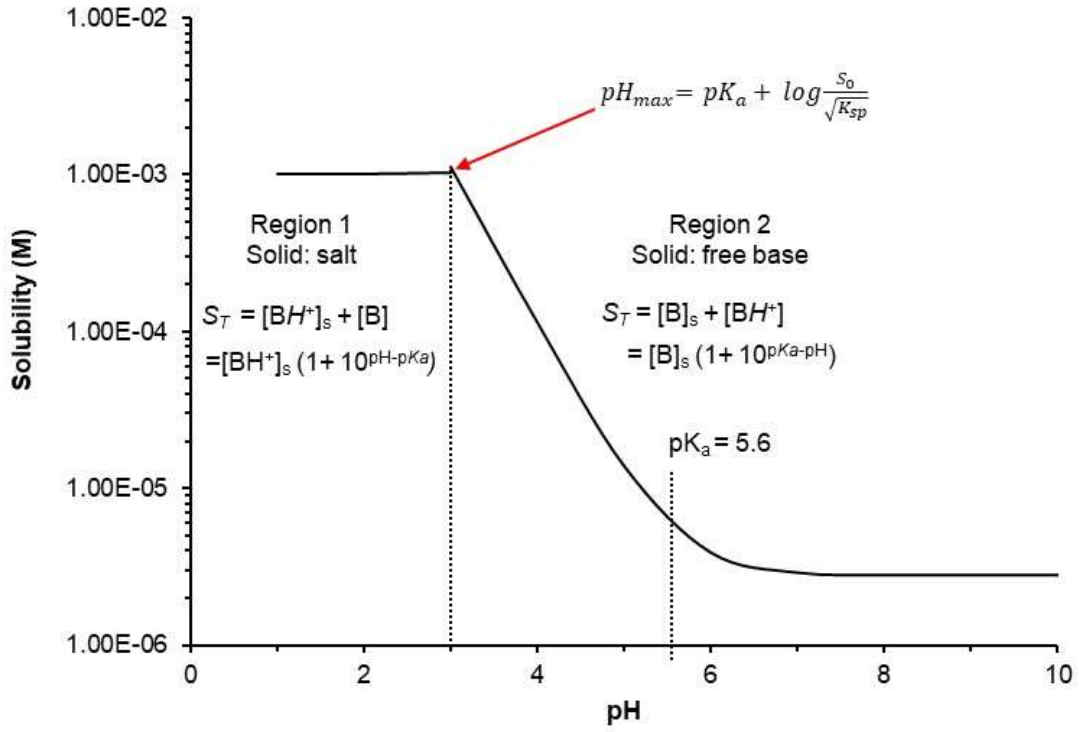

Figure 1.1. Theoretical pH-solubility profile of a monobasic compound with a pK_a value of 5.6. Details of the parameters shown are described in the text below.

When the weakly basic compound is dissolved in water, the ionization equilibrium can be expressed by Equation 1 and the corresponding equilibrium constant by Equation 2.

$$[BH^+] \rightleftharpoons [B] + [H^+] \qquad \text{Equation 1}$$

$$K_a = \frac{[H^+][B]}{[BH^+]} \qquad \text{Equation 2}$$

The pH-solubility profile of a weakly basic compound can be divided into two regions (Region 1 and 2) as shown in Figure 1.1. In Regions 1 & 2, the solution is saturated with the salt and free base respectively. These two curves intersect at a pH value that is termed as pH_{max}. The total solubility, S_T, is the sum of the solubility of both the free base [B] and the ionized species [BH^+] at a certain solution pH.

$$S_T = [B] + [BH^+] \qquad \text{Equation 3}$$

The total solubility in Region 1 (pH < pH_{max}), of the curve describing the pH-solubility profile of the weakly basic compound, where the solubility of the protonated form is limiting (denoted by subscript s), can be described mathematically as:

$$S_T(pH < pH_{max}) = [BH^+]_s + [B]$$

$$= [BH^+]_S \left(1 + \frac{K_a}{[H^+]}\right) \qquad \text{Equation 4}$$

The total solubility in Region II (pH > pH_{max}) can be described mathematically as:

$$S_T(pH > pH_{max}) = [BH]^+ + [B]_s$$

$$= [B]_S \left(1 + \frac{[H^+]}{K_a}\right) \qquad \text{Equation 5}$$

The two curves meet at pH_{max} (Figure 1.1) which represents the pH of maximal solubility because both free base and salt forms of the molecule contribute to the total solubility of the drug in solution.[29] Therefore, by setting the S_T equal in Equations 4 and 5, and solving the resultant quadratic equation, Bogardus et al.[29] derived an expression for the pH_{max} for a weakly basic compound.

$$pH_{max} = pK_a + log \frac{S_0}{\sqrt{K_{sp}}} \qquad \text{Equation 6}$$

where, S_0 is the intrinsic solubility of the free base, K_{sp} denotes the solubility product of the salt form and $\sqrt{K_{sp}}$ is thus the salt solubility, assuming no common ion effect.

According to Equation 6, the calculated pH_{max} value for a weakly basic compound depends upon the solubilities of the free base & salt forms and the pK_a of the compound. An analogous relationship may also be derived for a weakly acidic drug (Equation 7).

$$pH_{max} = pK_a + log\frac{\sqrt{K_{sp}}}{S_0} \quad \text{Equation 7}$$

where, S_0 is the intrinsic solubility of the free acid.

For a salt of a weakly basic drug with an acidic counter-ion, at a pH below pH_{max}, the salt is in equilibrium with the saturated solution, while above pH_{max}, it is the free base. The reverse is true for salt of a weakly acidic drug. Whether or not disproportionation is thermodynamically favored is determined by the pH of the microenvironment of the drug relative to its pH_{max}. For a weakly basic drug forming a salt with an acidic counter-ion, disproportionation is expected to occur when the pH of the formulation microenvironment swings above the pH_{max} of the salt. The use of different counter-ions will yield salts with different solubilities.[17,30] For a weakly basic compound, the more soluble the salt, the farther the pH_{max} will be shifted from its pK_a to lower pH values.[31] As a result, the pH stability window (where the salt would remain "as is") for a more soluble salt will be narrower compared to a less soluble salt, thereby making the former more susceptible to undergo disproportionation in the formulation microenvironment.[27] Thus, the pH_{max} and microenvironmental acidity play a major role in determining whether a salt would remain 'as is' or would convert to the corresponding free base form.

There are several examples in the literature where disproportionation could be rationalized by considering the microenvironmental pH of the system relative to the pH_{max} of the salt.[20,23,24,32,33] Hsieh et al., demonstrated a strong correlation between the pH_{max} value and extent of disproportionation for salts of miconazole and sertraline.[33]

When the salts were blended individually with a model basic excipient, tribasic sodium phosphate dodecahydrate (TSPd; 50:50 w/w), and stored at 57% RH (25 °C), the extent of disproportionation was observed to be higher in salts with lower pH_{max} (Figure 1.2).

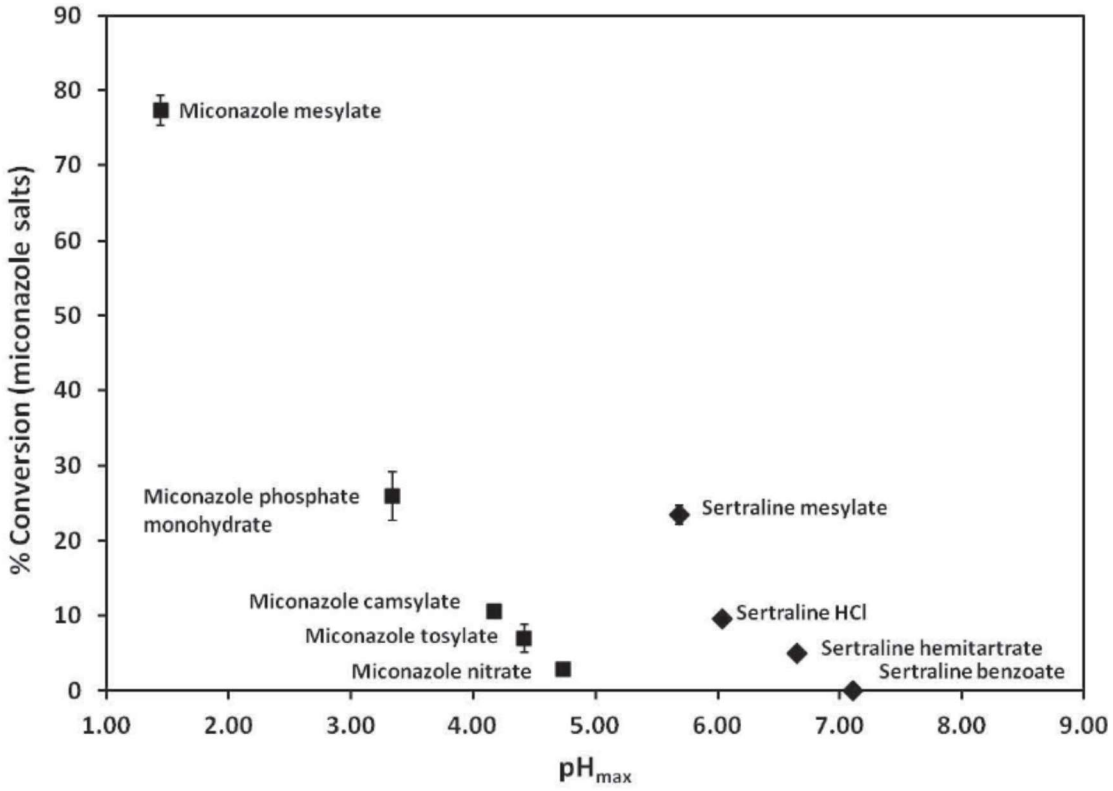

Figure 1.2. Relationship between pH_{max} and the extent of disproportionation for a series of miconazole and sertraline salts.[33]

Merritt et al. plotted the free base to salt solubility ratio versus pK_a for some Eli Lilly research and marketed compounds, and an imaginary boundary line was drawn to show the disproportionation risk (Figure 1.3).[34] The compounds above the boundary line (blue triangles) did not show any evidence of disproportionation. The molecules with low pH_{max}, i.e., with low pK_a and with high difference in free base and salt solubility, were predicted to have high risk of disproportionation.

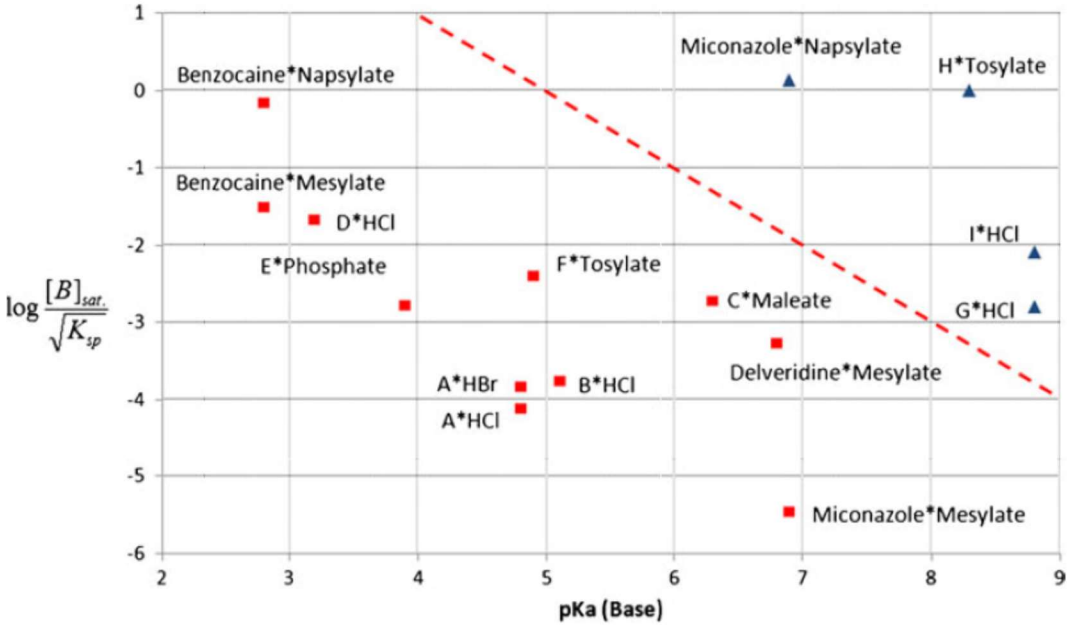

Figure 1.3. Graphical plot of the terms describing the equation for pH_{max} for weakly basic model compounds (including Lilly compounds). Disproportionation was observed for the square (red) data points under varying conditions however no disproportionation was observed for the data points given by the (blue) triangles. The dotted line is a guide for the eye based on the functional form of pH_{max} and represents a hypothetical boundary delineating disproportionation risk.[34]

While several studies have highlighted the importance of pH_{max}, there is still a lack of mechanistic understanding of how the microenvironmental acidity in the formulation controls the disproportionation behavior of a salt.

1.2.3 Factors Affecting Salt Disproportionation

Literature reports on salt disproportionation have shown that several environmental factors have a significant impact on the rate and extent of disproportionation. Specifically, the extent of disproportionation was observed to be influenced by water vapor pressure, formulation excipients, temperature, and mechanical activation (e.g. milling).[28,31,32,35] These factors are discussed in the following section:

1.2.3a Role of water vapor pressure and temperature

The detrimental effects of atmospheric moisture on the chemical stability of APIs in the solid state have been extensively documented.[36] In the case of solid-state reactions, water can act as a (i) reactant in hydrolytic reactions, (ii) medium for proton transfer by solvation of surface species or, (iii) plasticizer for the amorphous regions, thereby reducing the glass transition temperature (T_g) and promoting an increase in the molecular mobility.[36] With respect to the solid-state stability of salts, almost all of the literature reports on disproportionation have implicated water as a critical factor for disproportionation reactions. A direct relationship between water content of the sample and free base concentration was shown in the case of disproportionation of delavirdine mesylate salt.[23] In the study by Merritt et al., storage of prototype tablets of a model HCl salt at higher relative humidity increased the amount of free base formed.[34] When a binary mixture of benzocaine mesylate and a model basic excipient tribasic sodium phosphate dodecahydrate (TSPd; 50/50 w/w) was stored at 57% RH (25 °C), the disproportionation kinetics almost overlapped with the water sorption profile confirming the key role of water in disproportionation (Figure 1.4). In another case, the hydrochloride salt of an amine drug underwent disproportionation during aqueous wet granulation process whereas non-aqueous granulation with absolute ethanol, or 96 or 90% ethanol/water mixture caused no detectable disproportionation.[26] Binary compacts of compound 'A' HCl salt with magnesium stearate (10% w/w), exhibited a dramatic increase in disproportionation rate above 31% RH (40 °C), accompanied by a sharp increase in water uptake. This was attributed to the reaction between magnesium stearate and HCl salt resulting in the formation of deliquescent magnesium chloride hexahydrate as one of the

disproportionation products. Above the critical RH of 31%, the compacts sorbed more water and hence exhibited greater rate and extent of disproportionation.[35]

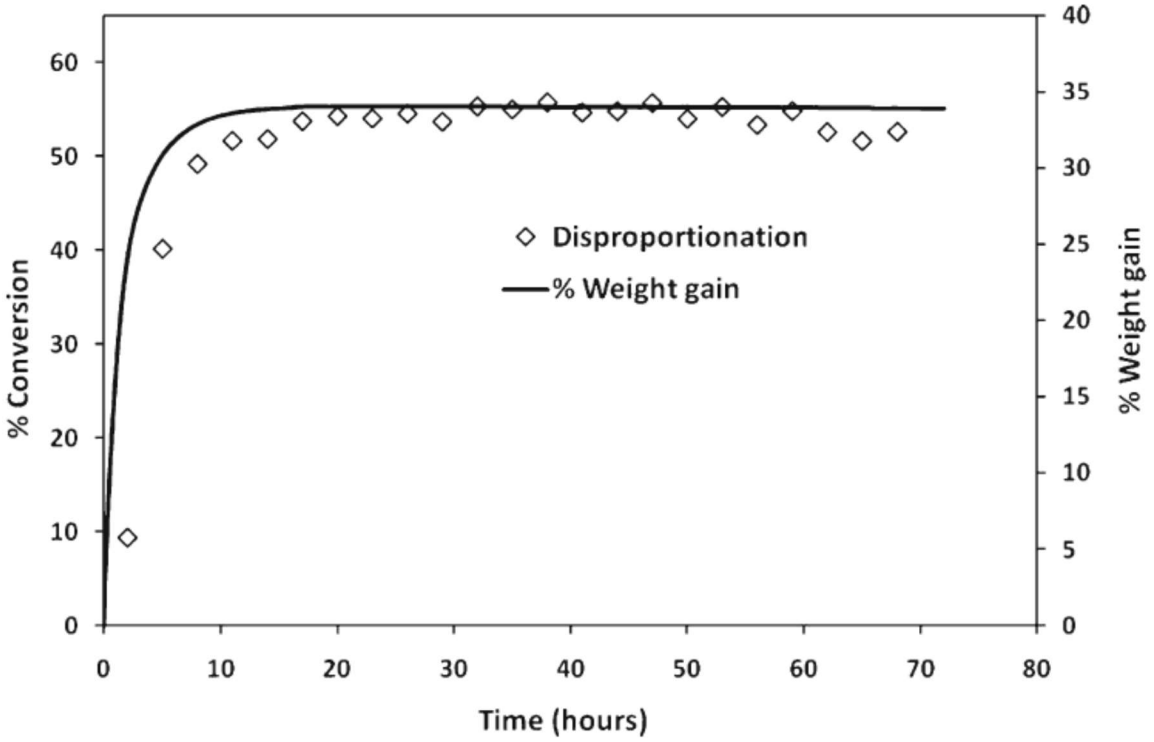

Figure 1.4. Disproportionation kinetics of benzocaine mesylate in the presence of TSPd (both particle sizes <53 mm) at 57% RH and 25 °C.[31]

For disproportionation of the salt of a weak base, loss of a proton is necessary, via hydration and possibly transfer to another component. The presence of at least some water is generally unavoidable in pharmaceutical solid formulations, and minimal amounts of residual water from processing or sorption from the environment are capable of providing a medium for proton transfer. In highly crystalline materials, although only a small amount of water is adsorbed on the surface, it may form localized regions on the surface which contain mobilized species of the solid[37–39]. The "activated solid" may then interact with other species in the water layer of an adjacent surface.[36] Disproportionation is generally

considered to be a "solution mediated" transformation occurring in the sorbed water layers. The salt to free base transformation will be dependent upon the microenvironmental pH of the sorbed water layer, which in turn will be related to the nature and concentration of solutes present in the microenvironment. The effect of temperature on salt disproportionation is more complex as additional factors that are impacted by temperature need to be considered. An increase in temperature caused an increase in the extent of disproportionation.[31,34,35] While an increase in temperature can cause a decrease in the water content of the system, the higher temperature also increases salt solubility. As a result, more salt molecules are mobilized in the sorbed water layers. Furthermore, if the salt solubility exhibits a more pronounced temperature dependence than the base solubility, there will be a decrease in the pH_{max} (Equation 6), thereby making the system more susceptible to disproportionation.[31]

1.2.3b Role of excipients and microenvironmental acidity

Important properties of excipients that have been reported to have a potential impact on salt disproportionation include: excipient acidity/basicity, solubility, hygroscopicity, molecular properties, particle size and surface area.[28,34] In addition, the presence of trace levels of impurities present either in the bulk or at the particle surface and residual levels of water trapped from processing and storage can also contribute to the API instability.[40,41] The role of excipients in the context of salt disproportionation is related to the ability of the excipients to bring about microenvironmental pH alterations. A problematic excipient is viewed as being able to swing the microenvironmental pH above (salts of weak bases) or below (salts of weak acids) the pH_{max} of the salt, thereby resulting in disproportionation. This is particularly important in the case of a highly potent drug, wherein the active

component will constitute a small fraction of the dosage form and the formulation microenvironmental pH will be largely controlled by the excipients. A direct measurement of proton activity in microenvironment of solid systems is challenging. Therefore as an alternative, traditionally the 'slurry' method has been used to estimate the potential risk posed by excipients to cause disproportionation. In this method, the acidity of a saturated aqueous solutions/suspension is conventionally measured in terms of the relative concentration of hydrogen ions present and is expressed in the pH scale ($pH = -\log [H^+]$). This measured pH value is designated to reflect the pH in the microscopic layer surrounding a solid particle in which the solid forms a saturated solution of adsorbed water.[27] While this approach has been shown to be empirically useful in some cases[24,28,42], there have been other cases wherein disproportionation was not observed even when the excipient slurry pH values were favorable to cause the transformation to the neutral species.[28,32,35] This may be due to the fact that pH estimated by the slurry method is very different from the actual microenvironments in solids, mainly due to the large difference in available water.[43,44] In addition, the measured pH may also depend on the concentration of the slurry, which could bias the outcome. Since disproportionation is expected to occur in the sorbed water layers present at the interface between the drug and excipients, measurement of the apparent acidity of the solid surfaces can be considered as a more reliable predictor of disproportionation. Recently, indicators have been used to probe the surfaces of pharmaceutical solids as well as the microenvironment of solid formulation blends and to measure the surface "acidity" in solid formulations.[44–48] In this method, the surface acidity of excipients is determined by depositing sulfonephthalein indicators (e.g. thymol blue, phenol red, bromocresol green etc.), as probes on the surface of solid samples

and the degree of indicator ionization is measured using diffuse reflectance UV-visible spectrophotometry.[45] The pH equivalent (pHeq) of the system is then calculated from a calibration curve constructed using buffered aqueous solutions of the same indicator. The pHeq of the solid surface is defined as the 'pH of an aqueous solution in which the ratio of the peak absorbance signals of the ionized to the unionized forms of the indicator is the same as in the given solid sample'.[43] The microenvironmental acidity in a physical mixture is expected to be influenced by each component of the mixture. This in turn can affect the ionization of the indicator, with water playing a facilitating role. The probe ionization extent can therefore be a measure of the interparticulate microenvironment and can provide a relative measure of the microenvironmental acidity in solid formulations.

Some authors have noted cases where pH_{max} and microenvironmental pH alone, could not predict disproportionation.[35] Instead, the proton accepting (buffering) capacity of the excipients used in the formulation was found to be critical. Disproportionation of HCl salt of a weakly basic drug (pK_a 5.6; calculated pH_{max} 3.0) was studied in presence of six excipients, by storing binary compacts of HCl salt with each excipient in a 90:10 % w/w ratio, at 40 °C/75% RH for 5 days.[35] Although the slurry pH measured for all excipients was higher than the pH_{max} of the salt, disproportionation was observed only in presence of excipients with proton accepting carboxylate groups (magnesium stearate, sodium stearyl fumarate, and sodium croscarmellose), having pK_a values higher than the pH_{max} of the salt.[35]

1.3 Pharmaceutical Cocrystals

Cocrystals are multi-component crystalline systems usually containing a stoichiometric ratio of API and a coformer, held together in a crystal lattice by nonionic/noncovalent interactions. In the past two decades, pharmaceutical cocrystals have emerged as new solid forms, providing opportunities to tailor the physicochemical and mechanical properties of drugs. Using a suitable coformer, properties of an API including solubility[49–51], dissolution rate[52–54], permeability[55–57], stability[58–60] and manufacturability[61–63] can be optimized. The coformer must be non-toxic, with generally regarded as safe (GRAS) status. The selection of coformers is often based on functional groups capable of complementary hydrogen bonding with the API. Cocrystal design and the selection of suitable coformers is guided by a detailed understanding of the supramolecular chemistry of relevant functional groups and the hierarchy of synthons (i.e. structural unit involving hydrogen bond).[64–66] Figure 1.5 shows examples of some commonly occurring synthons.

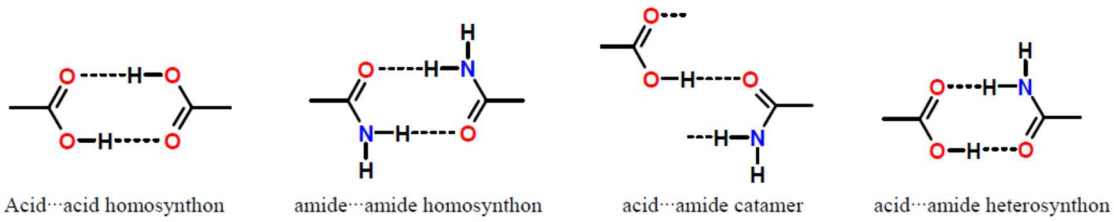

Figure 1.5. Common synthons found between carboxylic acid and amide functional groups.[67]

Although significant advancements have been made in the design, synthesis, and characterization of pharmaceutical cocrystals, their large-scale synthesis and stability in drug product environment, has not been adequately investigated.

1.3.1 Cocrystal Dissociation

Once a stable form of cocrystal API is identified, it is important to ensure that it remains unchanged both during the manufacturing and storage of the drug product prior to patient use. Formulating a cocrystal into a drug product involves the addition of function specific excipients, used to enhance drug product performance. The excipients, present in intimate contact with the cocrystal API, can compromise its stability either by directly reacting with the API or indirectly by providing microenvironmental conditions favorable to cause cocrystal dissociation, i.e., reversion to free drug and coformer. In addition to excipients, processing step (for instance wet granulation, milling and compaction) as well as storage conditions (temperature and relative humidity), can influence cocrystal stability. Cocrystal dissociation can have an adverse impact on the solubility, stability and bioavailability of a drug product. To develop a robust solid dosage form of a cocrystal API, a comprehensive understanding of its physical stability in the formulation environment is essential.

While disproportionation of salts has been extensively studied[27,28,31–33,35,68,69], very little information is available about the influence of formulation and processing on cocrystal stability. This is not surprising since only a few pharmaceutical cocrystals are available as marketed products. In contact with water (solution/slurry), many cocrystal systems have been observed to disproportionate.[50,70–73] Cocrystal dissociation can also occur during dissolution resulting in the precipitation of the poorly soluble parent drug on the surface of the cocrystal.[74–76] The physical instability of cocrystals in solution/suspension formulations was recently reviewed.[77]

Although cocrystals in general are stable in the solid-state, storage at high relative humidity (RH) and under elevated temperature have been implicated in cocrystal disproportionation.[78,79] The dicarboxylic acid (maleic, malonic, glutaric) cocrystals of caffeine and theophylline were reported to undergo dissociation within 7 days when stored at 98% RH (RT), resulting in the crystallization of the acid coformer and caffeine/theophylline hydrate. Eddleston et al. reported that the rate and extent of caffeine-glutaric acid cocrystal dissociation increased as a function of RH (RT).[78] In these cocrystal systems, the dissociation susceptibility was attributed to the large aqueous solubility difference between the drug and coformer and the propensity of the drug to form hydrates at high RH. Caffeine-theophylline cocrystal dissociated upon heating to a temperature below the melting points of caffeine and theophylline and was explained by entropically favorable conformation of caffeine as the driving force for cocrystal disproportionation.[80] The combined effects of temperature and water vapor pressure were investigated in pyrazine−phthalic acid cocrystal.[81] An elevation in temperature or water vapor pressure accelerated cocrystal dissociation. The dissociation mechanism was postulated to be dissolution of the cocrystal in sorbed water followed by crystallization of the individual components. Thus dissociation is favored when there is a large aqueous solubility difference between the cocrystal components.[78]

Most of the literature on cocrystal dissociation is focused on drug substance alone. There is limited information on the potential for cocrystals to dissociate when formulated as a drug product. Specifically, the influence of excipients and processing on cocrystal stability has not been thoroughly investigated. Dissociation of caffeine-oxalic acid cocrystal to form caffeine hydrate was observed in binary mixtures of the cocrystal with

ionizable excipients (1:1 w/w ratio) stored at 75% RH (RT).[82] Similar to salt disproportionation[23,35,68,69], the mechanism of cocrystal dissociation was proposed to be water mediated and involved proton transfer between coformer and carboxylate group of excipients. While such binary mixtures, containing equal amounts of both the cocrystal and excipient, are aimed at providing a rapid method for excipient screening, the excipient concentration may be unrealistically high. For example, the use of 50% w/w magnesium stearate in a binary drug-excipient mixture does not reflect a realistic formulation composition. Although the binary drug-excipient mixtures provide insight into the effect of each excipient, the complex interplay of the role of several excipients in a multicomponent dosage form will not be evident.

In order to realize the desired dissolution and bioavailability advantage offered by cocrystal forms, it is important to control and prevent any unintended phase transformations. This can be achieved by developing an understanding of the thermodynamic stability and solubility of cocrystal forms in aqueous media.

1.3.2 Cocrystal pH-Solubility Behavior and pH_{max}

Pharmaceutical cocrystals are often designed with molecules that exhibit different ionization properties (e.g. acidic, basic, amphoteric or zwitterionic) and stoichiometries. The pH-solubility behavior of cocrystals varies greatly depending on the ionization properties of the individual components. Theoretical equations that describe cocrystal solubility dependence on pH, solubility product (K_{sp}) of the cocrystal and acid ionization constant (K_a), for several types of cocrystal have been derived.[83]

Consider a 1:1 cocrystal RHA, where R is a non-ionizable drug and HA represents a weakly acidic monoprotic coformer. The cocrystal solubility can be determined by

considering the solution equilibria that describe cocrystal dissociation and coformer ionization. The cocrystal dissolves in an aqueous solution according to its K_{sp}, given by:

$$\mathrm{RHA_{solid}} \rightleftharpoons \mathrm{R_{aq}} + \mathrm{HA_{aq}}$$

$$\mathrm{K_{sp}} = [\mathrm{R}]_{\mathrm{aq}}[\mathrm{HA}]_{\mathrm{aq}} \qquad \text{Equation 8}$$

The monoprotic acidic coformer dissociates according to its ionization constant, K_a:

$$\mathrm{HA_{aq}} \rightleftharpoons \mathrm{A^-{}_{aq}} + \mathrm{H^+{}_{aq}}$$

$$K_a = \frac{[\mathrm{H^+}]_{\mathrm{aq}}\,[\mathrm{A^-}]_{\mathrm{aq}}}{[\mathrm{HA}]_{\mathrm{aq}}} \qquad \text{Equation 9}$$

When the cocrystal is in equilibrium with solutions of stoichiometry equal to the cocrystal (i.e., there is no excess coformer or drug in solution) then cocrystal solubility is equal to the total concentration of the drug or coformer in solution:

$$S_{cocrysta} = [\mathrm{R}]_{\mathrm{T}} = [\mathrm{A}]_{\mathrm{T}} \qquad \text{Equation 10}$$

where subscript T indicates total concentration (unionized + ionized). Therefore,

$$S_{cocrystal} = [\mathrm{R}]_{\mathrm{aq}} = [\mathrm{HA}]_{\mathrm{aq}} + [\mathrm{A^-}]_{\mathrm{aq}} \qquad \text{Equation 11}$$

Substituting Equation 8 and 9 in Equation 11, the stoichiometric solubility of cocrystal can be expressed as:

$$S_{cocrystal} = \sqrt{K_{sp}\left(1 + \frac{K_a}{[\mathrm{H^+}]}\right)} \qquad \text{Equation 12}$$

Thus, Equation 12 indicates that solubility of cocrystal RHA is dependent on cocrystal K_{sp}, coformer K_a and solution pH. The dependence of stoichiometric solubility of cocrystal RHA on pH is shown in Figure 1.6. When pH << coformer pK_a, cocrystal solubility approaches its intrinsic solubility ($\sqrt{K_{sp}}$). At pH = pK_a, the cocrystal solubility is equal to $\sqrt{2K_{sp}}$. When pH >> coformer pK_a, cocrystal solubility increases exponentially. The maximum concentration that can be experimentally achieved is, however, limited by the

solubilities of drug, coformer, and coformer salts. The pH value at which the cocrystal stoichiometric solubility and drug solubility are equal, is referred to as the pH_{max}. At pH_{max}, both cocrystal and drug solid phases are thermodynamically stable and can coexist in equilibrium with solution. At solution pH < pH_{max}, the drug is more soluble than the cocrystal, but at pH > pH_{max}, the cocrystal becomes more soluble than the drug. As with salts, cocrystal pH_{max} is an important parameter that identifies cocrystal stability regions.

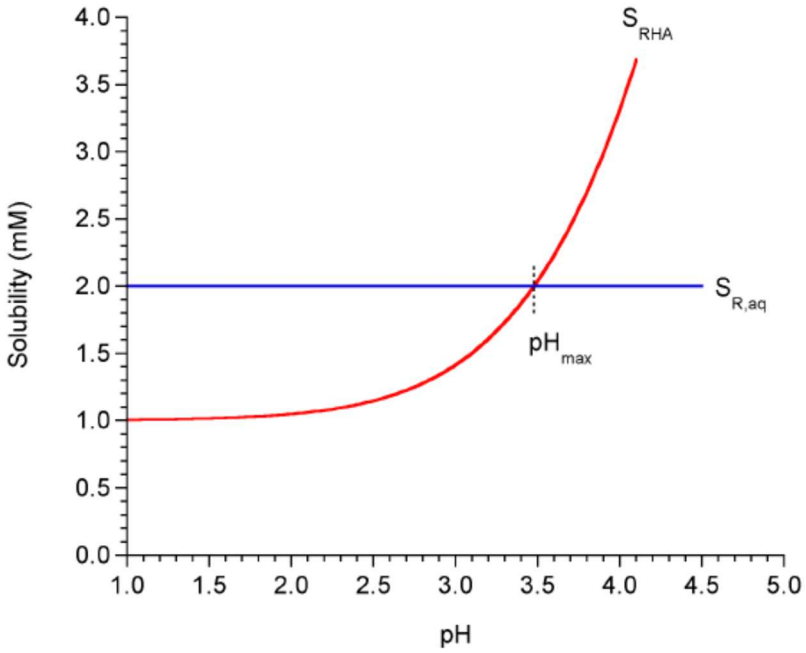

Figure 1.6. Dependence of cocrystal stoichiometric solubility and drug solubility on pH according to Equation 12 for a hypothetical cocrystal RHA. At pH_{max}, the cocrystal stoichiometric solubility equals drug solubility. K_{sp} = 1 mM^2, pK_a =3, $S_{R,aq}$ = 2 mM.[84]

The cocrystal solubility as a function of coformer concentration (which includes non-stoichiometric solution concentrations of drug and coformer) is determined from the mass balance on each of the cocrystal components.

$$[R]_T = [R]_{aq} \qquad \text{Equation 13}$$

$$[A]_T = [A^-]_{aq} + [HA]_{aq} \qquad \text{Equation 14}$$

By combining Equations 8, 9, 13, 14

$$[R]_T = \frac{K_{sp}}{[A]_T}\left(\frac{1+K_a}{[H^+]}\right) \qquad \text{Equation 15}$$

The total drug concentration at equilibrium, $[R]_T$ decreases with increasing $[A]_T$, which is a consequence of cocrystal solubility product behavior. Figure 1.7 shows the dependence of cocrystal solubility (given by $[R]_T$) on coformer concentration and pH according to Equation 15. The RHA cocrystal solubility is predicted to increase with increasing ionization ($pH > pK_a$) and decrease with increasing coformer concentration. The drug and cocrystal can be equally soluble under certain solution conditions, denoted by the intersection between drug and cocrystal solubilities.

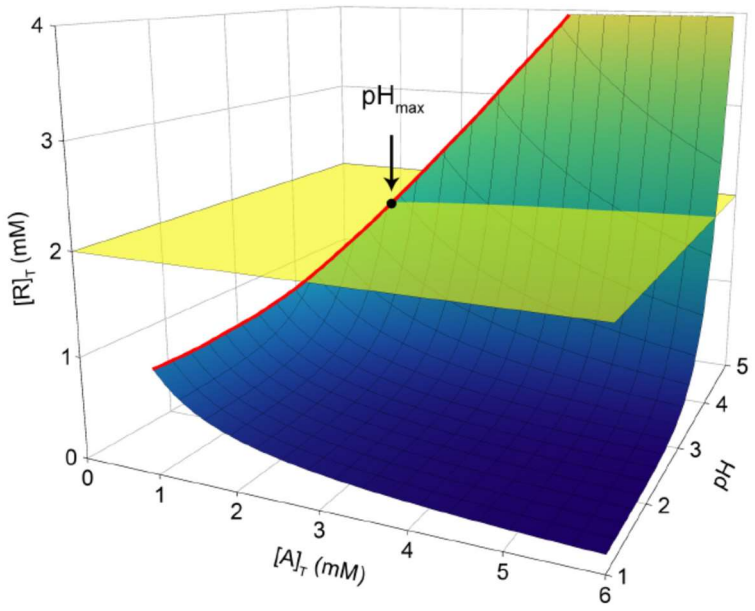

Figure 1.7. Dependence of drug concentration ($[R]_T$) on coformer concentration ($[A]_T$) and pH for a hypothetical cocrystal RHA and solution at equilibrium according to Equation 15. Blue/green surface indicates cocrystal solubility, red line indicates cocrystal stoichiometric solubility. Yellow plane indicates drug solubility. The intersection of the cocrystal stoichiometric solubility and drug solubility is the pH_{max}. K_{sp} = 1 mM^2, pK_a = 3, $S_{R,aq}$ = 2 mM.[84]

The theoretical pH-solubility profiles of cocrystals composed of drug and coformer with various ionization properties are compared against that of the parent drug in Figure 1.8.[83]

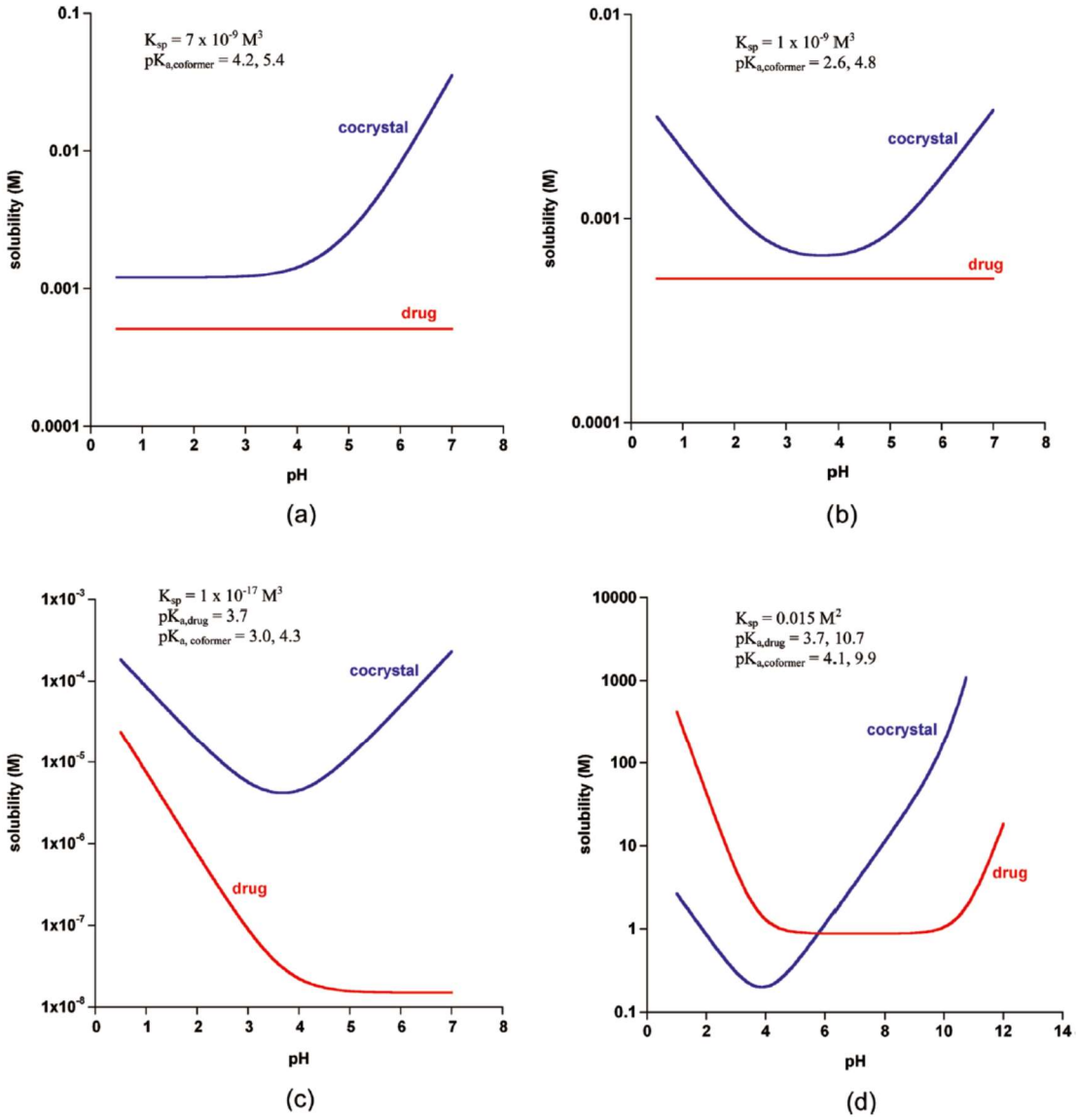

Figure 1.8. Cocrystal stoichiometric solubility-pH dependence for hypothetical cocrystals of different stoichiometry and ionization properties according to equations derived previously.[83] Cocrystals represented are (a) 2:1 R_2H_2A, (b) 2:1 R_2HAB, (c) 2:1 B_2H_2A, and (d) 1:1 $^-ABH^+H_2X$. Drug and coformer pK_a values and cocrystal K_{sp} are included in each graph.

For a non-ionizable drug (R) such as carbamazepine, the cocrystals solubility dependence on pH is based on the coformer ionization properties, while the drug solubility is constant

regardless of solution pH (Figure 1.8 a, b). A diprotic acid coformer (H_2A) causes the solubility to increase with pH (Figure 1.8 a), while an amphoteric coformer (HAB) leads to a U-shaped solubility curve (Figure 1.8 b). A cocrystal of a basic drug (B) such as itraconazole and an acidic coformer (H_2A) such as tartaric acid also exhibits a U-shaped solubility-pH profile, with both drug and coformer ionizations contributing to this phenomenon (Figure 1.8 c). In some cases, the cocrystal and drug solubility curves intersect at a characteristic pH value, referred to as the pH_{max} or transition point of the cocrystal. At pH_{max}, both cocrystal and drug solid phases are thermodynamically stable and can coexist in equilibrium with solution. An example of such a system exhibiting a characteristic pH_{max} is cocrystal of zwitterionic drug ($^-ABH^+$), gabapentin, with an acidic (H_2X) coformer, 3-hydroxybenzoic acid (Figure 1.8 d). At pH > 4, a steep increase in cocrystal solubility occurs, leading to an intersection of cocrystal and drug ($^-ABH^+$) solubility at pH of 5.8 (pH_{max}).[85] At solution pH < pH_{max}, the drug is more soluble than the cocrystal, but at pH > pH_{max}, this relationship reverses, and the cocrystal becomes more soluble than the drug.

Thus, in order to assess the stability and potential for dissociation of a cocrystal composed of ionizable constituents, it is essential to develop an understanding of the influence of pH on cocrystal solubility and stability.

1.3.3 Factors Affecting Cocrystal Disproportionation

The important considerations in solid-state dissociation of cocrystals include: (i) environmental factors (e.g. storage under high relative humidity and at high temperature, processing conditions), (ii) excipient properties (e.g. potential to interact with cocrystal

components, hydrophilicity) and (iii) physicochemical properties of the cocrystal including pH_{max}, and the solubility difference between cocrystal and parent drug.

1.3.3a Relative humidity stress

There are limited studies that report the long-term stability of cocrystals systems following storage under a range of RH conditions. Cocrystals of caffeine and theophylline with malonic, maleic, or glutaric acid, were stable for up to 7 weeks at 25 °C and under 0, 43, and 75% RH conditions. However, at 98% RH, the cocrystals dissociated within 7 days forming caffeine/theophylline monohydrate.[58,59] The dissociation was attributed to the inherent susceptibility of caffeine and theophylline to form hydrates at high RH. Cocrystal dissociation was also observed at high RH for cocrystals composed of non-hydrate forming constituents (e.g. dissociation of salicylic acid-urea cocrystal at 25 °C/98% RH and aspirin-acetamide cocrystal at 25 °C/75% RH).[78] In this case, the large solubility difference between the cocrystal components was suggested to be responsible for the dissociation.[78] While the relative solubility difference between coformer and drug explains dissociation in some cocrystals systems, it cannot be applied generally to all cocrystal systems.[86]

Thus, although cocrystal dissociation risk exists at high RH condition, each system needs to be evaluated on an individual basis. The exact mechanism of dissociation at high RH and the properties of cocrystal and its constituents that contribute to instability are not well understood.

1.3.3b Temperature stress

Thermal stresses are encountered during pharmaceutical unit operations such as drying, melt granulation, and accelerated storage conditions. It is therefore important to evaluate physical (and chemical) stability of cocrystals under pharmaceutically relevant temperature

conditions. In the context of cocrystal dissociation, there are only a few studies that have investigated the effect of temperature. Dissociation of caffeine-theophylline cocrystal was observed upon heating at a temperature below the melting points of caffeine and theophylline and was explained by entropically favorable conformation of caffeine as the driving force for cocrystal dissociation.[80] Cocrystals of paracetamol with 1,4-dioxane, N-methylmorpholine, morpholine, N,N-dimethylpiperazine, and piperazine, dissociated during heating with initial loss of the coformers followed by melting of paracetamol.[87] Cocrystal hydrates of acetazolamide with 2-aminobenzamide and NCT, dehydrated in the temperature range of 93 °C -104 °C followed by loss of coformer on further heating.[88] The combined effects of temperature and water vapor pressure were comprehensively investigated in pyrazine−phthalic acid cocrystal.[81] An elevation in temperature or water vapor pressure accelerated cocrystal dissociation. The dissociation mechanism was postulated to be dissolution of the cocrystal in sorbed water followed by crystallization of the individual components.[81]

1.4 Analytical Challenges in Detection and Quantification of Disproportionation

Predicting salt disproportionation and cocrystal dissociation in a complex, multi-component pharmaceutical systems is very challenging and even with simple drug substances, only limited success has been achieved in developing predictive quantitative models.[33] Therefore, early experimental detection of disproportionation can help in development of control strategies for its prevention. The disproportionation product formed has to be identified in the "as is" formulation. If it is a highly potent drug, the active component will constitute a small weight fraction of the dosage form and monitoring disproportionation can be analytically challenging. Solution based techniques such as

liquid chromatography cannot distinguish between salt/cocrystal and their disproportionation products. The use of spectroscopic methods such as Raman or FT-IR to analyze disproportionation in a multi-component formulation matrix is limited due to the spectral interference generated by the various excipients. In addition, conventional spectroscopic methods provide bulk information and they lack the sensitivity for the detection of low levels of analytes. Recently, a two-step Raman microscopic mapping approach was developed to investigate salt disproportionation on tablet surfaces with low drug loading (5% w/w).[89] In the first step, by using a statistically optimized sampling method, the areas of interest on the tablet surface where the drug particles reside were located. This was followed by a second close-step mapping approach to probe the tablet surface where the drug particles were concentrated. This method demonstrated a sophisticated approach with an improved limit of detection (LOD) compared to conventional Raman spectroscopy. However, this technique has several limitations: (i) The results obtained are qualitative in nature as the first step of sampling used in this method is derived from a binomial distribution with only "yes" or "no" information obtained for the target species. (ii) Information obtained from Raman microscopic mapping is predominantly "surface" biased. Because of the weak scattering signal, it is not possible to gain information from the tablet core (in an intact tablet). In addition, it is not representative enough to quantify a small portion (200 μm x 200 μm) of the tablet sample (5 mm x 5mm) since disproportionation is expected to exhibit spatial heterogeneity. (iii) The technique is time consuming.

In the identification and characterization of crystalline phases, X-ray diffractometry is considered to be the "gold-standard". However, since disproportionation tends to be very

slow in the solid-state, laboratory X-ray sources lack the sensitivity to detect very low levels of disproportionation (< 5%) at early stages. The detection is further complicated by the excipients in dosage forms. In tablets, the microenvironmental pH will not be uniform and disproportionation is expected to occur in a non-homogeneous manner. This necessitates analyzing multiple sample sites which will be tedious in a laboratory set-up. In order to obtain mechanistic insights into disproportionation in tablets, an ideal analytical technique should be able to (i) simultaneously quantify the reactant and product phases and (ii) provide the above information with spatial resolution. The latter reveals where the reaction is initiated and the distribution (from the surface to core) of both the reactant and product phases. The high intensity synchrotron radiation coupled with an area detector, can detect disproportionation at a very early stage.

1.5 Motivation and Thesis Overview

We aim to develop a comprehensive mechanistic understanding of the influence of formulation components (specifically excipients) and processing conditions (including storage) on physical instability of pharmaceutical salts and cocrystals, thus providing a scientific basis for the development of robust formulations. These studies will not only facilitate the development of a mechanism-based approach for the rational selection of counter-ions/coformer during salt/cocrystal screening stage but also guide the selection of optimum storage conditions (i.e., temperature and humidity). Furthermore, it will enable an understanding of the interplay between factors such as water, microenvironmental pH and excipients, which are potential determinants of instability.

This thesis is organized into four research chapters, with Chapters 2 and 3 focusing on salt disproportionation, and Chapters 4 and 5 focusing on cocrystal disproportionation. The

conclusions and future directions of this research are discussed in Chapter 6 and 7 respectively. A brief overview of the research Chapters is presented below:

1.5.1 Chapter 2

Our goal was to develop an understanding of the interplay between factors such as water content, excipient nature, and microenvironmental pH, which are potential determinants of salt instability. We hypothesized:

Salt disproportionation reaction, mediated by water, is attributed to the microenvironmental "acidity" experienced by the analyte. The microenvironmental acidity is dictated by the nature and concentration of the excipients used in the formulation.

Our objectives were (i) Design a temperature and humidity controlled chamber (40 °C/75% RH) for *in situ* monitoring of salt disproportionation in tables at the synchrotron beamline. (ii) Monitor the intact tablet continuously in the synchrotron beamline so as to detect the first evidence of disproportionation. (iii) Simultaneously quantify the crystalline salt (reactant) and the free base (reaction product) as a function of storage time. (iv) Determine the phase composition with spatial resolution by analyzing intact tablets in the transmission mode. (v) Finally, assess the potential role of water and microenvironmental acidity on the rates of disproportionation and spatial heterogeneity in phase composition.

Using pioglitazone HCl (PioHCl) as a model compound, *in situ* spatio-temporal mapping of disproportionation by synchrotron X-ray diffractometry (SXRD) revealed that the reaction was initiated on the tablet surface and progressed toward the core. The transformation was solution-mediated and the spatial heterogeneity in disproportionation could be explained by the migration of sorbed water. Disproportionation was most pronounced in the presence of magnesium stearate, a basic excipient, and good correlation

was observed between microenvironmental acidity (pHeq) and extent of PioHCl disproportionation.

1.5.2 Chapter 3

Salt disproportionation in lyophilized formulations, while posing a challenging problem, has not been extensively investigated. Using indomethacin sodium (IMCNa) as a model compound, we evaluated its disproportionation propensity during lyophilization in presence of sodium phosphate buffer.

The hypothesis was:

Selective crystallization of buffer component and the consequent pH shift will cause salt disproportionation during lyophilization.

Our objectives were to (i) investigate buffer salt crystallization and the consequent pH shifts during freeze concentration of indomethacin sodium buffered in sodium phosphate, and (ii) determine the effect of active pharmaceutical ingredient (indomethacin sodium) and excipient (buffer) concentrations on disproportionation.

The use of several complementary analytical techniques enabled an in-depth understanding of the phase behavior of the solutes. Low temperature X-ray diffractometry (XRD) of frozen solutions enabled us to detect buffer crystallization and identify the physical form of the crystallizing phase. The changes in solution pH brought about by buffer crystallization were measured using a low temperature pH probe. Differential scanning calorimetry (DSC) was used to characterize the frozen systems and infrared (IR) spectroscopy of the final lyophile enabled us to ascertain the disappearance of IMCNa and the formation of IMC free acid (disproportionation product).

1.5.3 Chapter 4

One of the key goals in drug development is to identify optimal dosage form compositions that can ensure the stability of API throughout its shelf-life. Currently, for cocrystal APIs, there is limited information on dosage form stability.[82] Specifically, the influence of excipients and processing on cocrystal stability has not been adequately investigated. Our overall goal was to develop a mechanistic understanding of the physical instability of cocrystal in a drug product environment.

The objectives were to (i) develop an analytical technique to monitor cocrystal disproportionation in intact tablets and (ii) understand the mechanism of cocrystal disproportionation in a complex multicomponent solid matrix.

We investigated the excipient induced dissociation of theophylline-glutaric acid (TG) cocrystal in prototype tablet formulations by synchrotron X-ray diffractometry. The water-mediated dissociation reaction occurred rapidly in tablets and was strongly influenced by the formulation composition. Excipient hygroscopicity and ionizability were identified to be critical attributes in the water mediated disproportionation reaction in intact tablets. Cocrystal – excipient compatibility studies, coupled with the effects of unit operations (milling, compression), can provide insights into the combined effects of formulation and processing on cocrystal stability.

1.5.4 Chapter 5

Our overall goal was to prevent excipient induced dissociation in theophylline cocrystals. In this Chapter, we attempted to gain insight into the role of coformer properties on cocrystal stability. Therefore, building upon our findings in theophylline-glutaric acid cocrystal discussed in Chapter 4, we investigated dissociation of theophylline cocrystals

composed of basic and neutral coformers. Powder X-ray diffractometry was used to investigate the dissociation in cocrystal−excipient binary tablets. We hypothesize water mediated dissociation in theophylline cocrystals under the following conditions:

(a) Cocrystals with a weakly basic coformer will dissociate in the presence of acidic excipients.

(b) Cocrystals with a weakly acidic coformer will dissociate in the presence of basic excipients.

(c) Cocrystals with a neutral coformer will be stable in the presence of acidic and basic excipients.

Since cocrystals of theophylline with an ionizable coformer exhibit pH dependent solubility, the formulation microenvironment, dictated by the excipients, can influence the ionization of the coformer. Therefore, following water sorption, acidic excipients caused dissociation of cocrystal with a weakly basic coformer, while basic excipients caused dissociation of cocrystal with a weakly acidic coformer. In contrast, theophylline cocrystal with a neutral coformer was resistant to dissociation caused by ionizable excipients.

Chapter 2 : Investigation of Spatial Heterogeneity of Salt Disproportionation in Tablets by Synchrotron X-ray Diffractometry*

2.1 Synopsis

Tablets which were binary mixtures of pioglitazone hydrochloride (PioHCl) with magnesium stearate (MgSt), croscarmellose sodium (CCS), microcrystalline cellulose or lactose monohydrate were prepared. Two sets of experiments, using intact tablets, were performed. (i) Tablets containing PioHCl (90% w/w) and MgSt were exposed to 25 or 40 °C and 75% RH in a custom-built temperature/humidity chamber. *In situ* spatio-temporal mapping of disproportionation was performed by transmission mode synchrotron X-ray diffractometry (SXRD; Argonne National Labs). Tablets were scanned in radial direction starting from top edge of the tablet and moving, in increments of 300 μm, towards the center. There was evidence of disproportionation after 10 minutes (at 40 °C). The reaction was initiated on the tablet surface and progressed toward the core. (ii) SXRD of tablets stored for longer time (up to 15 days) enabled the simultaneous quantification of the reactants and products of disproportionation and provided insight into the reaction progression. The influence of sorbed water and microenvironmental acidity on the disproportionation reaction was investigated. The most pronounced reaction was observed in presence of MgSt followed by CCS. The transformation was solution-mediated and the spatial heterogeneity in disproportionation could be explained by the migration of sorbed water. There was a good correlation between microenvironmental acidity (pHeq) and extent of PioHCl disproportionation.

2.2 Introduction

Salt formation is a commonly used strategy to modify and optimize the physicochemical properties of an ionizable drug. Important properties such as solubility, dissolution rate, stability, crystallinity, processability and powder characteristics can be influenced by using a variety of acceptable counter-ions.[15,17] Improvement in solubility and dissolution rate can, in turn, enhance (oral) bioavailability. However, a potential risk in the use of pharmaceutical salt forms is their propensity to undergo disproportionation resulting in reversion to the corresponding free base (or acid) form. This can negate the advantages of salt formation and can have undesirable consequences on product performance such as a decrease in dissolution rate and reduced bioavailability. Salt disproportionation has been reported in numerous pharmaceuticals.[23,24,32,90] In tablets of prasugrel, a platelet inhibitor, the hydrochloride salt transformed to the free base, raising regulatory concerns about altered bioavailability.[25] There was a decrease in the dissolution rate of delavirdine mesylate tablets following storage at 40 °C and relative humidity (RH) of 75% for a week. This was attributed to moisture mediated interaction between the drug and croscarmellose sodium, resulting in a disproportionation reaction leading to the formation of poorly soluble free base.[23]

The phenomenon of disproportionation can be understood by considering the pH solubility profiles of weak acids/bases. In these systems, the pH of maximum solubility is referred to as the pH_{max}. At pH_{max}, both the free form and salt coexist in equilibrium in the solid state with the saturated solution. For weak bases, at pH $> pH_{max}$, there will be disproportionation of the salt resulting in the formation of weak base (the opposite will be the case with weakly acidic compounds). In the "solid-state", including solid dosage forms,

disproportionation is generally considered to be a solution-mediated transformation[27,28] wherein the microenvironmental pH "experienced" by the salt particles in a formulation is believed to have a significant impact on its stability. The role of excipients in the context of salt disproportionation is related to the ability of the excipients to alter the microenvironmental pH above (salts of weak bases) or below (salts of weak acids) the pH_{max} of the salt, thereby resulting in disproportionation.[20,32–34] In one such example, during stability testing, the free base formed as a result of disproportionation of the maleate salt of a weakly basic experimental drug, vaporized, leading to a loss in potency.[24] The microenvironmental pH of the tablet formulation was higher than the pH_{max} favoring disproportionation. The addition of citric acid to the formulation lowered the microenvironmental pH below pH_{max}, thereby preventing the disproportionation reaction.[24]

The detection followed by quantification of salt disproportionation in complex multicomponent solid dosage forms (typically tablets), can be analytically challenging. Conventional solution based techniques such as liquid chromatography, are not typically designed to distinguish between different solid forms of the drug (salt versus the neutral form). Therefore, disproportionation reactions have to be studied directly in the solid dosage form, i.e. in the presence of the formulation excipients. In case of highly potent drugs, the active ingredient will constitute a small weight fraction of the dosage form and hence highly sensitive solid-state characterization techniques will be required.

In case of pioglitazone hydrochloride (PioHCl), our model compound, John et al. were the first to report excipient induced disproportionation upon storage at 40 °C/75% RH and 40 °C/35% RH.[35] Among the investigated excipients, magnesium stearate (MgSt), sodium

croscarmellose (CCS) and sodium stearyl fumarate (SSF) were observed to cause disproportionation with the rate and extent of disproportionation following the order: MgSt > CCS > SSF. This effect was attributed to the proton accepting capacity of the excipient carboxylate groups, evident from their pKa values being higher than the pH_{max} of the salt. MgSt was concluded to be the most problematic excipient owing to the formation of deliquescent $MgCl_2$ as a product of disproportionation reaction. Building upon this observation, to assess the impact of excipient counter-ion on the proton transfer reaction, Nie et al. investigated the disproportionation kinetics of PioHCl at 40 °C/65% RH in the presence of different cationic stearates - NaSt, CaSt and MgSt.[69] During the initial period of accelerated stability testing, the disproportionation kinetics was influenced by the hygroscopicity, alkalinity, and surface area of the stearate, while in the later stage, the hygroscopicity of the reaction products was the dominant factor.

While extensive studies are reported on the disproportionation kinetics in binary or multi-component powder physical mixtures, the information obtained is only "average" phase information and does not reveal spatial heterogeneity in phase composition. From a practical viewpoint, it is important and relevant to develop an understanding of the disproportionation reaction in complex multicomponent solid formulations, specifically tablets. As a result of compression, the drug and excipients particles come in intimate physical contact with the possibility of interactions between components at the points of particle contact.[91,92] Moreover, during tablet compaction, the restraint imposed by the die wall results in density gradients that affect physical and mechanical properties.[93] As a result, the particles on the surface could exhibit pronounced differences in properties (e.g. lower crystallinity/increased lattice disorder) compared to the particles in the tablet core.

In PioHCl tablets, at a low drug loading (5% w/w), a two-step Raman microscopic mapping approach was developed to investigate salt disproportionation on tablet surfaces.[89] The first step was to locate the drug particles on the tablet surface using a statistically optimized sampling method. This was followed by mapping the area of interest. This sophisticated approach led to an improved limit of detection (LOD) compared to conventional Raman spectroscopy. However, the technique has several limitations. (i) The results obtained are qualitative since the first sampling step is derived from a binomial distribution with only "yes" or "no" signal obtained for the target species. (ii) In spite of being time consuming, only information from the tablet surface is obtained. Because of the weak scattering signal, it is not possible to characterize the deeper layers of intact tablets. This issue is of particular relevance since disproportionation is not expected to occur in a homogenous manner in tablets. An added potential disadvantage of spectroscopic methods, such as Raman or IR, is the interference from the signals of the various excipients.

In order to obtain mechanistic insights into salt disproportionation in tablets, an ideal analytical technique should be able to (i) simultaneously quantify the reactant and product phases and (ii) provide the above information with spatial resolution of phase composition. The latter is expected to reveal the site of reaction initiation and the spatial distribution of both the reactant and product phases. X-ray diffractometry is a widely used technique to characterize crystalline phases. The XRD patterns of PioHCl and pioglitazone free base (hereafter referred to as free base) are sufficiently different with unique peaks for the reactant (PioHCl) as well as the product (free base). This provides an excellent opportunity to simultaneously monitor the loss of the crystalline reactant and the appearance of the crystalline product in the same sample using a single analytical technique. However,

disproportionation is expected to be slow in the solid state, and laboratory X-ray sources lack the sensitivity to detect low levels of free base (< 5%) formed at early stages of reaction progress. The detection can further be complicated by the excipients in dosage forms. The use of the high intensity synchrotron radiation coupled with an area detector, can enable detection and quantification of disproportionation at the onset of transformation. In addition to providing a two-dimensional image, the use of 2D SXRD in transmission geometry, reduces errors in phase quantification due to preferred orientation since the complete Debye-Scherrer rings are captured.[94]

Since disproportionation is considered to be a solution-mediated transformation, storage of tablets under accelerated stability conditions (for example, 40 °C/75% RH) provides an avenue to understand disproportionation reaction mediated by water. When tablets are stored under high RH conditions, the sorbed water, initially present only at the surface, is expected to gradually penetrate through the tablet and progress towards the tablet core. Depending on the water content and nature of excipients, these changes can alter the microenvironmental pH to favor disproportionation. The reaction is expected to be initiated at the tablet surface which is directly exposed to the high RH, and will progressively proceed towards the tablet core. In order to investigate the resulting spatial heterogeneity, it is imperative that the intact tablet is directly analyzed. In this paper, we report the use of synchrotron radiation for spatial mapping of salt disproportionation in tablet formulations. As disproportionation is expected to occur in the sorbed water layers present at the interface between the drug and excipients, measurement of the apparent acidity of the interparticulate microenvironment was expected to provide an insight into the environment inducing the disproportionation. In our work, we will attempt to correlate salt

disproportionation in solid formulations with the microenvironmental acidity estimated by the indicator dye sorption method. Our goal is to develop an understanding of the interplay between factors such as water content, excipient nature and microenvironmental pH, which are potential determinants of salt instability.

We hypothesize that the disproportionation reaction is initiated at the tablet surface which is directly exposed to high RH and proceeds towards the tablet core. We had five objectives. (i) Design a temperature and humidity controlled chamber (40 °C/75% RH) for *in line* monitoring of tablet disproportionation at the synchrotron beamline. (ii) Monitor the intact tablet continuously in the synchrotron beamline so as to detect the first evidence of disproportionation. (iii) Simultaneously quantify the crystalline salt (reactant) and the free base (reaction product) as a function of storage time. (iv) Determine the phase composition with spatial resolution by analyzing intact tablets in the transmission mode. (v) Finally, assess the potential role of water concentration and microenvironmental acidity on the rates of disproportionation and spatial heterogeneity in phase composition.

2.3 Experimental

2.3.1 Materials and Drug Substance Properties

Pioglitazone hydrochloride (PioHCl; Figure 2.1) and free base were generous gifts from Dr. Reddy's Laboratory (India). PioHCl is used in the management of type-2 diabetes mellitus and is commercially available as an oral formulation containing 15, 30 or 45 mg/tablet. Both, PioHCl and free base forms, are non-hygroscopic, and are reported to be chemically and physically stable at 40 °C/75% RH for 1 month. The pK_a of interest is 5.6, and the nitrogen of pyridine ring is protonated when the hydrochloride salt is formed. The

aqueous solubility of its free base is 1 µg/mL, whereas that of PioHCl is 0.4 mg/mL[35], resulting in a high salt to free base solubility ratio. The pH_{max} value is reported to be 2.8.[35]

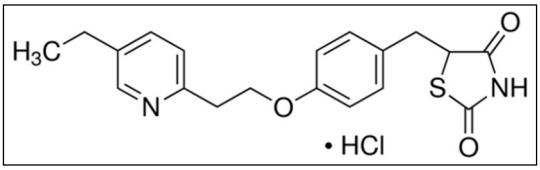

Figure 2.1. Chemical structure of PioHCl

Microcrystalline cellulose (MCC; Avicel PH-102; FMC BioPolymer), magnesium stearate (MgSt; Fischer Scientific Company), croscarmellose sodium (CCS; Ac-Di-Sol; FMC BioPolymer), lactose monohydrate (LM; Mallinckrodt) and sodium chloride (NaCl; Sigma Aldrich) were used as received.

2.3.2 Tablet Preparation and Storage

(i) Tablets containing excipient. Binary physical mixtures (200 mg) containing PioHCl and each excipient were prepared (compositions given in Table 2.1). Each mixture was filled into a tablet die, held in place with a flat-faced lower punch, and compressed in a hydraulic press (Carver model C laboratory press, Menomonee Falls, WI) to a compression pressure of 177 MPa (3 mm thickness). The tablet diameter was 8 mm and thickness 3 mm.

Table 2.1. Compositions of PioHCl tablets

	Composition, (% w/w)				
Pioglitazone hydrochloride (PioHCl)	100*	90	90	50	50
Magnesium stearate (MgSt)		10			
Croscarmellose sodium (CCS)			10		
Microcrystalline cellulose (MCC)				50	
Lactose monohydrate (LM)					50

*control (no excipient)

(ii) Calibration tablets - Quantification of free base and salt when present as a mixture. Tablets containing mixtures of PioHCl and free base were prepared, with the concentration of free base ranging from 0 to 100% w/w (8 compositions; n = 3 for each composition). Since only low levels of free base were expected in the test tablets, six compositions contained PioHCl in the range of 99.5 to 84.0% w/w. Two additional tablets of different composition were also prepared to challenge the validity of the calibration curves. SXRD was used to generate the calibration curve for quantification (described in later section). The unique peaks of free base and PioHCl at 2θ values of 4.3° and 6.0° respectively, were used for quantification (Figure 2.2E). The intensity (integrated) of the 4.3° 2θ peak of the free base was plotted as a function of the free base concentration. The relationship between peak intensity and free base concentration can be expressed by the equation y = 8.95x - 10.9 (R^2 = 0.995) where "y" is the peak intensity, and "x" is the free base concentration (Figure 2.13A; Supplementary Information). Similarly, the relationship between the intensity (integrated) of the 6.0° 2θ peak of the PioHCl can be expressed as y = 9.51x + 29.3 (R^2 = 0.996), (Figure 2.13B; Supplementary Information). Appropriate corrections for tablet drug content were used for phase quantification.

(iii) Tablet storage. The tablets were stored at 40 ºC/75% RH, and the salt disproportionation was monitored using synchrotron radiation. These experiments were conducted under two conditions: (i) For *in line* monitoring of tablet disproportionation at the beamline, a temperature/humidity chamber was custom built. Spatial mapping of tablet disproportionation was performed in the transmission mode using synchrotron radiation (Argonne National Laboratory). (ii) Longer term kinetic studies were conducted by storing the tablets in open pans in glass chambers maintained at 40 ºC/75% RH (saturated sodium

chloride solution). Tablets were withdrawn at specific time intervals and analyzed by SXRD.

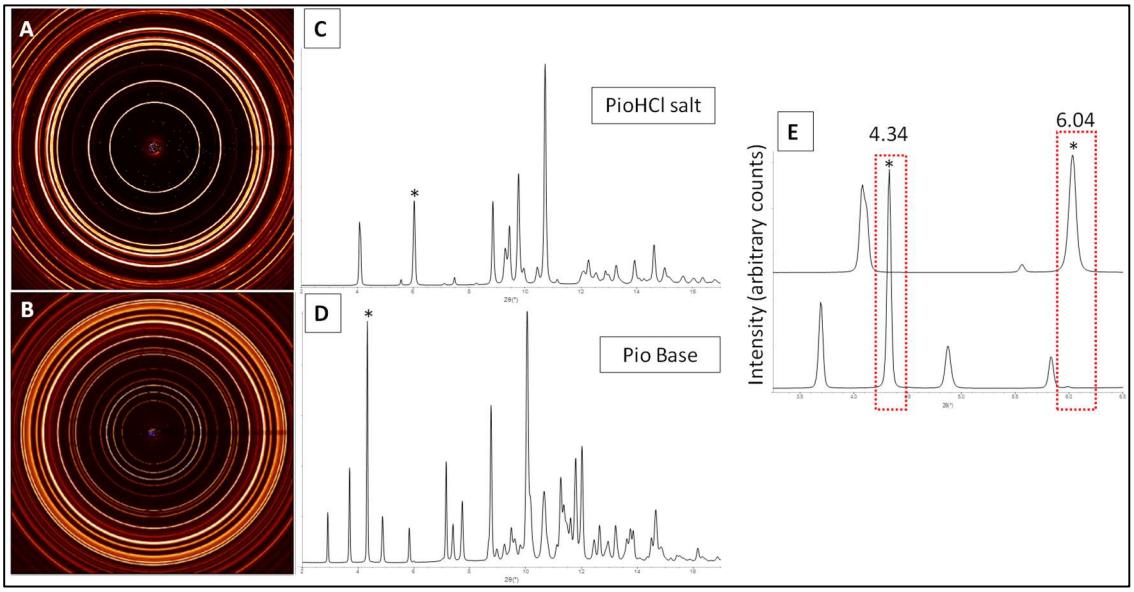

Figure 2.2. Two dimensional XRD patterns of (A) PioHCl and (B) pioglitazone free base obtained using synchrotron radiation (wavelength 0.72768 Å). To facilitate visualization, the corresponding one- dimensional XRD patterns of (C) PioHCl and (D) pioglitazone free base are also presented as intensity versus 2θ plots. The unique peaks corresponding to PioHCl and pioglitazone free base seen at 2θ values 4.34° and 6.04° respectively are shown in (E).

2.3.3 Chamber Design and Description

A schematic of the sample chamber and photographs of the chamber are presented in Figure 2.3. The sample chamber is comprised of a single aluminum block with a lid on top, that is held in place with six screws and a heat insulating tape to allow for a tight seal when closed. The chamber features a tablet sample holder, heaters, temperature probe, humidity and temperature sensor, a small air circulating muffin fan and glass beakers containing saturated sodium chloride solution. The temperature and relative humidity of the chamber was monitored continuously with the sensor (EK-H4, Sensirion AG, Switzerland)

positioned close to the tablet sample. Two circular windows, sealed with Kapton® tape, permitted the entrance and exit of the X-ray beam. More details of the temperature and humidity chamber are provided in the Supplementary Information.

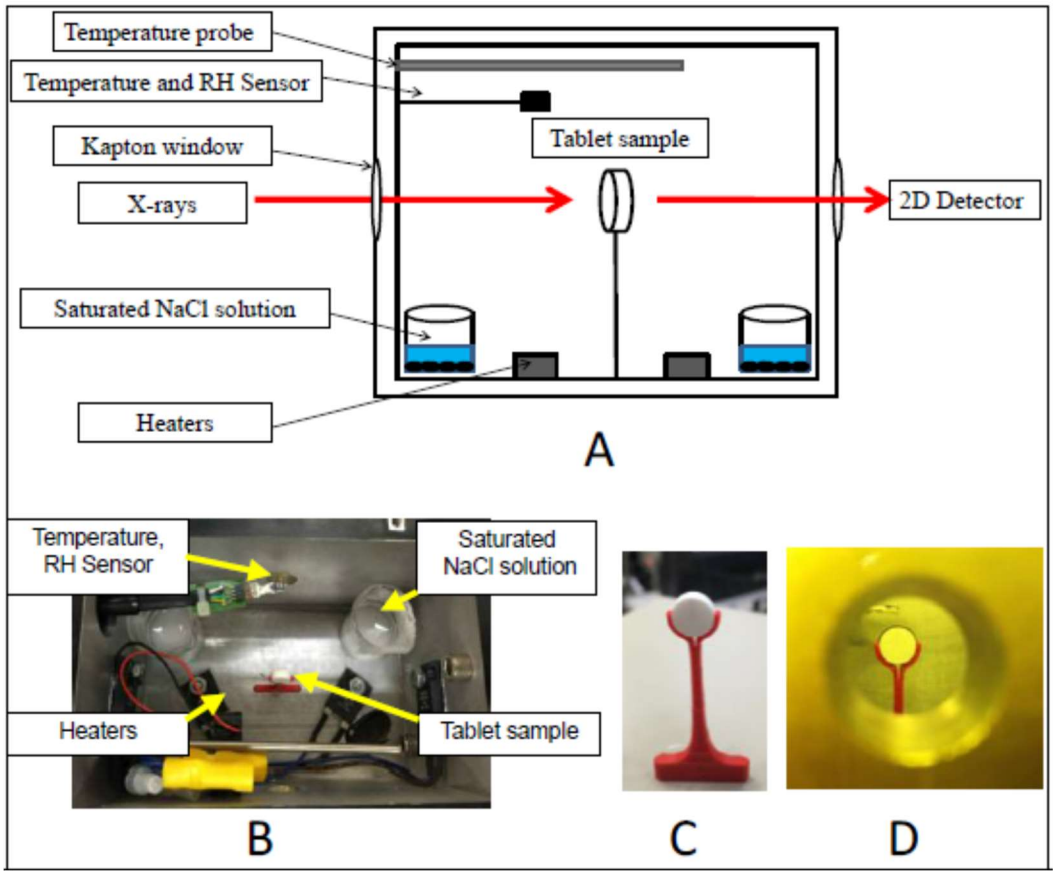

Figure 2.3. (A) Schematic of the temperature and humidity controlled chamber. (B) Top view of the temperature and humidity controlled chamber. (C) Tablet sample mounted on a custom tablet holder. (D) View of the tablet mounted inside the chamber, seen through the kapton window.

2.3.4 Synchrotron X-ray Diffractometry – Tablet Mapping

Experiments were performed in the transmission mode in the 17-BM-B beamline at Argonne National Laboratory (Argonne, IL, USA). A monochromatic circular X-ray beam [wavelength 0.72768 Å; beam diameter 300 μm and a two-dimensional (2D) area detector

(XRD-1621, PerkinElmer) were used. A triple-bounce channel-cut Si single crystal monochromator with [111] faces polished was used, which limited the line broadening to its theoretical low limit, i.e., the Darwin width. The flux of the incident X-ray was 8×10^{11} photons/sec at 17 keV. Calibration was performed using Al_2O_3 standard (SRM 674a, NIST).

***In situ* spatial mapping**. The intact tablet was mounted vertically on a holder and placed inside the custom-built chamber (40 ºC/75% RH) such that the tablet was positioned in the path of the synchrotron X-ray beam (Figure 2.3). For the spatial profiling, the tablet was scanned radially starting from the tablet edge and moving towards the tablet center, with a total of 15 steps constituting one cycle. At each step, the tablet was scanned 10 times, with an exposure time of 1s for each scan, and the results were averaged. The 2D diffraction rings were integrated to yield one-dimensional d-spacing (Å) or 2θ (deg) scans using the GSAS II software developed by Toby and Von Dreele.[95] Commercially available software (JADE 2010, Material Data, Inc.) was used for determining the integrated peak intensities.

Long term tablet mapping. For the tablets stored at 40 °C/75% RH, samples were withdrawn after 3, 5, 10 and 15 days and stored at -20 °C until analyzed by SXRD in transmission mode as described earlier.

2.3.5 Scanning Electron Microscopy (SEM)

SEM was used to characterize tablets containing PioHCl before and after storage. Tablet samples were placed on aluminum stubs using a double-sided carbon tape, coated with platinum (50 Å), and imaged in a scanning electron microscope (Jeol 6500 F microscope, Hitachi, Japan).

2.3.6 Confocal Laser Scanning Microscopy

The distribution of water within the tablet was visualized by using rhodamine, a fluorescent dye, which forms a complex with water and has a higher fluorescence emission than the "dry" dye. A separate set of tablets containing rhodamine 6G (Sigma Aldrich #4127; 1% w/w) were used to study moisture distribution in tablets. The tablets were stored at 40 °C/75% RH and were analyzed at select time points. Fluorescence images of the intact tablet face (top /bottom surface) as well as the split tablets (transverse sectional surface) were obtained (Olympus FluoView FV1000 IX2 inverted confocal microscope) using excitation and emission wavelengths of 543 and 591 nm respectively.[96]

2.3.7 Microenvironmental Acidity Measurements by Diffuse Reflectance UV Spectroscopy

Instrumentation. A UV visible spectrophotometer (Cary 100 Bio) equipped with a diffuse reflectance accessory (Labsphere, model DRA-CA-30I) having an inbuilt photomultiplier tube (PMT) was used. The inner surface of the sphere is coated with poly (tetrafluoroethylene). A "zero-degree" wedge in the sample port ensures that the powder sample surface was always perpendicular to the incident light. As a result, reflection back through the sample beam entrance port eliminates the specular component of the reflected light. The integrating sphere collects the light diffusely reflected by the sample and presents an integrated signal to the detector.

Indicator Selection and Solution Measurements. To estimate the microenvironmental acidity in solid samples, thymol blue (pK_{a1} 1.6, pK_{a2} 8.9) was selected as an indicator based on reported slurry pH measurements of PioHCl – excipient blends.[35] The ionization of thymol blue can be represented as shown in Figure 2.4.

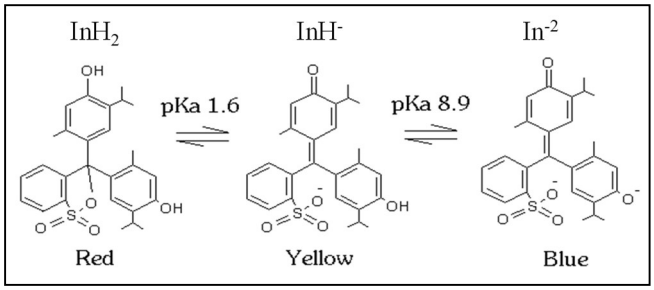

Figure 2.4. Ionization of thymol blue

Thymol blue solutions (20 µg/ml) were prepared using HCl buffers in the pH range of 1.4 - 2.6, which includes pK_{a1}. The solution pH values were measured using a pH meter (Mettler Toledo, SevenMulti series), which was calibrated using standard buffer solutions (pH 4.01, 7.00 and 10.01, Mettler Toledo, Columbus, OH). The concentration of thymol blue was selected such that the absorbance of the ionized, as well as unionized forms, were within the linear range of the Beer-Lambert Law. The ratio of the peak absorbance signals of the unionized to the ionized forms of the indicator was plotted as a function of solution pH (Figure 2.14, Supplementary Information).

Indicator deposition on solid sample. A solution of thymol blue (1 mg/ml) in methanol was mixed well with each solid powder sample and dried. The choice of methanol as the solvent was based on solubility of the probe used and "insolubility" of the solid sample. The indicator concentration used (0.4 mg/g) was based on earlier reports[45] and theoretical indicator coverage calculations reported in an earlier publication.[97] Each solid sample treated similarly but without the indicator served as 'blank' in the spectral measurements.

pHeq Calculation. Solid powder samples of neat PioHCl and PioHCl - MgSt (90:10 w/w) mixtures containing thymol blue were stored at 40 °C/75% RH and their diffuse reflectance spectra were recorded as a function of storage time. The ratio of the Kubelka–Munk functions, F(R), at the peaks corresponding to the ionized and unionized forms of the

indicator (peak height ratios) were determined.[43] The peak ratios provide a measure of the extent of the indicator ionization. The pHeq was calculated by substituting these peak ratios in the calibration equations constructed for thymol blue in buffered aqueous solutions.

2.4 Results and Discussion

Baseline characterization of PioHCl and free base, carried out by differential scanning calorimetry, thermogravimetric analysis, and XRD, yielded results that were in excellent agreement with earlier findings. The XRD pattern of PioHCl was virtually superimposable on the calculated powder pattern published in the Cambridge Structural Database.[98]

2.4.1 Disproportionation in Tablets

Intact tablets (compositions in Table 2.1) were placed in chambers maintained at 40 °C/75% RH and analyzed periodically. The excipient selection was based on previous reports and they represent different functionalities - lubricant, disintegrant, and diluents.[35,89] SXRD enabled the simultaneous quantification of PioHCl (reactant) and free base (product) formed in these tablets. As a first step, tablets were positioned in such a way that the synchrotron radiation passed through the center of the tablet. In this transmission mode, “average” information along a three dimensional (3D) cylindrical section of the tablet was obtained. The diameter, reflecting the beam size, was set to 0.3 mm and the length of the cylinder would correspond to the tablet thickness of 3 mm. In tablets formulated with either MCC or lactose MH, even after 9 days of storage at 40°C / 75% RH, there was no detectable decrease in intensity of the characteristic peaks of PioHCl. In addition, the peaks uniquely attributable to the free base were not observed (data not shown). We therefore concluded that there was no disproportionation. In contrast, disproportionation of PioHCl to form crystalline free base was observed in tablets

formulated with MgSt or CCS. In Figure 2.5, the weight fractions of the crystalline PioHCl salt (reactant) and free base (product) are plotted as a function of time. At any time point, the extent of disproportionation was higher in presence of MgSt than CCS (Figures 2.5A and 2.5B). These findings are consistent with previous reports.[35,69,89] Since we were simultaneously quantifying the reactant as well as the product, the sum of the weight fractions of reactant and product (base weight fractions normalized to corresponding weights of salt) was also plotted (Figure 2.5). At all time-points, this was close to unity, indicating the absence of amorphous phases.

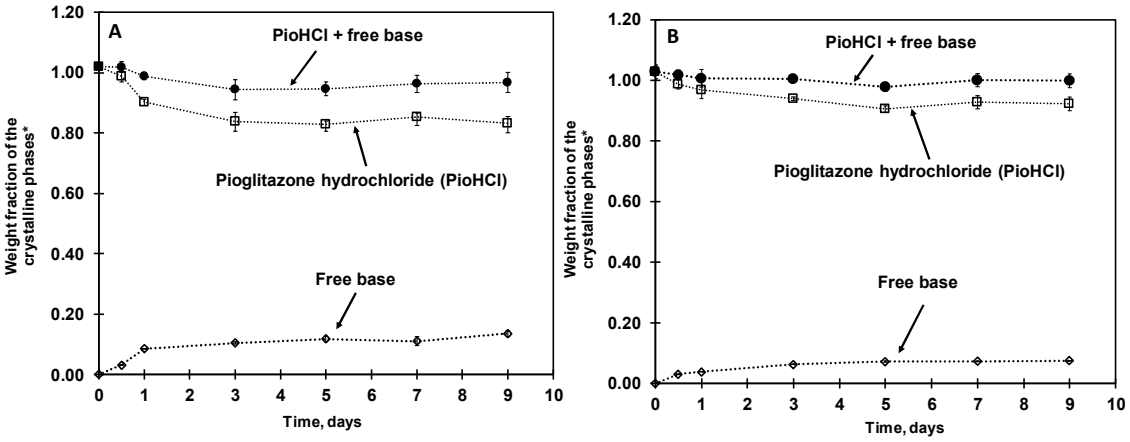

Figure 2.5. Weight fractions of PioHCl and free base as a function of time following storage of PioHCl tablets containing (A) MgSt (10% w/w) and (B) CCS (10% w/w). The tablets were stored at 40 °C/75% RH (n = 3). The dotted lines are drawn to assist in visualization of trends. (*Weight fractions are expressed in terms of PioHCl).

2.4.2 Spatial Mapping of Disproportionation

In order to investigate the spatial heterogeneity in phase composition, tablet mapping studies were performed. The experimental details were presented earlier. Figure 2.6 shows the results of the spatial mapping in tablets containing PioHCl and MgSt, placed inside the chamber. Since the chamber, maintained at 40 °C/75% RH, was placed in the path of the X-ray beam, the results represent kinetic studies conducted in real time in the beamline. As

described previously, tablet mapping was performed in the radial direction starting from tablet edge and moving, in increments of 300 microns, towards the tablet center. Tablet mapping experiments revealed the first evidence of PioHCl disproportionation after 10 minutes (Figure 2.6). About 1% free base was observed along the tablet edge, while the tablet center region showed approximately 0.3% transformation. After 2 hours, the transformation at the edge was ~3.5%, while at the center, it was ~0.6%. Thus, the extent of transformation at the edge was about 5 times that in the core.

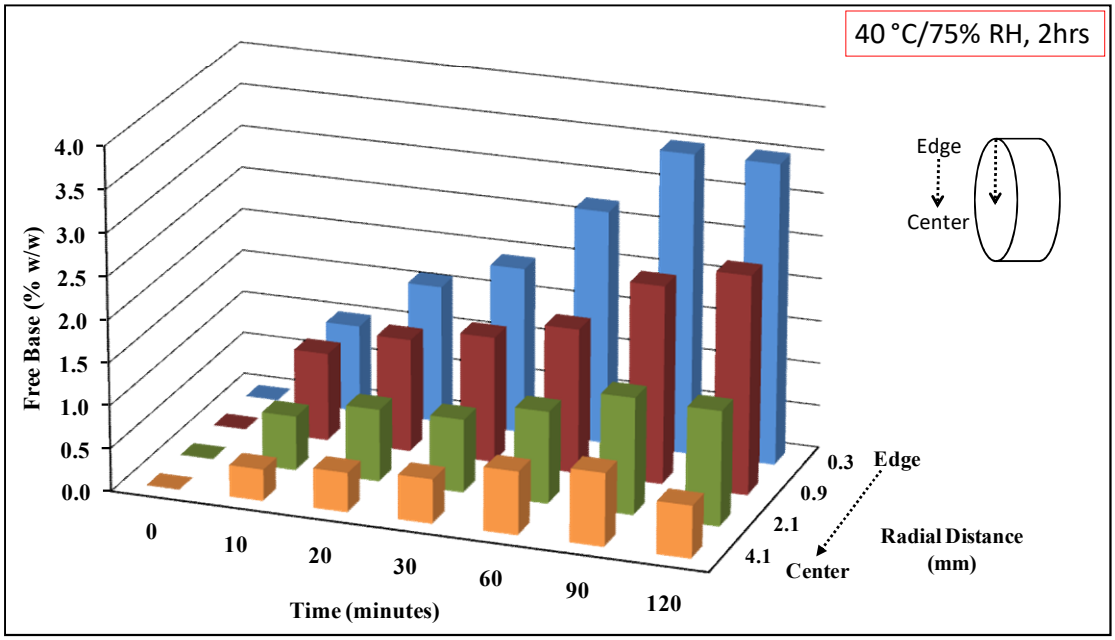

Figure 2.6. Spatial mapping of PioHCl disproportionation in a tablet containing MgSt (10% w/w) and stored at 40 °C/75% RH. The mapping was performed in transmission mode by scanning the tablet in radial direction, starting from the top edge towards the center. While the mapping was performed in 15 steps, for the sake of clarity, only a few steps are shown.

We were surprised at the pronounced disproportionation observed in such a short time. In order to determine the effect of temperature, the experiments were repeated at 25 °C/75% RH (Figure 2.7). At 25°C, the first evidence of disproportionation was observed after 30

mins with ~1.4% free base formed along the tablet edge and ~ 0.4% along the tablet center. After 3 hours, the extent of free base transformation on the edge was ~ 3% while the transformation in the center increased to ~ 0.8%. A comparison of the kinetics at 40°C with 25 °C revealed that the increase in temperature caused a pronounced acceleration in kinetics. This increase in temperature will also cause a pronounced increase in water vapor pressure from 23.8 to 55.4 torr. Thus the combined effects of temperature and water vapor pressure can explain the observed acceleration in disproportion kinetics.

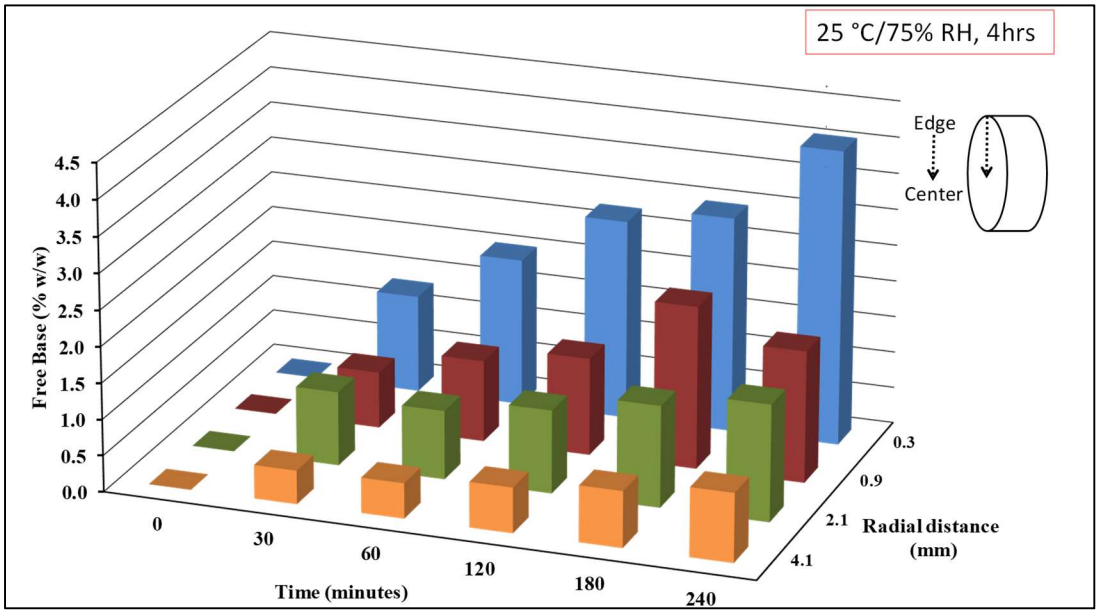

Figure 2.7. Spatial mapping of PioHCl disproportionation in a tablet containing MgSt (10% w/w) and stored at 25 °C/75% RH.

In an effort to characterize the surface morphology of the tablets, SEM images were obtained before and after exposure of the tablets to 40 °C/75% RH. These studies were conducted using both the salt and free base tablets formulated with or without MgSt (Figure 2.8). The surface morphologies of the freshly prepared free base and PioHCl tablets (no excipient) exhibited pronounced differences. PioHCl tablet consisted predominantly of

needle-shaped crystals with particles ranging in size between 2 and 100 µm, while the neat free base tablet consisted of large plate-like crystals (Figure 2.8A and 2.8B). Addition of 10% MgSt did not cause an observable/significant change in surface morphology (not shown). Exposure to 40 °C/75% RH caused a pronounced change in the surface of the PioHCl tablets formulated with MgSt, attributable to the disproportionation reaction. Upon disproportionation, large plate-like crystals appeared on the tablet surface (pointed by arrows in Figure 2.8C and 2.8D).

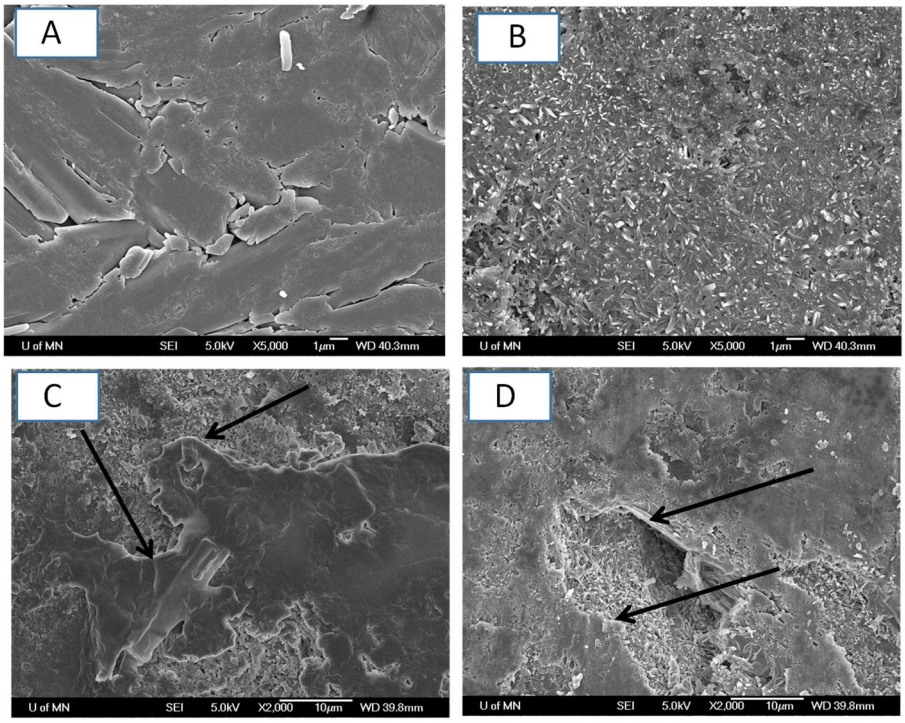

Figure 2.8. SEM images of (A) free base tablet surface (B) PioHCl tablet surface. (C) & (D) two regions of PioHCl tablets containing MgSt (10% w/w) exposed to 40 °C/75% RH for 2 hrs. The change in the surface morphology is attributed to free base formation (The arrows indicate the phase boundary).

Longer-term storage studies provided additional insights into the disproportionation reaction. In these cases, the tablets were stored at 40 °C/75% RH for the desired time

period and then the mapping was conducted using synchrotron radiation. The free base concentration in three different regions - at the tablet edge, center and between the edge and center were determined at different times (Figure 2.9). For each time point, a fresh set of tablets were used. The free base formation was very rapid along the tablet edge, with 12.9% (± 0.6%; mean ± SD; n = 3) free base after 3 days. Thereafter, the reaction was observed to have reached a plateau with about 15.5% (± 1.4%) formed in 15 days. Along the central region of the tablet, only 6.5% (± 0.4%) free base formation was observed in 3 days. Thus, after 3 days of storage, the free base concentration in the edge was approximately twice that in the center. However, the concentration in the center progressively increased with storage time and reached 11.4% (± 0.6%) in 10 days. The free base concentration seemed to be levelling off after 10 days.

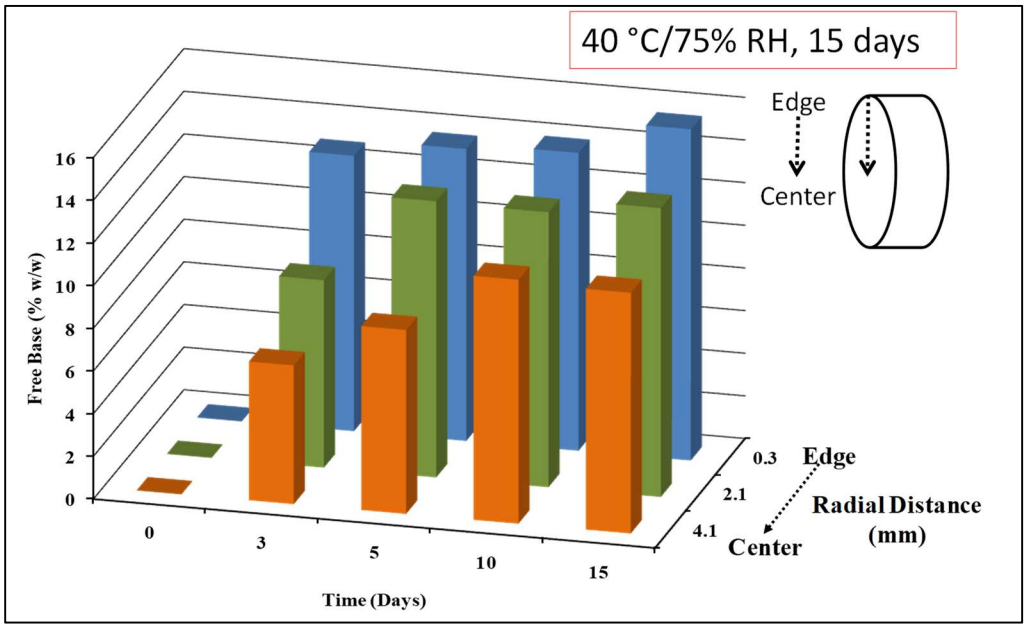

Figure 2.9. Spatial mapping of PioHCl disproportionation in tablets containing MgSt (10% w/w) and stored at 40 °C/75% RH for up to 15 days.

Analysis of the XRD patterns provided detailed insights into the disproportionation reaction. The 2D XRD patterns were converted into one dimensional (conventional) XRD patterns (Figure 2.10). One characteristic peak of free base (4.3° 2θ), magnesium stearate (2.5° 2θ) and stearic acid (10.1° 2θ) are pointed out. The XRD patterns obtained from the tablet edge reveal: (i) significant decrease in the intensity of the MgSt peak (2.5° 2θ) in 3 days and complete disappearance of this peak after 5 days, (ii) simultaneous appearance of the peaks attributable to the free base (for example at 2.9°, 3.6°, 4.3°, 4.8°, 5.8° and 7.7° with the most intense peak at 4.3° 2θ) and (iii) appearance of two new peaks at 3.2° and 10.1° 2θ after 3 days which can be attributed to two polymorphs of stearic acid.[99,100] Very similar results were obtained from the XRD analysis of the center of the tablet (Figure 2.10B). However, in this tablet region, the MgSt peaks completely disappeared much later (after 10 days) compared to the tablet edge. These observations provide conclusive evidence for the previously proposed disproportionation reaction.[35,69,89]

$$(2)\text{PioH}^{+}\text{Cl}^{-} + (\text{R-COO}^{-})_2\,\text{Mg}^{2+} \longrightarrow (2)\text{ free base} + (2)\text{ R-COOH} + \text{MgCl}_2 \quad (1)$$

Pioglitazone hydrochloride — Magnesium stearate — Pioglitazone free base — Stearic acid — Magnesium chloride

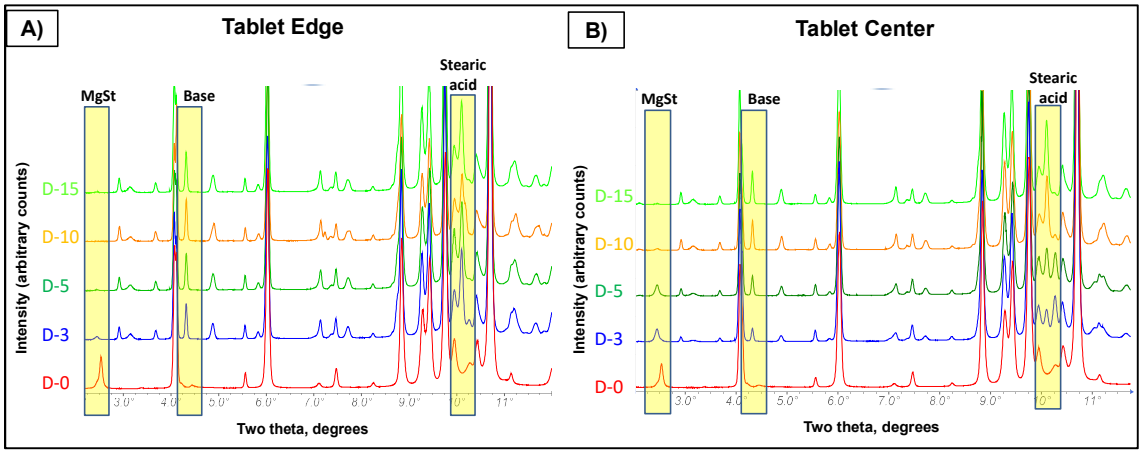

Figure 2.10. Overlay of the XRD patterns of PioHCl tablets containing MgSt (10% w/w). The tablet edge (A) and tablet center (B) were analyzed following storage at 40

°C/75% RH for 3, 5, 10 and 15 days. The peaks highlighted from left to right are attributed to MgSt (2.5° 2θ), free base (4.3° 2θ) and stearic acid (10.1° 2θ).

In the tablets, the reaction is expected to be initiated at the interface of PioHCl and MgSt particles. During blending, which precedes compression, there will be a pronounced coverage of the surface of PioHCl particles by MgSt. This process will be facilitated by the intrinsic nature of the lubricant.[101,102] As a result of compression, PioHCl and MgSt particles come in intimate physical contact increasing the interface between particles. In addition, compression can introduce significant lattice disorder.[103,104] The sorption of water in these "disordered regions" can cause pronounced plasticization, resulting in increased molecular mobility and will enhance the reaction rate.

It is now instructive to think of the water-solid interactions at the particulate level. Both crystalline and amorphous particles are expected to adsorb water. The amount adsorbed will be a function of surface area, is expected to increase as a function of RH, and can account for only a very low water content (typically < 0.1% w/w).[105] The water – solid interactions in amorphous particles is fundamentally different from that in crystalline materials.[36,105] When amorphous particles take up water, the sorbed water can "dissolve" in the amorphous phase. In contrast, when a crystalline anhydrous phase is subjected to elevated RH, assuming that it does not form a hydrate, dissolution in the adsorbed water will occur only if the RH $\geq$ RH_0 (where RH_0 is the critical relative humidity).

Our findings indicate that the disproportionation reaction is initiated very rapidly (Figure 2.5). This is surprising in light of the extremely low aqueous solubility of crystalline magnesium stearate. The lattice disorder in the PioHCl - MgSt particle interface, the

plasticization and the attendant increase in molecular mobility, facilitates the rapid reaction initiation yielding the free base, stearic acid and $MgCl_2$ as reaction products (reaction 1). Interestingly, after just one day of storage, the characteristic XRD peak (2.5° 2θ; Figure 2.5) of MgSt had essentially "disappeared". Thus, the reaction once initiated, progressed rapidly to completion. The critical relative humidity (RH_0) of $MgCl_2$ hexahydrate, one of the reaction products, is 33% at 40 °C. Since this is substantially less than the storage RH (75%), it is expected to have a pronounced tendency to sorb water and exist in solution. The continued uptake of water would progressively plasticize the system. With increased water content, the aqueous phase would serve as a medium, facilitate dissolution of the crystalline phases, and enable solution mediated transformation.

The other two reaction products, the free base and stearic acid, may attain a concentration substantially above their saturation solubility values, leading to their rapid crystallization. This explains the rapid appearance of the characteristic peaks of the stearic acid and free base (Figure 2.10). It is worthwhile to point out that there is a 400-fold difference in solubility between the PioHCl salt and free base.[35]

Thus, from our XRD data we can draw two conclusions. (i) The salt disproportionated as a result of its interaction with MgSt. The water sorbed by the tablet components enabled this solution mediated reaction. (ii) There is spatial heterogeneity in the disproportionation reaction; the reaction initiated at the tablet surface and progresses towards the tablet core.

2.4.3 Distribution of Water

Since disproportionation is a solution mediated transformation, the observed differences in disproportionation kinetics between the edge and center can be explained on the basis of spatial distribution of sorbed water into the tablet. The migration of sorbed water from the

surface to the interior of the tablet during storage at 40 °C/75% RH was confirmed using rhodamine. At first, the intact tablet face was analyzed by keeping the tablet sample horizontal on the glass slide of the inverted confocal fluorescence microscope. Initially, the tablet surface did not exhibit a strong fluorescence signal indicating that it was "dry" (Figure 2.11B). However, upon storage at 40 °C/ 75% RH, the sorbed water on the tablet surface could be readily discerned by the increase in fluorescence intensity (Figure 2.11C and 2.11D). In the split tablets, a gradient in the water concentration was evident after 5 days, wherein tablet regions closer to the exposed surfaces exhibited the presence of greater amount of water but the tablet core was relatively "dry" (Figure 2.11H).

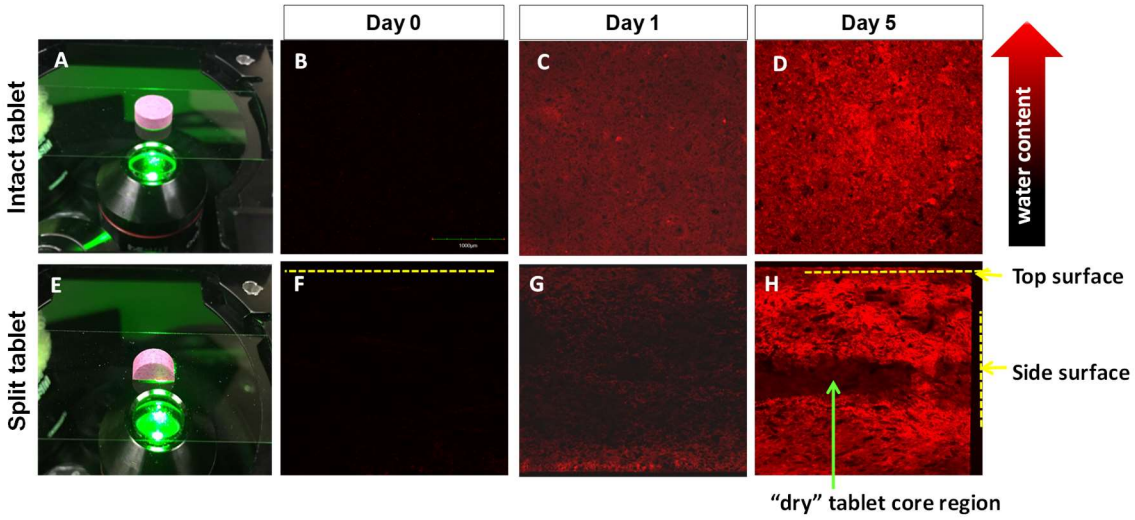

Figure 2.11. Visualization of water distribution (measured by fluorescence of rhodamine 6G) on the tablet face (B, C, D) and on the sectional surface of a split tablet (F, G, H) of PioHCl tablets containing MgSt (10% w/w), stored at 40 °C/75% RH. The photographs of intact tablet and split tablet are shown in A and E respectively.

These results are consistent with the spatial disproportionation trend observed in tablets. If we consider the tablet edge region, the sorbed water can penetrate from the top and bottom surfaces of the tablet as well as through the tablet 'band' surface. For example, to reach the

center of the tablet, the sorbed water entering from the top and bottom faces has to travel a distance of 1.5 mm (half of tablet thickness) while the sorbed water entering from the edges has to travel radially 4 mm to reach the center. This could explain our observation that the free base formation at the tablet edge tends to reach a plateau earlier compared to the center of the tablet. While there is enough evidence to support the role water in salt disproportionation reaction, it important to note that the presence of water is a *necessary but not sufficient condition* for disproportionation. Mechanistically, as the sorbed water migrates into the tablet interior, a "basic microenvironment" is created owing to the presence of MgSt in the tablet. As the "pH" of the microenvironment exceeds the pH_{max} of the PioHCl salt, disproportionation of salt to the free base occurs. Therefore, our final objective was to understand the role of microenvironmental acidity in the disproportionation reaction.

2.4.4 Microenvironmental Acidity

While there is agreement in literature on the pivotal role of microenvironmental acidity and pH_{max} in the context of salt disproportionation, a direct measurement of proton activity in microenvironment of solid systems is challenging. Recently, indicator dyes have been used to probe the microenvironments in pharmaceutical solid compositions.[44–48,106] In this method, the acidity is expressed as pH equivalent (pHeq), and is defined as the 'pH of an aqueous solution in which the ratio of the peak absorbance signals of the ionized to the unionized forms of the indicator is the same as in the given solid sample'.[43] This method provides a practical means for estimating and rank ordering microenvironmental 'acidity'. Hence, the indicator dye method was used to gain an insight into the environment inducing the disproportionation. It is important to note here that, although the pHeq provides a

measure of the environment within the solid sample, it is not an absolute measure of the acidity of the microenvironment and represents an empirical acidity scale. The limitations of this approach are discussed elsewhere.[43]

Solid powder samples of neat PioHCl and PioHCl - MgSt (90:10 w/w) mixtures containing thymol blue were stored at 40 °C/75% RH and their diffuse reflectance spectra were recorded as a function of storage time. From the signal intensities of the unionized (InH_2) and ionized (InH^-) species of thymol blue, the pHeq values were calculated using the calibration curve as described elsewhere[43,45] (Figure 2.14, Supplementary Information). The free base formed was also simultaneously quantified by XRD using a separate set of physical mixtures (without dye).

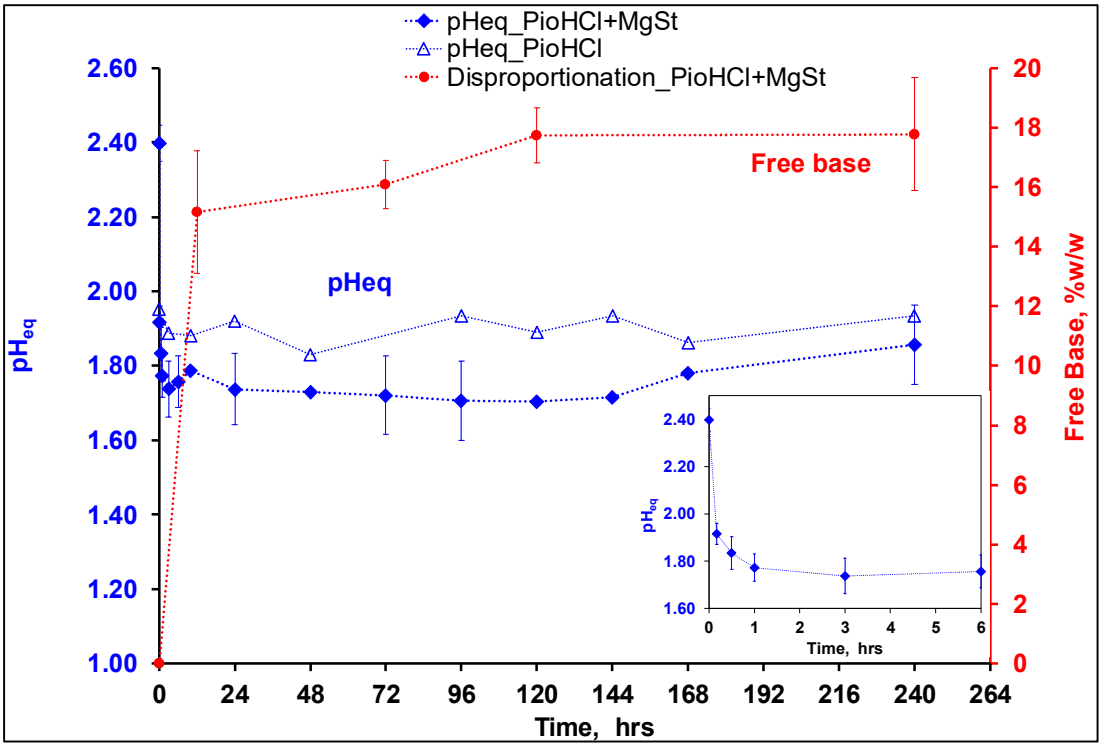

Figure 2.12. pHeq (left y-axis) versus time for (i) neat PioHCl and (ii) PioHCl - MgSt (90:10 w/w) physical mixture stored at 40 °C/75% RH. The inset shows a magnified view of the pHeq values monitored at early time points up to 6 hrs. The percentage of free base formed as a function of storage time for the PioHCl -MgSt (90:10 w/w) physical mixture is plotted on the right y-axis.

Figure 2.12 shows the pHeq values (left y-axis) measured for the two systems and the free base formation (right y-axis) as a function of storage time. For the PioHCl-MgSt (90:10 w/w) physical mixture, the initial pHeq was higher (pHeq = 2.40 ± 0.05) than for neat PioHCl (1.90 ± 0.02). In addition, an increase in the MgSt concentration (20 and 30% w/w) further raised the pHeq of the system in a concentration dependent manner (data not shown). This was expected due to the basic nature of MgSt coupled with MgO as an impurity.[40,107] Initially, a rapid decrease in the pHeq value from 2.40 (± 0.05) at 0 hr to 1.77 (± 0.06) after 1 hr was observed (inset, Figure 2.12). This initial steep decrease in pHeq also correlates well with the very rapid disproportionation kinetics. At later time points, the pHeq was similar to that of neat PioHCl salt and eventually levelled off at ~1.74. In contrast, the pHeq values measured for the neat PioHCl salt stored at 40 °C/75% RH, remained essentially unchanged for 10 days and there was no evidence of free base formation (by XRD). This indicates that the salt by itself is stable and the pHeq determined for the neat salt represents a microenvironment that does not favor disproportionation. In presence of a basic excipient, MgSt, the initial high pHeq value may be the driving force for the disproportionation reaction and the subsequent decrease in the pHeq values reflects the altered phase composition of the system. While the presence of the basic excipient, MgSt, is responsible for the observed disproportionation reaction, its reaction and complete consumption coincides with the observed decrease in the pHeq. Since this altered pHeq value is close to that of the 'as is' salt, it is likely that the microenvironmental conditions no longer favors disproportionation.

To validate this, a fresh physical mixture containing stoichiometric proportions of PioHCl salt, free base, stearic acid and $MgCl_2$ was prepared assuming all the MgSt in the system has reacted (reaction 1). We recognize that this physical mixture is unlikely to accurately represent the stored blend that underwent disproportionation. The microstructure and particulate properties of the two systems are unlikely to be identical. However, the pHeq of this freshly prepared physical mixture (1.82) matched the pHeq value (1.86) of the stored physical mixture. An increase in the acidity (a lowered pHeq), is likely to represent a shift in the microenvironment that does not favor further salt to base transformation.

2.5 Significance

For the salt of a weakly basic active pharmaceutical ingredient having a low pH_{max} value, the presence of a basic excipient can cause the microenvironmental acidity "experienced" by the salt to exceed the pH_{max}. This water-mediated disproportionation reaction can occur in extremely short timescales. As seen in the case of PioHCl, even at room temperature and 75% RH, the reaction was evident in a few hours. This rapid reaction is particularly surprising in light of the fact that the tablet water content was < 5% w/w and magnesium stearate is practically insoluble in water. It will be interesting to evaluate the effect of processes such as wet granulation, wherein there is direct contact with water and a strong disproportionation propensity.[26] While the undesirable effects of disproportionation on the API properties are well recognized, the tablet disintegrant, croscarmellose sodium, by participating in this reaction can lose its functionality. This was evident in the case of delavirdine mesylate wherein disproportionation of the salt due to solid-state reaction with croscarmellose sodium caused a dramatic reduction in dissolution rate.[23]

We believe that this is the first report of spatial heterogeneity of salt disproportionation in tablets. The disproportionation reaction was initiated at the tablet surface and moved towards the core. Thus, while the overall extent of disproportionation may be low, it can be pronounced on the tablet surface. It is instructive to recognize that disproportionation on the tablet surface can profoundly affect tablet dissolution. The free base crystallized on the surface can dramatically slow down the dissolution because of the very high salt to free base solubility ratio (400 fold). In addition, it is well known that *in situ* phase transition leading to "crystallization" of a new phase in tablets, can seriously compromise excipient functionality.[108]

2.6 Conclusions

Salt disproportionation reaction, mediated by water, is attributed to the microenvironmental pH “experienced” by the analyte. The microenvironmental acidity is dictated by the nature and concentration of the excipients used in the formulation. The *in situ* tablet mapping experiments show that the disproportionation reaction is initiated at the tablet surface and progresses towards the tablet core as a function of time. By taking a two-pronged approach of quantifying disappearance of reactant (salt) and appearance of free base (product), it is possible to determine the reaction kinetics. Our investigation, carried out in model tablet formulations, enabled an in-depth understanding of the disproportionation mechanism. This will aid in the development of strategies for preventing, or at least controlling, disproportionation.

2.7 Supplementary Information

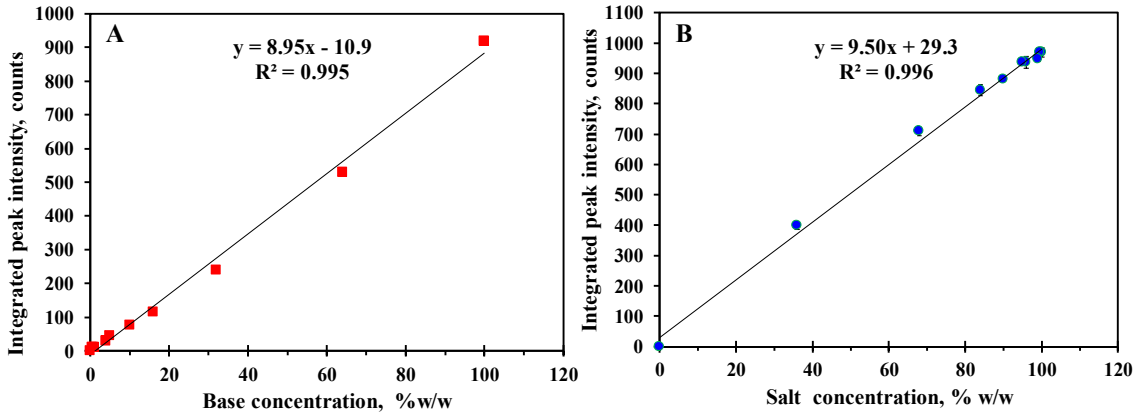

Figure 2.13. Calibration curve (A) Plot of the intensity of the 4.3° 2θ peak of pioglitazone free base and, (B) Plot of the intensity of the 6.0° 2θ peak of PioHCl salt as a function of concentration in PioHCl salt - free base tablets of different compositions. (Error bars show standard deviation where n = 3).

Sample Chamber Details

The system consists of a heated aluminum chamber containing the tablet sample and the humidity inside the chamber is controlled by use of saturated salt solution. The chamber is comprised of a single aluminum block with a wall of 12.7 mm thickness and an internal chamber measuring 127 X 76.2 X 101.6 mm ($l \, X \, w \, X \, h$) in size. Windows with a diameter of 13 mm are drilled through the aluminum to enable X-ray diffraction. The windows are sealed with kapton tape. The lid of the chamber is a piece of aluminum with six screws and a heat insulating tape to allow for a tight seal when closed. One of the walls of the chamber that is parallel to the X-ray beam features three holes: (i) for inserting the temperature and humidity sensors close to the tablet sample, (ii) a temperature probe and (iii) outlet for 5 feet umbilical cable to a control system enclosure. The other wall features holes for three screws for mounting the chamber on a base plate (Newport Kinematic stage BKL-4) used at the beamline.

Temperature and Humidity Control

The temperature of the chamber is controlled by a Newport/Omega PT32-305 PID process controller sensing temperature with a 100 ohm Platinum RTD. It controls power using a time proportioned relay to the four 100 ohm Caddock M9100 power resistors used as heaters. There are two DC power supplies in the control enclosure, 48 VDC/3Amp for the heaters, and a 12V/0.5Amp supply for the muffin fans. One 60 mm fan cools the control enclosure, and one 25mm fan circulates air in the sample chamber. Both are brushless DC type. At 48V, each resistor dissipates 23W into the 1/2-inch-thick aluminum walls of the chamber, for a total of 92W at 100% output from the PID controller. The temperature and relative humidity of the air surrounding the tablet placed inside the chamber, was monitored throughout the experiment. This was accomplished by sealing a sensor (EK-H4, Sensirion AG, Switzerland) into the chamber and positioning it close to the tablet sample. The sensor was connected to a computer and the time-dependence of temperature and relative humidity of the air in the chamber was logged. The water vapor content of the air in the chamber is achieved through the use of saturated salt solutions placed in 5 ml glass beakers inside the chamber. The equilibrium RH is specific to the salt, and varies with temperature. Saturated solution of NaCl was used to maintain the desired RH of 75% at 40 °C. The air inside the chamber was circulated by a muffin fan for maintaining a uniform environment. The RH inside the chamber was monitored during the course of the experiment by means of a RH sensor present in the chamber. While this paper is limited to 75% RH maintained by saturated salt solution of NaCl, other saturated solutions could, in principle, be used based on the temperature dependence of humidity. To collect XRD data,

tablet sample was quickly mounted into the pre-equilibrated chamber, in which the RH was 75% and temperature was 40°C.

Sample Chamber Performance

The sealed chamber design enables excellent temperature and humidity control. Chamber temperature fluctuations were less than ±0. 2°C of the set point and the humidity inside the chamber is acceptably uniform. The humidity sensor was physically moved to five different locations in the sample chamber. At temperature set point of 40 °C, the measured RH generated by saturated solution of NaCl was close to 75%, with a maximum deviation of 0.8%. During data acquisition runs, the humidity sensor is placed in close proximity to the tablet sample to ensure accurate control of the humidity around it. Stable control around the set-point with no overshoot was observed. It does, however, take several minutes for the chamber to equilibrate. Once the chamber was equilibrated, the tablet sample was quickly mounted inside the chamber by opening the lid.

Calibration Curve for Thymol Blue

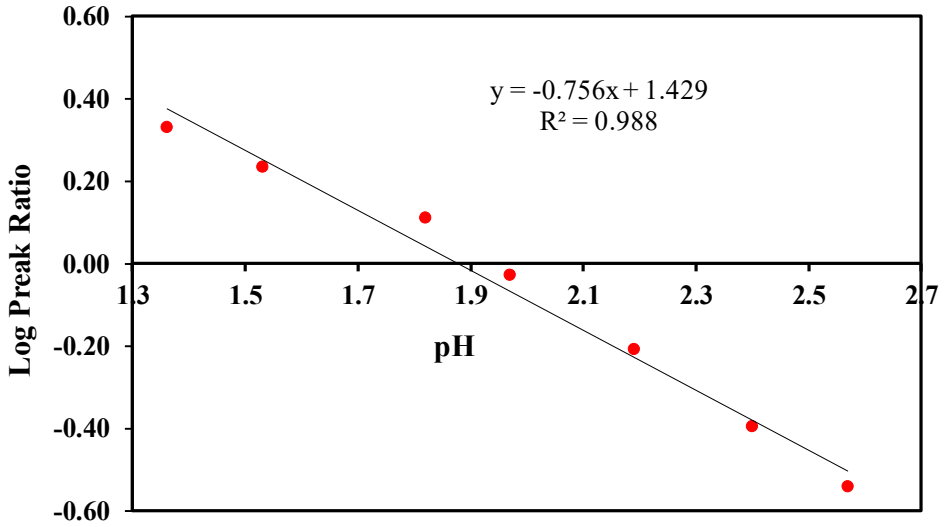

Figure 2.14. Calibration curve for thymol blue in HCl buffer solutions at different pH values. The log of the peak ratios of the unionized form (InH_2) to the ionized form (InH^-) is plotted as a function of solution pH.

Chapter 3 : Effect of Formulation and Process Parameters on the Disproportionation of Indomethacin Sodium in Buffered Lyophilized Formulations*

*Reprinted by permission from: Springer Nature [Pharmaceutical Research] Koranne, S.; Thakral, S.; Suryanarayanan, R. Effect of Formulation and Process Parameters on the Disproportionation of Indomethacin Sodium in Buffered Lyophilized Formulations. *Pharm. Res.* **2018**, *35* (1), 21. COPYRIGHT (2018)

3.1 Synopsis

Purpose. (i) To investigate buffer salt crystallization and the consequent pH shifts during the freezing stage of the lyophilization of indomethacin sodium (IMCNa) in aqueous sodium phosphate buffer. (ii) To determine the effect of pH shift on the disproportionation of IMCNa in lyophilized formulations.

Methods. Prelyophilization solutions containing IMCNa in sodium phosphate buffer, at initial buffer concentrations ranging from 10 to 100 mM (pH 7.0), and at IMCNa concentrations of 5, 10 & 15 mg/ml, were investigated. Their phase behavior during cooling was monitored by low temperature X-ray diffractometry (XRD), differential scanning calorimetry (DSC) and pH measurements. The final lyophiles were characterized by infrared spectroscopy (IR) and XRD.

Results. Upon cooling to −25 °C, pronounced pH shifts were observed only in IMCNa buffered solutions containing high initial buffer concentration (100 mM), due to crystallization of $Na_2HPO_4 \cdot 12H_2O$. In the final lyophiles, disproportionation of IMCNa to the free acid (IMC) was observed in systems with buffer concentrations ≥ 50 mM, but not low buffer concentration (10 mM). At intermediate buffer concentrations (35 & 20 mM) the disproportionation depended on IMCNa concentration. The initial concentrations of both buffer and IMCNa influenced the buffer crystallization.

Conclusions: During freeze drying, selective crystallization of a buffer component and the consequent pH shift can cause disproportionation of IMCNa. This can prolong the reconstitution time or retain particles of the poorly soluble free acid in the reconstituted solution.

3.2 Introduction

Lyophilization (or freeze drying) is a commonly used method for the dry state stabilization of thermolabile small molecules, proteins and other biological products. Lyophilized formulations are generally multicomponent systems containing the active pharmaceutical ingredient (API) and excipients. The stability (physical and chemical) and performance (for example, reconstitution time) of the lyophilized product can be dictated by the physical form of the API and excipients.

The first step in freeze-drying, cooling of the prelyophilization solution, results in ice crystallization leading to freeze concentration of the solutes. The second step is primary drying where ice is sublimed under reduced pressure followed by secondary drying for the removal of the residual sorbed water. During the process of freeze-drying, unintended API-excipient interaction can occur, with the potential to affect the final product performance. Lyophilization of bortezomib with mannitol, resulted in bortezomib - mannitol ester, which upon reconstitution existed in equilibrium with its hydrolysis product, monomeric boronic acid.[109] Freeze-drying of indomethacin in tris buffer resulted in the formation of indomethacin-tris salt with a very short reconstitution time, an attribute highly desired in lyophilized parenteral formulations.[110]

During the freezing step, selective crystallization of a buffer component can lead to a drastic shift in the pH of the freeze-concentrate. Such pH shifts in phosphate buffer systems (sodium and potassium) have been extensively investigated.[111–113] In the sodium phosphate buffer system, selective crystallization of the disodium phosphate (as $Na_2HPO_4 \cdot 12H_2O$) during freezing caused a decrease in pH of up to ~ 4 units. In contrast, in the potassium phosphate buffer system, pH increase of ~ 2 units was observed due to selective crystallization of KH_2PO_4. In case of succinate buffer solution, a 'pH swing' was observed with the pH increasing from 4.0 to 8.0 followed by a drop to 2.2 caused due to the sequential crystallization of succinic acid, monosodium succinate, and disodium succinate respectively.[114,115] There are numerous examples of loss in API activity in protein formulations attributed to pH shifts caused by buffer crystallization.[112,116–119] Such pH shifts upon freezing can also induce instability in small molecules. Benzylpenicillin sodium decomposes to penicillenic acid when cooled to -5 °C in sodium phosphate buffer (70 mM; pH 6.5).[120] Sucrose underwent acid hydrolysis when freeze-dried in a formulation containing sodium phosphate buffer (pH 7.0).[121]

When the drug substance is a salt and is lyophilized, the pH shift brought about by selective crystallization of a buffer component can cause disproportionation i.e. salt → free acid (or base) transformation. This will happen if the pH swings above (salts of weak bases) or below (salts of weak acids) the pH_{max} of the salt.[24,27,34] Salt disproportionation has been extensively studied in the context of solid oral dosage forms. The disproportionation reaction is considered to be water mediated and influenced by the microenvironmental acidity "experienced" by the salt particles in a formulation. Salt disproportionation in tablets can lead to a decrease in dissolution rate[23], increase in tablet

hardness[122] and reduced bioavailability.[25] In pioglitazone hydrochloride (PioHCl) tablets, using synchrotron radiation, we had investigated the spatial heterogeneity in disproportionation.[68] Upon storage of the tablets at 40 °C/75% RH, water sorption was initiated at the tablet surface and progressed towards the core, lending insights into the observed heterogeneity. There was also a good correlation between microenvironmental acidity (pHeq) and extent of PioHCl disproportionation.

Salt disproportionation in lyophilized formulations, while posing a challenging problem, has not been extensively investigated. The neutral form (free acid or base) in the final lyophile, at the very least will increase the reconstitution time and at worst result in incomplete dissolution. If the drug is formulated for intravenous administration, the consequences can be serious. Additionally, the formation of an unstable neutral form of the drug can adversely affect the shelf-life of the final drug product.[123].

Indomethacin (IMC; free acid), the drug of interest, has low aqueous solubility (5 μg/mL at 25 °C; γ-IMC) and is susceptible to hydrolysis.[124] .The carboxylic acid group (pK_a = 4.5) in the molecule enables salt formation and IMC is commercially available, both as a sodium and as a meglumine salt.[125,126] The sodium salt is used parenterally in the treatment of patent ductus arteriosus.[127] In spite of its commercial availability, there are numerous challenges and unresolved issues with this injectable IMC formulation.[128,129] In 2011, some lots of lyophilized indomethacin sodium for injection were recalled due to the presence of drug particulate matter upon reconstitution.[128] This was a FDA Class I recall, wherein product exposure to the patient may provoke serious adverse health consequences or death. In the present study, using indomethacin sodium (IMCNa; as trihydrate) as a model compound, we evaluated its disproportionation propensity during lyophilization in

presence of sodium phosphate buffer. We hypothesize that the selective crystallization of buffer component and the consequent pH shift will cause salt disproportionation during lyophilization. Specifically, crystallization of dibasic sodium phosphate (as $Na_2HPO_4 \cdot 12H_2O$) will lower the pH sufficiently to cause disproportionation of IMCNa (the model compound) yielding the poorly soluble free acid (IMC).

Our objectives were to (i) investigate buffer salt crystallization and the consequent pH shifts during freeze concentration of indomethacin sodium buffered in sodium phosphate, and (ii) determine the effect of active pharmaceutical ingredient (indomethacin sodium) and excipient (buffer) concentrations on disproportionation. The use of several complementary analytical techniques enabled an in-depth understanding of the phase behavior of the solutes. Low temperature X-ray diffractometry (XRD) of frozen solutions enabled us to detect buffer crystallization and identify the physical form of the crystallizing phase. The changes in solution pH brought about by buffer crystallization were measured using a low temperature pH probe. Differential scanning calorimetry (DSC) was used to characterize the frozen systems and infrared (IR) spectroscopy of the final lyophile enabled us to ascertain the disappearance of IMCNa and the formation of IMC free acid (disproportionation product).

3.3 Experimental

3.3.1 Materials

Indomethacin sodium trihydrate (IMCNa; Figure 3.1) was obtained from Sinder Technology Co. Ltd., (Qingdao, China.) and indomethacin free acid (IMC, γ- form) was purchased from CSPC Ouyi Pharmaceutical Co. Ltd., (Shijiazhuang, China). Monosodium

dihydrogen phosphate monohydrate ($NaH_2PO_4 \cdot H_2O$) and disodium hydrogen phosphate heptahydrate ($Na_2HPO_4 \cdot 7H_2O$), having purity ≥ 99%, were purchased from Sigma-Aldrich and were used as received. The pH meter (Mettler Toledo, SevenMulti) was calibrated with standard buffer solutions (Oakton standard buffers; pH 2.00, 4.01, 7.00, and 10.00 at 24 ±1 °C; certified by NIST). Deionized (DI) water was used to prepare the solutions.

Preparation of solid forms of IMC and IMCNa

Amorphous IMC was prepared by melting IMC γ- form at 165 °C followed by quench cooling in liquid nitrogen.[130] Amorphous IMCNa was prepared by freeze drying an aqueous solution of IMCNa as previously described.[131] The IMC α- form was obtained by heating solution ofIMC γ- form in ethanol (80 °C), followed by the addition of water.[132] The IMC ε- form was generated by stirring a suspension of amorphous IMC (20 mg/ml) in 0.1 M aqueous phosphate buffer (pH 6.8) at 25 °C for 5 min and the excess solid was isolated by vacuum filtration.[133]

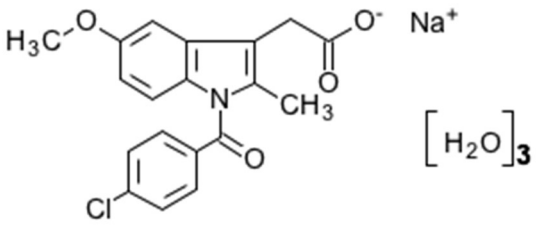

Figure 3.1. Chemical structure of indomethacin sodium trihydrate (IMCNa).

Preparation of buffer solutions

A total of five buffer solutions were prepared by dissolving the monosodium and disodium phosphate salts in the appropriate ratios to obtain the desired pH (7.0 ± 0.1 at 25 °C) and buffer concentration (10, 20, 35, 50 and 100 mM). At each buffer concentration, IMCNa, at concentrations of 5 (11.5 mM), 10 (23.0 mM) & 15 (34.6 mM) mg/ml were investigated.

All the solutions were membrane filtered (0.45 μm, PTFE) and used immediately after preparation. Sodium phosphate buffer solutions (NaP; 10 - 100 mM) without IMCNa and solutions of IMCNa in DI water served as controls.

3.3.2 Lyophilization

Freeze-drying was carried out in a bench-top (VirTis® AdVantage™, Gardiner, NY) freeze-dryer. USP Type I borosilicate glass vials (VWR®) with 20 mm neck size and 10 ml fill volume were used. The prelyophilization solutions were filtered, 5 mL added to each vial, covered with a rubber stopper (20 mm, 2 Leg Lyo, Gry Butyl Sil, Wheaton) and loaded into the lyophilizer. The shelf was cooled to −50 °C at 0.5 °C/min and held for 2 hours. Primary drying was conducted at −25 °C (200 mTorr) for 48 hours. During secondary drying, the shelf temperature was programmed to −10 °C (48 hours), 0 °C (24 hours), +25 °C (24 hours), +45 °C (24 hours) and +60 °C (48 hours). At the end of the cycle, the vials were stoppered under dry nitrogen purge and stored in a desiccator containing anhydrous calcium sulfate at −20 °C.

3.3.3 IR Spectroscopy

The IR Spectra (Vertex 70, Bruker, Ettlingen, Germany; equipped with a globar mid-IR source) were obtained using an attenuated total reflectance (ATR) accessory (single reflection germanium crystal) and a DLaTGS detector. The resolution was 4 cm^{-1}, and 64 scans were acquired in the range of 4000 – 400 cm^{-1}. The peak positions were determined using OPUS software peak picking function.

3.3.4 Differential Scanning Calorimetry

A differential scanning calorimeter (Q2000, TA Instruments, New Castle, DE) equipped with a refrigerated cooling accessory was used. Dry nitrogen gas was purged at 50 mL/min.

Approximately 20 μL of prelyophilization solution was weighed in an aluminum pan, sealed hermetically, cooled from RT to −50 °C at 1 °C/min, held for 30 min and heated to RT either at 1 or 10 °C/min.

3.3.5 Temperature and pH measurements during freezing

The buffer solution (75 ml) was placed in a jacketed beaker (250 ml) connected to a water bath with an external controller unit (Neslab RTE 740, Thermo electron, NH). The bath fluid (HC-50 heat transfer fluid, Dynalene Inc., PA), with a working temperature range of -40 °C to 80 °C, was used. A low temperature pH electrode (Inlab®cool, Mettler Toledo, Switzerland) was placed in the center of the sample and connected to a pH meter (pH 500 series, Oakton, Singapore) to monitor the electromotive force (EMF). The measured EMF was then used to calculate the solution pH. The reference electrolyte containing glycerol and formaldehyde (Friscolyte-B Mettler Toledo, Switzerland) allowed pH measurements down to -25 °C. A copper-constantan thermocouple (0.05 inch diameter, Omega, Stanford, CT) with Teflon insulation connected to a digital bench top read-out device (± 0.2 °C; Omega MDSi8 Series, Stanford, CT) was used to monitor the temperature changes in the sample upon cooling. The thermocouple was placed in the middle of the sample close to the electrode bulb.

The electrode was calibrated using standard buffer solutions of pH values 2.0, 4.0, 7.0, and 10.0 at different temperatures (20, 15, 10, 5 and 0 °C). At each temperature, the EMF and pH of buffer solutions was recorded. From the EMF vs pH plots (Figure 3.11; Supplementary Information), the slope m(T) and intercept b(T) were determined. The pH of the cooled solutions was calculated from the measured EMF values at temperatures ranging from 0 to −25 °C, as described previously.[115,134] During the entire experiment, both

the temperature and pH probes were placed in the center of the beaker. Since the two probes were in close proximity, it was reasonable to assume that the temperature and pH measurements represented the same sample "environment". Initially, the solutions were allowed to equilibrate at 0 °C, and then cooled to −25 °C at 0.5 °C/min simulating the cooling conditions in the lyophilizer. Both the temperature and pH of the solution were monitored throughout the experiment. The pH measurements of the frozen solutions were reproducible (standard deviation of ±0.1).

3.3.6 X-ray Diffractometry

Low temperature XRD: An X-ray diffractometer (D8 Advance; Bruker AXS, Madison, WI) equipped with a variable temperature stage (TTK 450; Anton Paar, Graz-Straßgang, Austria) and Si strip one-dimensional detector (LynxEye; Bruker AXS, Madison, WI) was used. The sample solution was cooled at 0.5 °C/min down to −50 °C where it was held for 1 hour and XRD patterns were collected. The solutions were exposed to Cu Kα radiation (1.54 Å; 40 kV× 40 mA) over an angular range of 5 – 35 °2θ with a step size of 0.02° and dwell time of 0.5 seconds.

Two-Dimensional XRD: Samples were mounted on an xyz stage and exposed, at room temperature, to Co Kα radiation (1.79 Å; 40 kV × 35 mA) in a two-dimensional X-ray diffractometer (D8 Discover 2D, Bruker with a 140 mm diameter window VÅNTEC-500 detector). The sample-to-detector distance was set at 20 cm and XRD patterns were collected using a 0.8 mm collimator. Two measurement frames were scanned at 10° angle of incidence with detector set, first at 20° and then at 40° 2θ. The two-dimensional XRD patterns were integrated to generate the corresponding one-dimensional patterns that were

converted to Cu Kα radiation (1.54 Å) and analyzed using commercially available software (JADE 2010).

3.4 Results and Discussion

3.4.1 Characterization of Lyophiles

IR spectroscopy

The FT-IR spectra of IMCNa trihydrate, amorphous IMCNa, IMC free acid (α-, γ-, and ε-forms) and amorphous IMC acid are overlaid in Figure 3.2. The characteristic peak positions associated with the acid C=O stretch in the IMC acid and the asymmetric COO^- stretch in IMCNa that occur in the 1800 - 1400 cm^{-1} range are used to distinguish between the free acid and salt. The IMC acid is reported to exist in five different anhydrous polymorphic forms, namely, α-, β-, γ-, δ- and an unnamed crystal form, several solvates and an amorphous form.[133,135,136] In addition, a recent study reported the appearance and characterization of three new polymorphic forms of indomethacin, namely ε-, ζ-, and η-forms.[133] Under ambient conditions, the γ- form is the thermodynamically stable form, while the α- form is the most commonly observed metastable form.[124] The IR spectrum of the α- form is characterized by a shoulder at 1681 cm^{-1} to the benzoyl peak (C=O) at 1688 cm^{-1} and weak vibration at 1649 cm^{-1}, attributed to hydrogen bonded acid C=O group, while the non-hydrogen bonded acid C=O vibration occurs at 1735 cm^{-1} [130]. The IR spectrum of IMC γ- form shows a characteristic peak at 1717 cm^{-1} attributed to the asymmetric C=O stretch due to cyclic acid dimer [130]. In case of the ε- form, the peak position of the acid carbonyl (C=O) is close to that of γ- form, but the peak for benzoyl carbonyl (C=O) is shifted to about 1672 cm^{-1}.[133] For the amorphous IMC, the asymmetric C=O stretch due to cyclic acid dimer is observed as a weak vibration at 1710 cm^{-1}, while

the non-hydrogen bonded acid C=O vibration occurs as a shoulder at 1735 cm^{-1}.[130] On the other hand, the acid C=O peaks are absent in the IR spectrum of IMCNa due to loss of the carboxylic acid proton and instead the asymmetric COO^- stretching vibration appears at 1560 cm^{-1} in IMCNa trihydrate and at 1589 cm^{-1} in amorphous IMCNa.[110,131,137]

The results of lyophile characterization, based on IR spectroscopy, are summarized in Table 3.1.

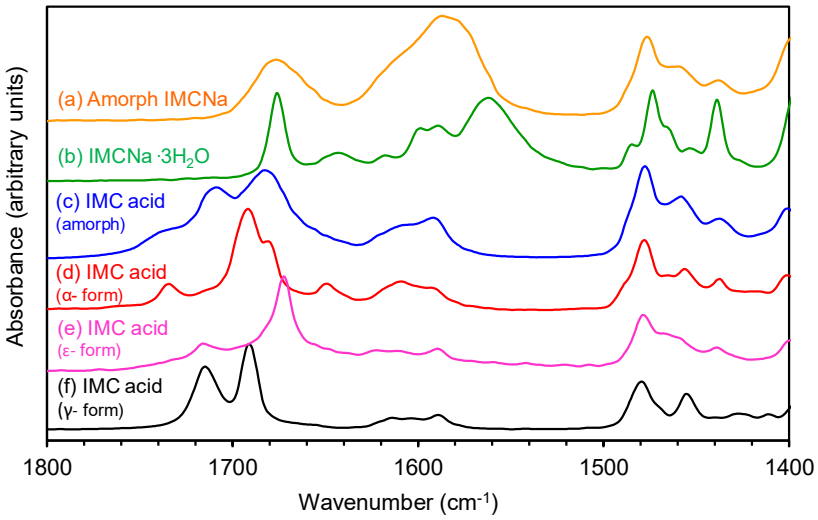

Figure 3.2. FT-IR spectra of (a) amorphous IMCNa, (b) IMCNa trihydrate, (c) amorphous IMC acid, (d) IMC acid α- form, (e) IMC acid ε- form and (f) IMC acid γ- form. (Amorph = amorphous)

Table 3.1. Disproportionation of IMCNa during lyophilization - influence of concentrations of sodium phosphate (NaP) buffer and IMCNa.

NaP concentration, mM	IMCNa trihydrate concentration		
	15 mg/ml (34.6 mM)	10 mg/ml (23.0 mM)	5 mg/ml (11.5 mM)
100	D	D	D
50	D	D	D
35	ND	D	D
20	ND	ND	D
10	ND	ND	ND

D: Disproportionation (IMC acid formation) observed, ND: No disproportionation

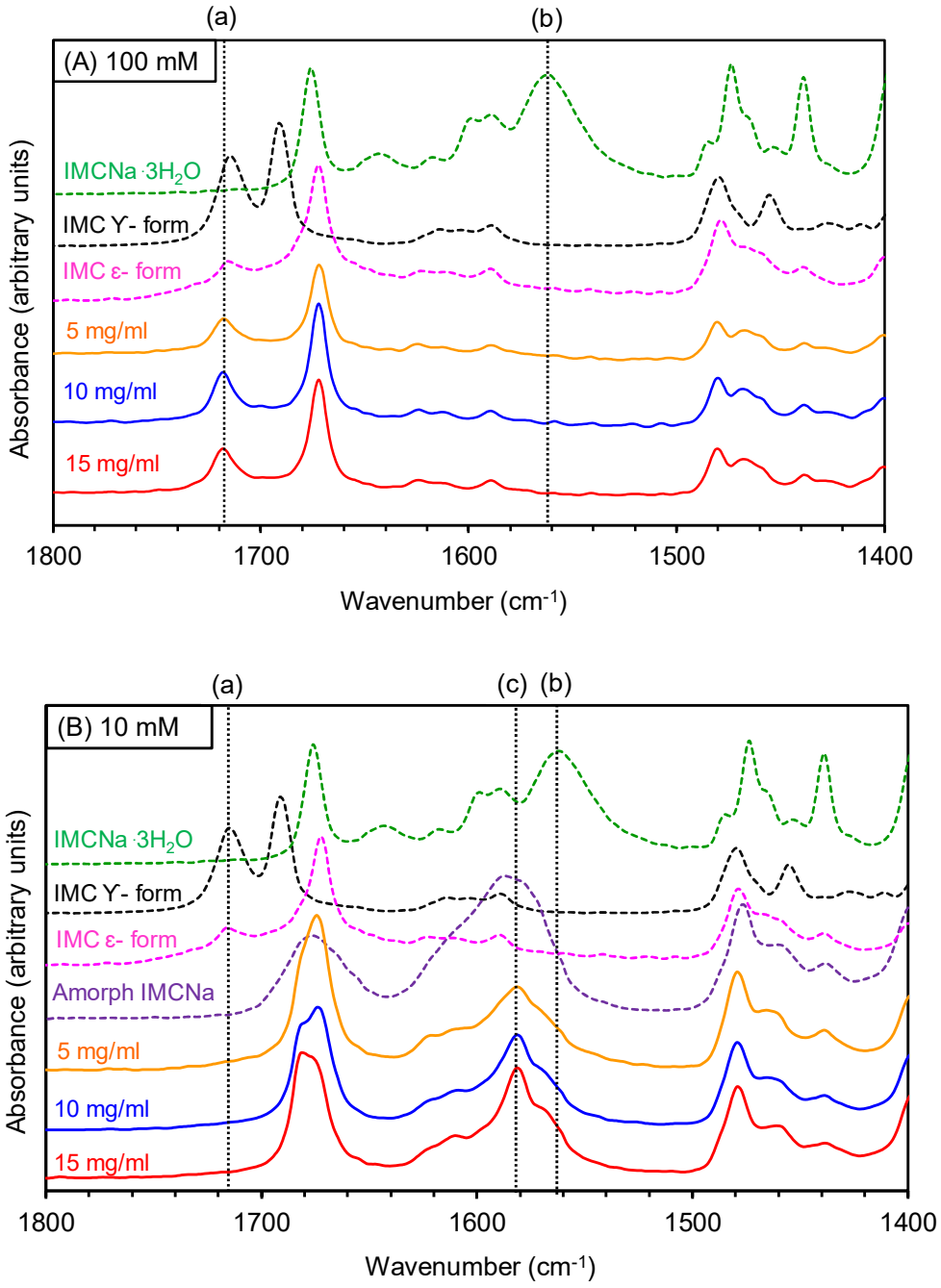

Figure 3.3. Overlay of FT-IR spectra of IMCNa lyophiles (solid lines) prepared using (A) 100 and (B) 10 mM NaP buffer. The 'reference' spectra of IMCNa trihydrate, amorphous IMCNa, IMC γ- and ε- forms (dashed lines) are also provided. Vertical broken lines: (a) carboxylic acid carbonyl (C=O) vibration (observed in the IMC acid), (b) & (c) asymmetric stretch due to carboxylate anion (COO^-) observed in IMCNa trihydrate and amorphous IMCNa salt respectively.

Figure 3.3A contains the IR spectra of IMCNa lyophiles, formulated at the highest buffer concentration (100 mM). Irrespective of the IMCNa concentration in the prelyophilization solutions, a new peak at 1717 cm^{-1}, attributed to the acid carbonyl (C=O) vibration was observed and the benzoyl carbonyl peak was shifted to 1672 cm^{-1}. The IR spectra of the lyophiles closely matched with that of IMC ε- form.[133] In addition, the characteristic peak at 1560 cm^{-1}, attributed to the asymmetric COO^- stretching vibration in IMCNa salt, was absent in the final lyophiles. Thus, at 100 mM buffer, the disproportionation of the IMCNa to IMC acid was confirmed by the disappearance of the carboxylate anion peak (COO^-) and simultaneous appearance of the unionized carboxylic acid peak in the lyophiles. Similar results were observed in the IMCNa lyophiles containing 50 mM sodium phosphate buffer (Figure 3.12; Supplementary Information). On the other hand, the IR spectra of IMCNa lyophiles formulated at the lowest buffer concentration, i.e. 10 mM, revealed the absence of acid C=O peak at 1717 cm^{-1} (Figure 3.3B). Moreover, there was a shift in the COO^- ion peak from 1560 cm^{-1} (in IMCNa trihydrate) to a broad peak around 1580 cm^{-1}. This closely matches with the asymmetric COO^- stretching vibration in amorphous IMCNa. These results indicate that at lower buffer concentration, IMCNa converted to amorphous IMCNa upon freeze drying, with no evidence of IMC free acid formation.

At an intermediate buffer concentration of 35 mM, at 5 and 10 mg/ml IMCNa concentrations, the IR spectra of the lyophiles revealed the acid C=O peak at 1717 cm^{-1}, indicating the formation of IMC acid (Figure 3.4A). However, this peak was not observed in the IR spectra of the lyophile prepared with 15 mg/ml IMCNa solution. Instead, a broad peak at ~1580 cm^{-1} was observed, indicating the presence of amorphous IMCNa. Thus, the concentration of IMCNa also has an impact on disproportionation. A similar

concentration dependent effect of IMCNa on disproportionation was observed in IMCNa lyophiles prepared from 20 mM buffer solutions. In these lyophiles, IMC free acid formation (Figure 3.4B; acid C=O peak at 1717 cm^{-1}), was observed only in lyophile prepared from 5 mg/ml solution of IMCNa.

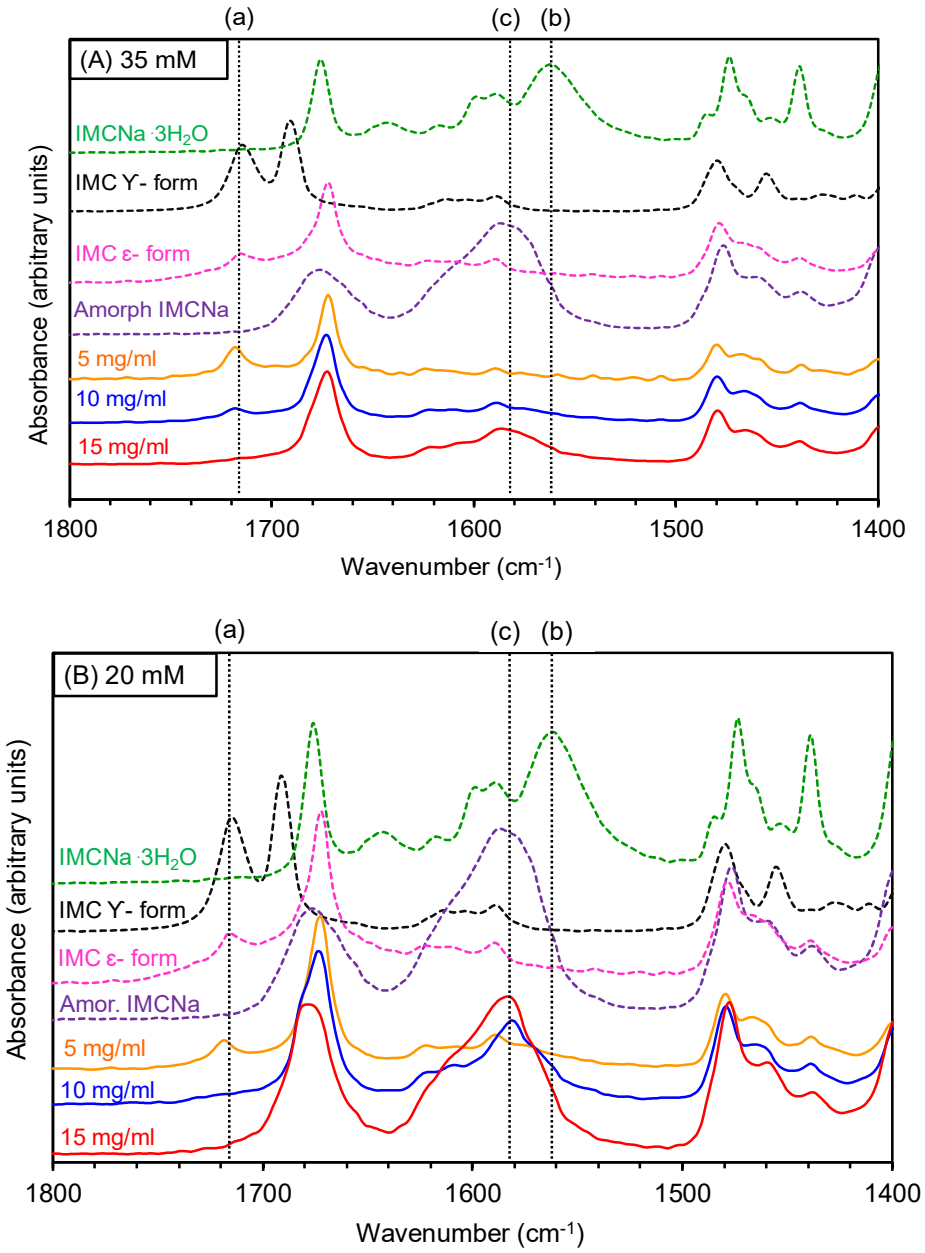

Figure 3.4. Overlay of FT-IR spectra of IMCNa lyophiles (solid lines) prepared using (A) 35 and (B) 20 mM NaP buffer. The 'reference' spectra of IMCNa trihydrate, amorphous IMCNa, IMC γ- and ε- forms (dashed lines) are also provided. Vertical

broken lines: (a) carboxylic acid carbonyl (C=O) vibration (observed in the IMC acid), (b) & (c) asymmetric stretch due to carboxylate anion (COO^-) observed in IMCNa trihydrate and amorphous IMCNa salt respectively.

Powder X-ray Diffractometry

Figure 3.5 shows the XRD patterns of IMCNa (10 mg/ml) lyophiles prepared from aqueous unbuffered or buffered (NaP) solutions. The freeze-drying of an aqueous IMCNa solution, resulted in an X-ray amorphous lyophile. In conjunction with IR spectroscopy (discussed earlier), we can therefore confirm the formation of amorphous IMCNa upon lyophilization from an aqueous solution. When IMCNa in 100 mM buffer was lyophilized, numerous characteristic peaks of anhydrous Na_2HPO_4 (d-spacings of 4.9 (18.0 °2θ), 3.9 (22.3 °2θ), 3.8 (23.1 °2θ), 3.4 (26.0 °2θ), 2.9 (31.0 °2θ), 2.8 (31.9 °2θ), 2.7 (32.8 °2θ), and 2.6 Å (33.7 °2θ) were readily evident. In the final freeze-dried cakes, the anhydrous Na_2HPO_4 is generated during the drying step from dehydration of the dodecahydrate formed during freezing step.[134,138] In addition to the buffer peaks, several additional peaks were observed (11.6, 12.6, 13.7, 15.3, 19.5, 22.0, 24.6 and 26.6 °2θ) all of which could not be assigned to a single physical form of anhydrous indomethacin. At 10 mM buffer concentration, in addition to Na_2HPO_4 peaks, several new peaks (for e.g. lines with d-spacings of 12.0 (7.3 °2θ), 10.2 (8.6 °2θ), 7.6 (11.6 °2θ), 6.9 (12.7 °2θ), 6.0 (14.6 °2θ) and 4.8 Å (18.6 °2θ) were also observed in the powder pattern of the lyophile (Figure 3.5, panel C). The IR spectroscopy results indicate that disproportionation does not occur at this low buffer concentration (Figure 3.3B). These peak positions did not match with that of IMCNa trihydrate reported in the literature.[139] Based on the powder diffraction files, the peaks could also not be attributed to any of the polymorphs of the IMC free acid. Interestingly the XRD pattern matches with that reported by Tong and Zografi.[139] They had prepared

amorphous IMCNa by lyophilization and stored it at 56% RH (30 °C). After 24 hours of storage, numerous new peaks were observed. Our XRD pattern is in good agreement with this new form. Tong and Zografi have speculated that this phase is either an "intermediate structure" or a metastable polymorphic trihydrate which eventually transformed to the stable trihydrate.[139] In light of the poor crystallinity of this phase, its in-depth X-ray characterization was challenging. However, from the perspective of this investigation, it is evident that, at low buffer concentration, disproportionation does not occur.

Thus, a higher buffer concentration was detrimental to the formulation stability. One possible explanation is that the pH shifts on cooling the solutions become more pronounced as the initial buffer concentration is increased. This has been observed in phosphate buffer [112] as well as in succinate buffer systems.[140] In an effort to understand the role of buffer and IMCNa concentrations on the observed disproportionation, the prelyophilization solutions were characterized.

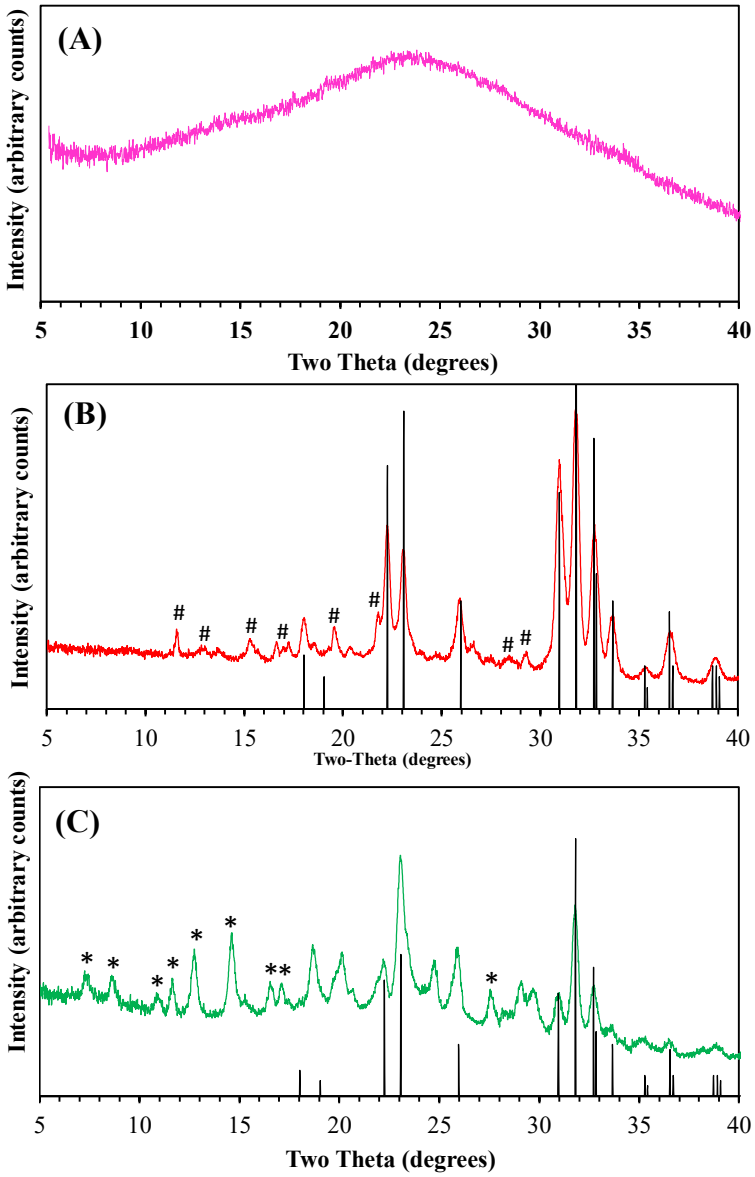

Figure 5. Powder XRD patterns of IMCNa (10 mg/ml) lyophiles prepared from (A) DI water, (B) (i) 100 mM buffer and (C) 10 mM buffer. The stick pattern of anhydrous Na_2HPO_4 is provided in both panels B and C. The unidentified peaks (panel B and C) are pointed out (#, *). While the XRD patterns were obtained using Co Kα radiation (1.79 Å), they were converted to Cu Kα radiation (1.54 Å), so as to enable direct comparison with published data.

3.4.2 Characterization of Frozen Systems

Low temperature pH measurements

In an effort to correlate the observed disproportionation (data presented in Table 3.1) with pH shifts during freezing, buffered (100, 35 & 10 mM) IMCNa trihydrate (10 mg/ml) solutions were subjected to low temperature pH measurements. The NaP buffers (100, 35 & 10 mM) served as controls. Additionally, since IMCNa exerted a concentration dependent effect on disproportionation, pH measurements during cooling were performed at all three IMCNa concentrations (5, 10 and 15 mg/ml) keeping the buffer concentration constant at 35 mM. The results are summarized in Table 3.2.

The pH of the NaP solution (100 mM), when cooled at a controlled rate, is provided in Figure 3.6 (panel A). The sample temperature progressively decreased until the release of the latent heat of ice crystallization resulted in a small but sharp increase in sample temperature to ~ 0 °C. Following equilibration at 0 °C for 10 minutes, as the cooling was continued, a drop in sample temperature to -25 °C was readily evident. The decrease in temperature was accompanied by a sharp drop in the pH of the freeze-concentrate to ~ 3.0, attributed to the selective crystallization of disodium hydrogen phosphate dodecahydrate ($Na_2HPO_4 \cdot 12H_2O$). This was confirmed by the XRD of the frozen solution (Figure 3.13; Supplementary Information). The presence of IMCNa (10 mg/ml) did not seem to influence the crystallization behavior of the buffer (Figure 3.6, panel B). The pH shift in the presence and absence of IMCNa was about the same.

At a lower initial buffer concentration (10 mM), the observed pH shift was ~ 3.7. Thus, the observed pH shift was not affected in a pronounced manner by the initial buffer concentration. However, the presence of IMCNa (10 mg/ml), had a pronounced attenuating effect on the pH shift. When cooled to –25 °C, there was a small increase in pH of ~ 0.2 units.

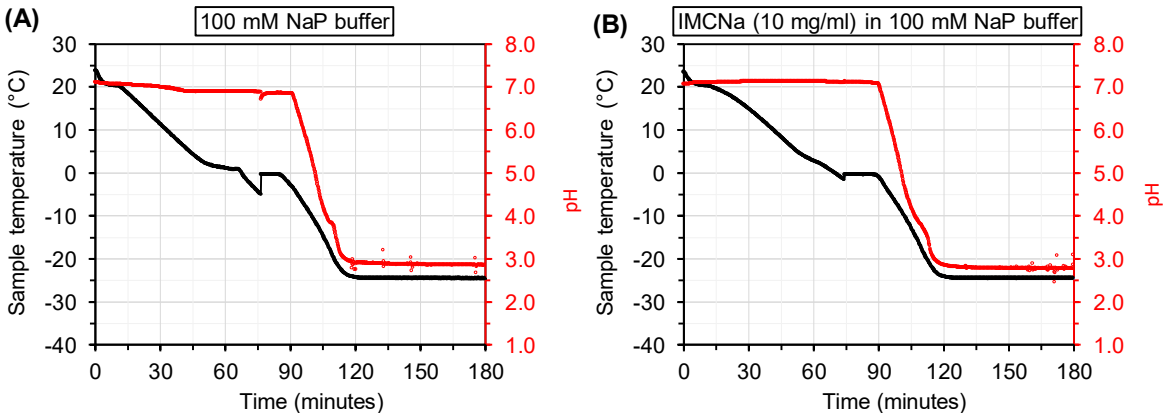

Figure 3.5. pH (right y-axis) and temperature (left y-axis) changes during freezing of 100 mM NaP buffer solutions (initial pH of 7.0 at 20 °C): (A) only buffer, and (B) with IMCNa (10 mg/ml or 23 mM). The solutions were cooled at 0.5 °C/min and held at –25 °C for 2 hours.

The pH shifts observed in 10 & 100 mM buffer solutions can explain the disproportionation evident in the lyophiles (FT-IR data; Table 3.1). The drastic pH shift in 100 mM buffer systems, triggered by selective buffer salt crystallization, lowered the pH below pH_{max} of the IMCNa salt, resulting in disproportionation of IMCNa. On the other hand, in the 10 mM buffer system, since there was a negligible pH shift in presence of IMCNa, there was no disproportionation. At the lower buffer concentration, the presence of IMCNa may have inhibited buffer crystallization and the consequent pH shift. If IMCNa is capable of inhibiting buffer crystallization, this effect is expected to be concentration dependent.

Table 3.2. Change in pH of NaP buffer solutions when cooled from 20 °C to -25 °C. The effect of IMCNa concentration on the pH shift was investigated at a buffer concentration of 35 mM.

NaP concentration, mM	IMCNa · $3H_2O$ concentration, mg/ml (mM)	pH at 20 °C[a]	pH at -25 °C[b]	ΔpH[c]
100	-	7.1	2.9	4.2
100	10.0 (23.0)	7.1	2.8	4.3
35	-	7.2	3.1	4.1
35	15.0 (34.6)	7.2	6.7	0.5
35	10.0 (23.0)	7.2	5.2	2.0
35	5.0 (11.5)	7.1	5.6	1.5
10	-	7.2	3.5	3.7
10	10.0 (23.0)	7.2	7.4	-0.2

[a]Initial pH
[b]pH after the buffer solution was cooled to -25 °C and held for 2 hours
[c]ΔpH= (pH at 20 °C) – (pH at -25 °C)

The influence of the buffer to IMCNa concentration ratio on the salt disproportionation behavior is clearly evident from Table 3.1. When the molar concentration ratio was > 1, disproportionation of IMCNa was observed in the final lyophiles. Whereas, when the ratio was ≤ 1, no disproportionation was observed. The concentration effect is readily evident at 35 and 20 mM buffer concentrations. To investigate this further, the pH shifts upon freezing different concentrations of IMCNa, were determined at a fixed buffer concentration of 35 mM (Figure 3.7). In the absence of IMCNa, the pH shift in 35 mM buffer was 4 units. At IMCNa concentration of 34.6 mM, the pH shift was ~ 0.4 units while much higher shift of ~ 2 units was observed at 23.0 mM and 11.5 mM. The salt disproportionation observed in the final lyophiles (Table 3.1) correlated with the observed pH shifts. Disproportionation was observed only at IMCNa concentration of 23.0 and 11.5 mM. The observation can be explained by the buffer crystallization lowering the pH below

the pH_{max} of IMCNa, causing salt → acid conversion. A comprehensive understanding of the system would be possible if the pH_{max} value of IMCNa was known. Unfortunately, the pH_{max} value has not been reported. Based on the information in the Handbook on Injectable Drugs, the pH_{max} for IMCNa is ~6. Therefore, at pH values < 6, precipitation of the free IMC acid can occur. [141]

When the molar concentration ratio of buffer to IMCNa is ≤ 1, IMCNa can inhibit selective crystallization of $Na_2HPO_4 \cdot 12H_2O$ and thereby cause a negligible effect on pH and thus prevent disproportionation. To investigate the effect of IMCNa on buffer crystallization, XRD and DSC analyses of frozen solutions was performed and the results are discussed in the next section.

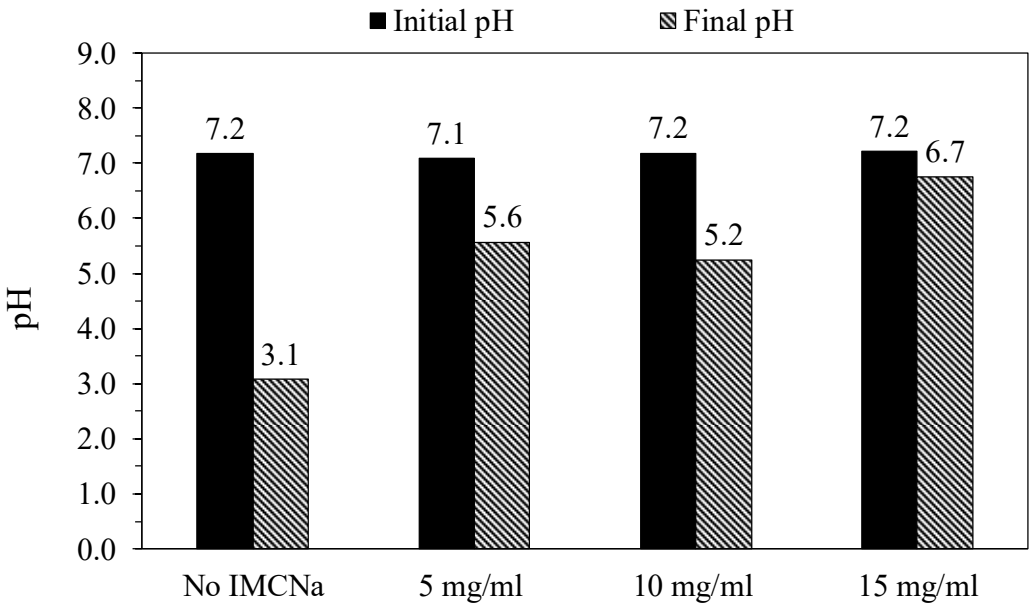

Figure 3.6. The initial and final (after 2 hours at -25 °C) pH of 35 mM NaP buffer solutions containing different concentrations of IMCNa.

X-Ray Diffractometry (XRD) of Frozen Solutions

When the buffer solution (35 mM) was cooled to -50 °C, crystallization of hexagonal ice was evident from the peaks at 22.7 (3.9 Å), 24.4 (3.6 Å), 25.8 (3.5 Å), and 33.5 (2.7 Å) °2θ (Figure 3.8). The disodium hydrogen phosphate crystallized as the dodecahydrate ($Na_2HPO_4 \cdot 12H_2O$) with a characteristic peak at 16.1 (5.4 Å) °2θ. Using synchrotron radiation, we had earlier observed crystallization of this phase, even from a 1 mM buffer solution.[138] Addition of IMCNa caused a pronounced decrease in the intensity of the buffer salt peak, indicating inhibition of buffer crystallization (Figure 3.8). However, the inhibitory effect of IMCNa concentration could not be quantified due to the limited sensitivity of the XRD method. The phase behavior of indomethacin will be discussed later (after the discussion of DSC results).

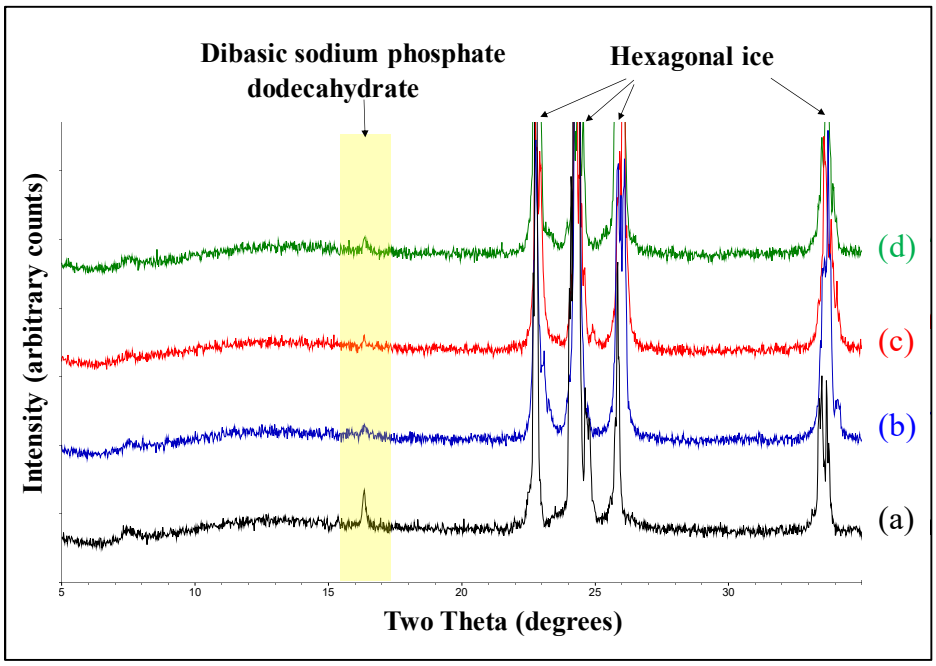

Figure 3.7. Overlay of XRD patterns of frozen aqueous NaP buffer (35 mM) containing IMCNa at concentrations of (a) 0 mg/ml (35 mM buffer only), (b) 15 mg/ml, (c) 10 mg/ml and (d) 5 mg/ml. The solutions were cooled from RT (initial pH of 7.0) to -50 °C, at 0.5 °C/min, held for 60 min and the XRD patterns were obtained. The angular range of the buffer salt peak is highlighted and the characteristic peaks for ice and $Na_2HPO_4 \cdot 12H_2O$ are pointed out.

Differential Scanning Calorimetry (DSC) of Frozen Solutions

The DSC heating curves of the frozen prelyophilization solutions of IMCNa (10 mg/ml) in 10 & 100 mM buffer, are overlaid in Figure 3.9. The buffer solutions (10 and 100 mM; no IMCNa) and aqueous IMCNa solution (10 mg/ml) served as controls. As pointed out in Table 3.1, no disproportionation was observed at the lower buffer concentration, while the free acid formation was complete when the buffer concentration was 100 mM. In the absence of buffer as well as at a low buffer concentration (10 mM), during the reheating (at 1 °C/min), an exotherm was observed at ~ −15.6 °C which could be attributed to crystallization of IMCNa and the associated unfrozen water (Figure 3.9). Thus this exotherm in the DSC is an evidence of the retention of the salt (i.e. no disproportionation) in the freeze concentrate.

In the DSC heating curve, crystallization of IMCNa should be preceded by the glass transition of the freeze-concentrate (Tg′). However, a discernible Tg′ was not observed (Figure 3.9). In an effort to detect Tg′, we increased the solute concentration (15 mg/mL) as well as the heating rate (10 °C /min).[142] Now, a Tg′ was observed at -18.2 °C, followed by an exotherm at -11.4 °C (Figure 3.10). At a higher IMCNa concentration of 50 mg/ml (115.2 mM) in water, interestingly, the Tg′ was unaffected, revealing it to be independent of the solute concentration (Figure 3.14; Supplementary Information). Thus, irrespective of the initial solute concentration, amorphous freeze-concentrate of constant composition was obtained for solutions of IMCNa in water.

Kumar et al. observed a Tg′ at -35 °C, followed by an exotherm at ~ -23 °C.[143] The IMCNa concentration was 140 mM and the cooling rate was 17 °C/min. Since we cooled the solution at a slower rate of 1 °C/min, ice crystallization could have been much more

complete resulting in a freeze-concentrate with a higher solute concentration. We believe that at the slower heating rate (Figure 3.9), there could be a pronounced overlap of the Tg′ and the crystallization events and as a result, the former event is not readily discernible. Interestingly, there was no evidence of IMCNa crystallization when the buffer concentration was increased to 100 mM (Figure 3.9). This is in line with the FT-IR results for IMCNa lyophiles prepared with 100 mM buffer, wherein IMCNa had disproportionated to the free acid. Thus the absence of the crystallization exotherm, appears to be an indirect evidence of salt disproportionation.

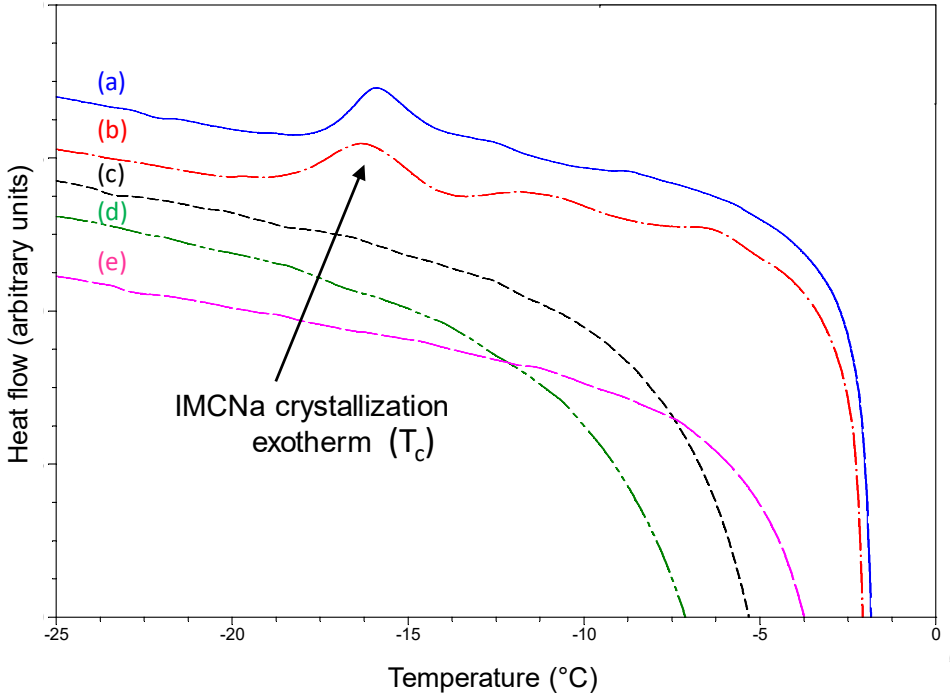

Figure 3.8. Overlay of DSC heating curves of frozen aqueous IMCNa solutions in (a) water, (b) 10 mM, and (c) 100 mM NaP buffer. The concentration of IMCNa in the solutions was 10 mg/ml (23 mM). Curves (d) and (e) are for 10 and 100 mM NaP buffer in the absence of IMCNa. The solutions were initially cooled from RT to −50 °C at 1 °C/min, held for 30 minutes, and heated to 20 °C at 1 °C/min. Only the heating curves are shown. Crystallization exotherm (T_c) attributed to the presence of IMCNa is pointed out. Additional weak exotherms were observed in some systems (a,b). One possible explanation is the crystallization of IMCNa in two stages. A similar thermal behavior was observed in IMC potassium salt.[143]

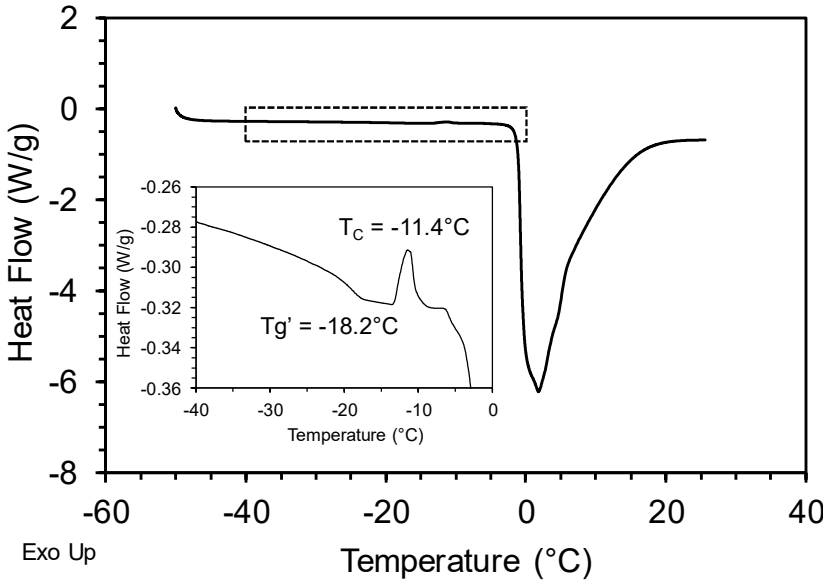

Figure 3.9. DSC heating curve of frozen aqueous IMCNa solution (34.6 mM; unbuffered). The solution was initially cooled from RT to −50 °C at 1 °C/min, held for 30 min, and heated to 30 °C at 10 °C/min. A select region has been expanded to enable the visualization of the glass transition of the freeze-concentrate (Tg′) and crystallization exotherm (T_c). The midpoint of Tg′ is reported. Only the heating curve is shown.

The results confirm that IMCNa disproportionation is dependent on the concentrations of both NaP buffer and IMCNa (results based on FT-IR are presented in Table 3.2). We hypothesize that the selective crystallization of Na_2HPO_4 (as the dodecahydrate) during freezing causes a shift in the pH. If this shift results in pH < pH_{max}, disproportionation can occur. Our results indicate that the IMCNa concentration influences the crystallization behavior of the buffer during freezing. When the molar concentration ratio of IMCNa to buffer is ≥ 1, IMCNa can substantially inhibit buffer crystallization. *IMCNa, by remaining amorphous, appears to inhibit buffer salt crystallization.* The increase in viscosity of the system upon cooling, can inhibit crystal growth, and the effect can become pronounced as the temperature approaches Tg′.[144,145] Cosolutes have been shown to influence buffer crystallization in sodium phosphate and succinate buffer systems. The initial concentration

of the cosolute as well as its physical form (amorphous or crystalline) in the freeze concentrate influences buffer crystallization. Pikal-Cleland et al. demonstrated that glycine, at low concentrations (≤ 50 mM), effectively prevented pH change when 10 and 100 mM NaP buffer were frozen.[146] However, when the initial glycine concentration was ≥100 mM, buffer salt crystallization was facilitated. Subsequently, Varshney et al. developed an XRD method, using synchrotron radiation, to monitor NaP buffer crystallization in presence of glycine.[138] When a solution with a 1:3 molar ratio of glycine to NaP buffer was freeze-dried, buffer component crystallization was completely inhibited in frozen systems. On the other hand, at higher molar ratios of glycine to buffer (3:1), there was pronounced glycine crystallization. Gomez et al. observed that addition of sucrose or mannitol to NaP buffer (>3:1 molar ratio of additive to buffer) decreased the crystallization-induced pH changes to 0.5 units.[134] In case of succinate buffer systems, Sundaramurthi et al. studied the effect of crystallizing (glycine, mannitol, trehalose) and non-crystallizing (sucrose) solutes on buffer crystallization and consequent pH shift.[140] They concluded that sucrose and trehalose, when retained amorphous, inhibited succinate buffer component crystallization and the consequent pH shift. However, upon crystallization of trehalose or degradation of sucrose to yield a crystalline decomposition product, buffer crystallization was observed. These studies highlight that the crystallization behavior of buffer components during freezing can be modulated by the addition of cosolutes.

However, from our results it is obvious that much like the cosolutes, the physical form of API in the frozen system, can influence the phase behavior of buffer salt. In case of IMCNa/NaP system, presence of common ion, Na^+, can influence the crystallization of

Na_2HPO_4. If the crystallization of Na_2HPO_4 is diffusion controlled, by the addition of excess IMCNa (containing the common ion Na^+), the growth rate of Na_2HPO_4 crystals will be governed by the diffusion of the uncommon ion, HPO_4^{2-}.[134] The net effect will be a decrease in the growth rate of Na_2HPO_4, i.e. inhibition of buffer salt crystallization. A similar mechanism was proposed in case of Na_2HPO_4, wherein the addition of NaCl led to an increase in molar ratio of Na^+/ HPO_4^{2-}, thereby decreasing the overall crystal growth rate.[134] There is also the possibility of the adsorption of the bulky IMC anion on the surface of growing crystals of Na_2HPO_4 thereby inhibiting its growth.

3.5 Significance

Phosphate buffers are widely used in lyophilized protein formulations.[147] It is well known in the freeze-drying community that selective crystallization of a buffer component (in this case, disodium hydrogen phosphate dodecahydrate) during freezing has the potential to significantly alter the freeze-concentrate pH and thereby influence the API stability.[116–118] In this investigation, we have documented the disproportionation of a soluble salt (indomethacin sodium) to an insoluble free acid as a consequence of buffer crystallization during freeze-drying. Such a disproportionation reaction will prolong the reconstitution time, and in extreme cases, result in incomplete dissolution of the lyophile.

The concentration of the API (IMCNa) influenced the crystallization behavior of the buffer and thereby the salt → acid conversion. In other words, a complex interplay of the API and excipient concentrations dictated the API stability. When the molar concentration ratio of buffer to IMCNa ≤ 1, buffer crystallization was inhibited and the API was retained in the desired state (i.e. as the salt). Therefore, decrease in the API content (the dose), at a fixed buffer concentration, can have a bearing on product performance. For example, at a

NaP concentration of 35 mM and at a IMCNa concentration of 34.6 mM, there was no disproportionation. Decreasing the IMCNa concentration to 23.0 mM or 11.5 mM, resulted in disproportionation. In systems exhibiting such complexity, a robust formulation can only be developed by understanding the influence of the concentrations of all the formulation components on buffer crystallization propensity. These issues warrant consideration during the early stages of formulation development.

Finally, conventional solution-based analytical techniques including chromatography, will not reveal disproportionation. It is meaningful to study disproportionation reactions directly in the solid dosage form (i.e., in the presence of the formulation excipients), using solid-state techniques.

3.6 Conclusions

The pH shift brought about by the selective crystallization of a buffer component (disodium phosphate dodecahydrate) during cooling resulted in disproportionation of indomethacin sodium. The buffer to indomethacin sodium concentration ratio was a determinant of the buffer crystallization propensity. Low temperature pH measurement was an effective tool to identify salt disproportionation during freeze-drying.

3.7 Supplementary Information

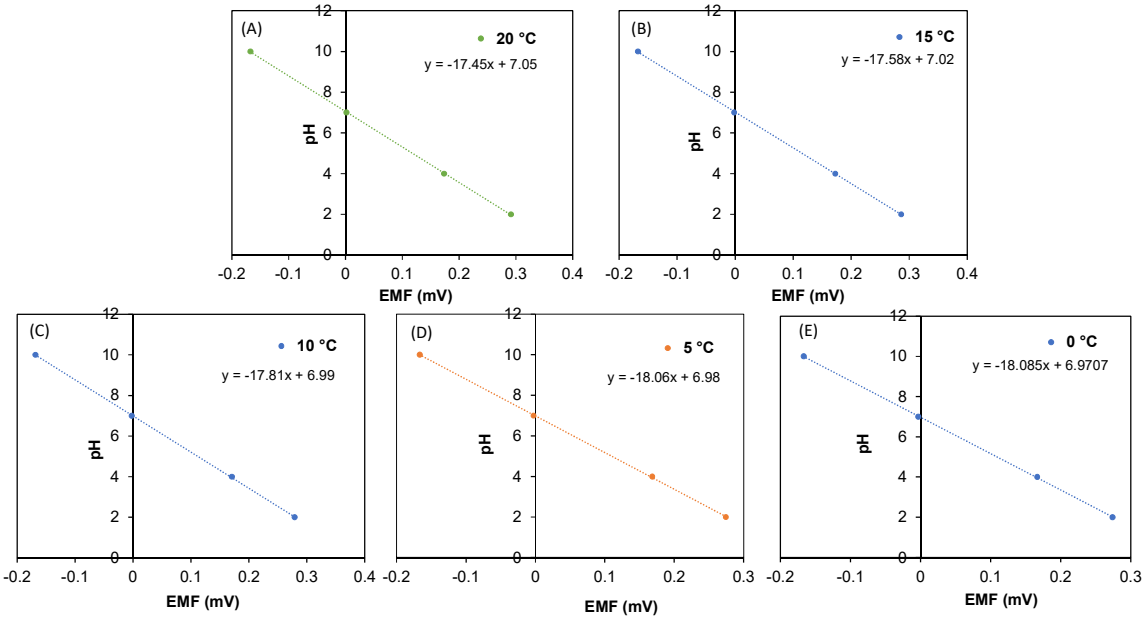

Figure 3.10. Electrode calibration- EMF vs pH plots for standard buffer solutions (pH 2.0, 4.0, 7.0 and 10.0) at (A) 20 °C, (B) 15 °C, (C) 10 °C, (D) 5 °C, and (E) 0 °C.

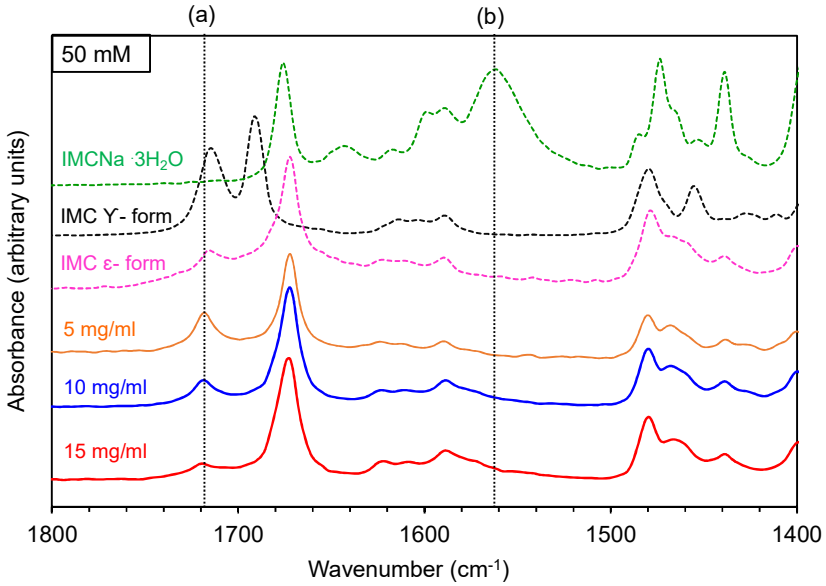

Figure 3.11. Overlay of FT-IR spectra of IMCNa lyophiles (solid lines) prepared using 50 mM NaP buffer. The 'reference' spectra of IMCNa trihydrate, amorphous IMCNa, IMC γ- and ε- forms (dashed lines) are also provided. Vertical broken lines: (a) carboxylic acid carbonyl (C=O) vibration (observed in the IMC acid), (b) asymmetric stretch due to carboxylate anion (COO^-) observed in IMCNa trihydrate salt.

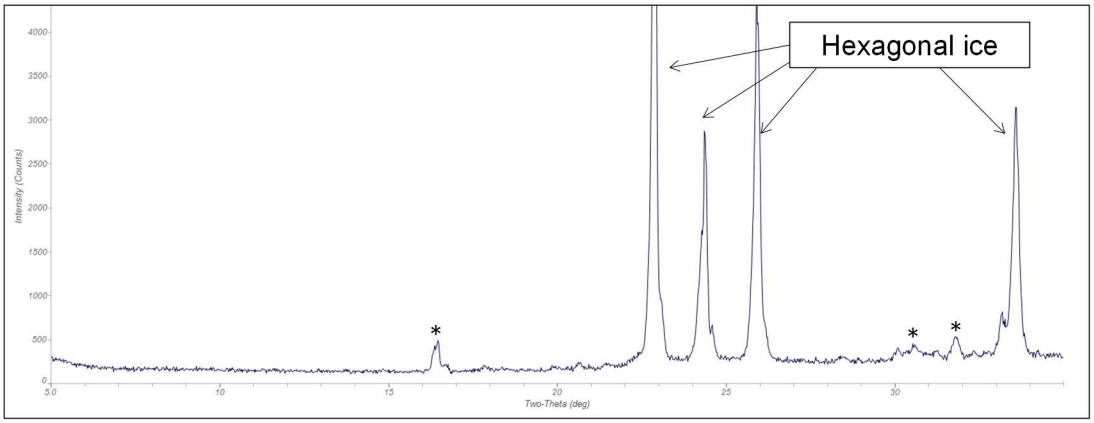

Figure 3.12. XRD pattern of frozen aqueous NaP buffer (100 mM). The solution was cooled from RT (initial pH of 7.0) to -50 °C, at 0.5 °C/min, held for 60 min and the XRD pattern was obtained. The characteristic peaks for ice and $Na_2HPO_4 \cdot 12H_2O$ (*) are pointed out.

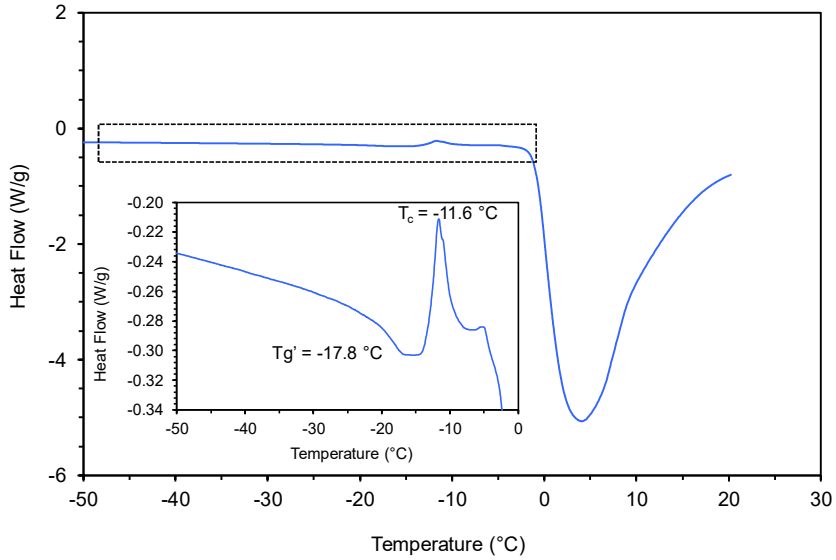

Figure 3.13. DSC heating curve of frozen aqueous IMCNa solution (115.2 mM). The solution was initially cooled from RT to −50 °C at 1 °C/min, held for 30 min, and heated to 25 °C at 10 °C/min. A select region has been expanded to enable the visualization of the glass transition of the freeze-concentrate (Tg′) and crystallization exotherm (T_c). The midpoint of Tg′ is reported. Only the heating curve is shown.

Chapter 4 : Challenges in Transitioning Cocrystals from Bench to Bedside: Dissociation in Prototype Drug Product Environment

4.1 Synopsis

Tablets containing theophylline-glutaric acid (TG) cocrystal dissociated rapidly forming crystalline theophylline (20 – 30%), following storage at 40 °C/75% RH for 2 weeks. Control tablets of TG containing no excipients were stable under the same conditions. The dissociation reaction was water mediated and the theophylline concentration (the dissociation product), monitored by synchrotron X-ray diffractometry, was strongly influenced by the formulation composition. Investigation of binary compacts of TG cocrystal with each excipient revealed the influence of excipient properties (hydrophilicity, ionizability) on cocrystal stability providing mechanistic insights into dissociation reaction. Ionizable excipients with a strong tendency to sorb water, for example sodium starch glycolate and croscarmellose sodium, caused pronounced dissociation. MCC, while a neutral but hydrophilic excipient, also enabled solution mediated cocrystal dissociation in intact tablets. Magnesium stearate, an ionizable but hydrophobic excipient, interacted with the cocrystal to form a hygroscopic product. The interaction is believed to be initiated in the disordered cocrystal-excipient particle interface. In contrast, the cocrystal was stable in the presence of lactose, a neutral excipient with no tendency to sorb water. The risk of unintended cocrystal dissociation can be mitigated by avoiding contact with water both during processing and storage.

4.2 Introduction

In recent years, the design and development of cocrystals has gained significant interest in the pharmaceutical industry primarily as an approach to modify the physicochemical

properties of the active pharmaceutical ingredients (API). A pharmaceutical cocrystal is a multicomponent crystal, containing the API and coformer held together by nonionic/noncovalent interactions.[148] Cocrystallization strategy is useful when the API does not contain readily ionizable functional groups and salts are not a viable option. Pharmaceutical cocrystals provide a unique avenue to customize the physicochemical properties of the API. Cocrystal formation has been shown to exhibit improved solubility and dissolution behavior and enhanced physical stability of the API. Cocrystals of fluoxetine hydrochloride salt (active ingredient in Prozac®), with succinic acid, exhibited an approximately two-fold increase in aqueous solubility compared to fluoxetine HCl.[50] Cocrystals of the antifungal drug, itraconazole, with succinic, malic and tartaric acid exhibited a 4 to 20 fold solubility increase compared to crystalline itraconazole.[49] Cocrystallization of the anti-epileptic drug carbamazepine with saccharin significantly improved the physical stability relative to the anhydrous polymorph (form III).[149] In addition, administration of the cocrystal in dogs resulted in higher C_{max} and comparable T_{max} when compared with the marketed product (Tegretol®), a formulation of the anhydrous form III.[149] Apart from offering potential improvements in solubility, dissolution rate, bioavailability and physical stability, pharmaceutical cocrystals can modulate other essential properties of the APIs such as flowability, chemical stability, compressibility and hygroscopicity.[150]

A potential risk in the use of a pharmaceutical cocrystal is its propensity to undergo unintended dissociation, resulting in reversion to the corresponding free API and coformer. This can negate the solubility, stability and bioavailability advantages conferred by cocrystal formation. In contact with water (solution/slurry), many cocrystal systems have

been observed to dissociate.[50,70–73] Although cocrystals in general are stable in the solid-state, storage at high relative humidity (RH) and under elevated temperature has been implicated in cocrystal disproportionation.[78,81] The dicarboxylic acid (maleic, malonic, glutaric) cocrystals of caffeine and theophylline were reported to undergo dissociation within 7 days when stored at 98% RH (RT), resulting in the crystallization of the acid coformer and caffeine/theophylline hydrate.[58,59] Eddleston et al. reported that the rate and extent of caffeine-glutaric acid cocrystal dissociation increased as a function of RH (RT).[78] In these cocrystal systems, the dissociation susceptibility was attributed to the large aqueous solubility difference between the drug and coformer and the propensity of the drug to form hydrates at high RH. Caffeine-theophylline cocrystal disproportionated upon heating to a temperature below the melting points of caffeine and theophylline and was explained by entropically favorable conformation of caffeine as the driving force for cocrystal dissociation.[80] The combined effects of temperature and water vapor pressure were investigated in pyrazine−phthalic acid cocrystal.[81] An elevation in temperature or water vapor pressure accelerated cocrystal dissociation. The dissociation mechanism was postulated to be dissolution of the cocrystal in sorbed water followed by crystallization of the individual components.

To develop a robust solid dosage form of a cocrystal API, a comprehensive understanding of its physical stability in the formulation environment is essential. In order to realize the solubility enhancement and other advantages of a cocrystal, it must remain unchanged both during the manufacturing and storage of the product prior to patient use. While dissociation of salts has been extensively studied[27,28,31–33,35,68,69], very little information is available

about the influence of formulation and processing on cocrystal stability. This is not surprising since only a few pharmaceutical cocrystals are available as marketed products.

Dissociation of caffeine-oxalic acid cocrystal to form caffeine hydrate was observed in binary mixtures of the cocrystal with ionizable excipients (1:1 w/w ratio) stored at 75% RH (RT).[82] Similar to salt dissociation[23,35,68,69], the mechanism of cocrystal dissociation was proposed to be water mediated and involved proton transfer between coformer and carboxylate group of excipients. While such binary mixtures, containing equal amounts of both the cocrystal and excipient, are aimed at providing a rapid method for excipient screening, the excipient concentration may be unrealistically high. For example, the use of 50% w/w magnesium stearate in binary drug-excipient mixture does not reflect a realistic formulation composition. While these binary drug-excipient mixtures provide insight into the effect of each excipient, the complex interplay of the role of several excipients in a multicomponent dosage form will not be evident. We advocate the use of "prototype" formulations since there is limited information on excipient induced cocrystal dissociation in tablets.[151] This will provide formulation scientists a comparative data set of excipient mixtures, across different functional classes, typically used in tablet manufacture. Six common excipients (shown in Table 4.1) were chosen: three diluents/fillers (lactose, microcrystalline cellulose, dibasic calcium phosphate anhydrate), two disintegrants (croscarmellose sodium, sodium starch glycollate) and one lubricant (magnesium stearate). We have investigated the ability of these excipients to induce dissociation in prototype tablet formulations of theophylline-glutaric acid cocrystal (TG; 1:1 stoichiometry of drug to coformer). Additionally, binary mixtures of TG cocrystal with each excipient were also investigated. Since cocrystal dissociation is considered to be a solution-mediated

transformation, storage of tablets at 40 °C/75% RH provides an avenue to understand dissociation reaction mediated by water.

Our overall goal was to develop a mechanistic understanding of the physical stability of TG cocrystal in a drug product environment. The specific objectives were to (i) develop an analytical technique to monitor cocrystal dissociation in intact tablets and (ii) understand the mechanism of cocrystal dissociation in a complex multicomponent matrix. The ideal analytical technique should detect low levels of analyte in a complex matrix and also simultaneously quantify the reactant and product phases. The selection of the appropriate technique will hinge on the physical form of the analyte(s). Powder X-ray diffractometry (XRD) and spectroscopic techniques (IR, Raman, solid-state NMR) have been used for phase quantification in solid dosage forms (tablets).[35,68,89,96,152] The interference in the analyte signal, because of the multiple matrix components, often limits the use of spectroscopic methods. This can be overcome to a limited extent by combining spectroscopy with chemometric modeling.[89] XRD is a highly selective and sensitive technique, provided the analytes are crystalline. Our preliminary studies revealed rapid TG cocrystal dissociation in tablets resulting in the formation of crystalline theophylline (TH; anhydrous form). Since both the reactant (TG cocrystal) and product (TH) phases were crystalline, XRD was chosen as the analytical technique. Additionally, the use of two dimensional (2D) XRD using synchrotron radiation, enabled rapid data collection and enhanced the signal intensity. Moreover, the reduction in errors due to preferred orientation make this technique particularly well suited for quantitative analyses.

4.3 Experimental

4.3.1 Materials

Theophylline anhydrate (TH) and glutaric acid (GA), (> 99% pure; Figure 4.1), were obtained from Sigma–Aldrich. The powder X-ray diffraction patterns (XRD) of TH and GA agreed with their respective simulated patterns from the crystal structures of theophylline anhydrate (CSD reference code BAPLOT01)[153] and glutaric acid (β-polymorph; CSD ref code: GLURAC13).[154] The chemical structures are shown in Figure 4.1.

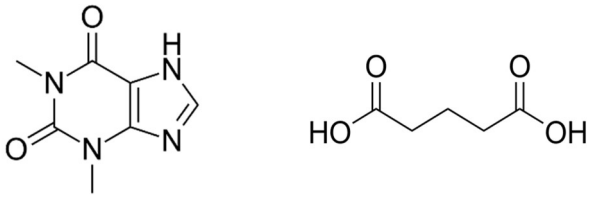

Theophylline Glutaric acid

Figure 4.1. Chemical structure of anhydrous theophylline and glutaric acid.

Microcrystalline cellulose (MCC; Avicel PH 101; NF grade), lactose monohydrate (LM; FastFlo 316, Foremost Farms; NF grade), dibasic calcium phosphate, anhydrous (DCPA; A-TAB from Rhodia Pharma Solutions; USP grade), magnesium stearate (MgSt; Vegetable source, Mallinckrodt Laboratory Chemicals; NF grade), sodium starch glycolate NF (SSG; Explotab, Edward Mendell; NF grade), and croscarmellose sodium (CCS; Ac-di-sol, FMC BioPolymer) were used as received.

4.3.2 Preparation of Theophylline - Glutaric acid (1:1; TG) Cocrystal

TG cocrystal was prepared in bulk by the isothermal slurry conversion crystallization method using chloroform as solvent.[155] In a 250 mL glass bottle, theophylline (9.0 g) and β-glutaric acid (6.6 g) were added into 100 mL chloroform. This slurry was maintained at

30 °C and stirred continuously for 24 hours. The solid was separated by vacuum filtration, dried, and characterized by powder XRD. The powder XRD showed a better match with the simulated pattern (CSD reference code XEJXIU)[58] at low 2θ values than at high 2θ values because of temperature difference for data collection of powder XRD (298 K) and simulated patterns (180 K). Therefore, single crystal data was collected at room temperature and was found to be in excellent agreement with that of the powder XRD pattern.

4.3.3 Tablet Preparation

Cocrystal tablets for stability study. Four tablet formulations, having compositions listed in Table 4.1 and with a drug (TH) load of 15% w/w, were prepared. Cocrystal and excipient powders were weighed, geometrically mixed and 222 mg of each composition was filled into a circular tablet die. It was compressed to 177 MPa in a hydraulic press (Carver model C laboratory press, Menomonee Falls, WI) using flat faced punches. The tablets, 8 mm diameter and 3 mm thick (n = 3), were stored in stability chambers maintained at 40 °C/75% RH. Cocrystal dissociation in the intact tablets was monitored at select time points using both laboratory and synchrotron source XRD.

Table 4.1 Composition of TG cocrystal tablets.

Tablet Formulations[a]	Excipients – 85% w/w					
	MCC (mg)	LM (mg)	DCPA (mg)	SSG (mg)	CCS (mg)	MgSt (mg)
F1	108	54	-	6	-	2
F2	108	-	54	6	-	2
F3	108	-	54	-	6	2
F4	108	54	-	-	6	2

[a]Each tablet weighed 222 mg and contained 52 mg of TG.
Placebo tablet formulations were prepared without the addition of TG.

Preparation of Tablets for Generating Standard Curves - Quantification of Cocrystal Dissociation. For each formulation, tablets containing known concentrations of TG cocrystal, coformers (TH and GA) and excipients were prepared (five compositions; n = 3 for each composition). In each formulation, the excipients cumulatively constituted 85% w/w of the dosage form. The concentrations of the cocrystal and its coformers were adjusted to account for 0 - 30% dissociation. The unique peak of TH at 12.7 °2θ was used for quantification (Figure 4.2). It was necessary to establish the relationship between the integrated peak intensity and the analyte (theophylline) concentration. Such a "standard curve" was generated for each of the four formulation compositions (Table 4.1). The integrated intensity of the 12.7° 2θ peak of TH was plotted as a function of its concentration (Figure 4.10; Supplementary Information). There was a linear relationship between peak intensity and concentration (Figure 4.10; Supplementary Information).

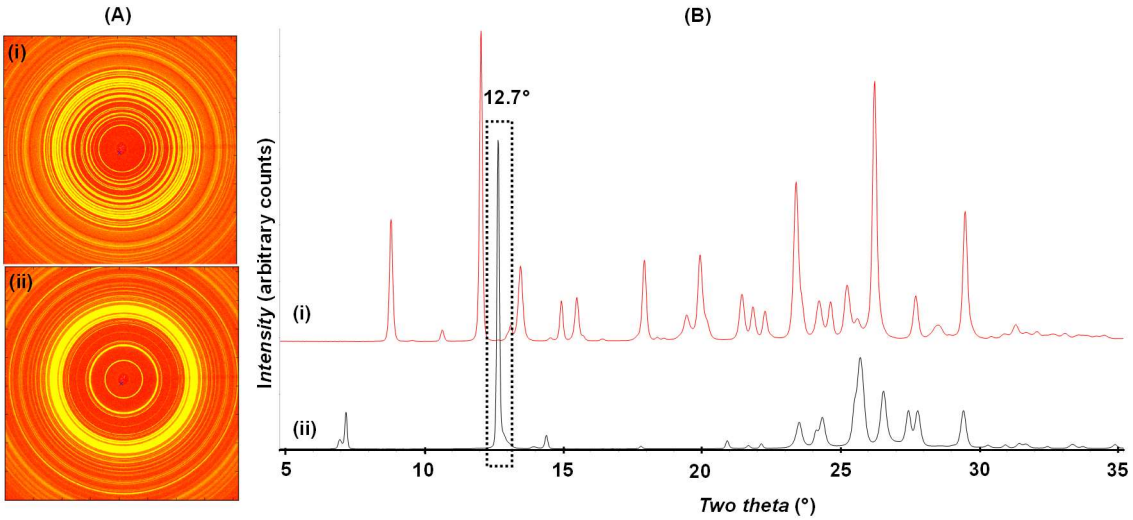

Figure 4.2. (A) Two-dimensional XRD patterns of (i) TG cocrystal and (ii) TH obtained using synchrotron radiation (λ = 0.45212 Å). To facilitate visualization and to enable comparison with the reported patterns, (B) shows the corresponding one-dimensional XRD patterns, presented as intensity versus 2θ plots (calculated for Cu Kα radiation, λ = 1.54 Å) of (i) TG cocrystal and (ii) TH. The "unique" peak of TH, at 12.7° 2θ, is pointed out with the dotted rectangle in (B).

4.3.4 Synchrotron X-ray Diffractometry (SXRD)

Experiments were performed in transmission mode in the 17-BM-B beamline at Argonne National Laboratory (Argonne, IL, U.S.A.). A monochromatic circular X-ray beam (wavelength 0.45212 Å; beam diameter 300 μm) and a two-dimensional (2D) area detector (XRD-1621, PerkinElmer) were used. A triple-bounce channel-cut Si single crystal monochromator with [111] faces polished was used, which limited the line broadening to its theoretical low limit (i.e., the Darwin width). The sample to detector distance was set at 900 mm. Calibration was performed using Al_2O_3 standard (SRM 674a, NIST). Intact tablets were loaded vertically on a custom-built sample holder mounted on a motorized sample stage that enabled multiple sample analyses. The tablets were positioned in the path of the synchrotron X-ray beam and, using a stepper motor, the sample was oscillated (±1

mm from the center along the horizontal axis) during data collection. Every sample was scanned 10 times, with an exposure time of 1 s for each scan, and the results were averaged. The 2D diffraction rings were integrated to yield corresponding one-dimensional d-spacing (Å) or 2θ (°) scans using the GSAS II software developed by Toby and Von Dreele.[95] Commercially available software (JADE 2010, Materials Data, Livermore, CA) was used for determining the integrated peak intensities.

4.3.5 Water Sorption Analysis

Powder blends, both placebo and with TG cocrystal (compositions in Table 4.1), were dried at 40 °C/ 0% RH for 6 hours in an automated vapor sorption system (Q500SATA Instruments, New Castle, DE). This was followed by exposure to 40 °C/75% RH. All the water sorption data were analyzed using Universal Analysis software. The water sorption profiles of individual excipients were obtained using the Dynamic Vapor Sorption Analyzer (DVS-1000 Advantage, Surface Measurement Systems, Middlesex, U.K.). Approximately 15.0 mg of powder was placed in a quartz sample pan and equilibrated at 0% RH (25 °C) for 1 h under a nitrogen flow rate of 200 mL/min. The relative humidity (RH) was progressively increased from 0% to 90% RH, in increments of 10% RH, and then decreased back from 90% to 0% RH in steps of 10% RH. At each RH, the attainment of equilibrium was assumed if the mass change was < 0.005% in 10 minutes. The maximum hold time at each RH was not more than 2 hours. The weight gain in tablet samples, following storage at 40 °C/75% RH, was determined gravimetrically.

4.3.6 Slurry pH

Solutions/suspensions of the excipients were prepared (10% w/v) using deionized water. The samples, in sealed vials, were stirred for 24h. Their pH values, as well as those of saturated solutions of selected excipients, were measured (Oakton pH 500 pH meter) at ambient temperature (25 °C). The pH meter was calibrated using standard buffer solutions of pH 4.01, 7.00, and 10.01 (Oakton Instruments).

4.3.7 Microenvironmental Acidity Measurements by Diffuse Reflectance UV-Visible Spectroscopy

Instrumentation. A UV visible spectrophotometer (Cary 100 Bio) equipped with a diffuse reflectance accessory (Labsphere, model DRA-CA-30I) having an inbuilt photomultiplier tube (PMT) was used. The inner surface of the sphere is coated with poly-(tetrafluoroethylene). A "zero-degree" wedge in the sample port ensures that the powder sample surface was always perpendicular to the incident light. As a result, reflection back through the sample beam entrance port eliminates the specular component of the reflected light. The integrating sphere collects the light diffusely reflected by the sample and presents an integrated signal to the detector.

Indicator Selection and pHeq Measurements. To estimate the microenvironmental acidity in the solid samples (placebo blends and cocrystal formulations), bromocresol green and thymol blue were selected as indicators. The first ionization of bromocresol green (pK_{a1} 4.7) and thymol blue (pK_{a1} 1.6) are shown in Figure 4.3. To deposit indicators onto the solid samples, indicator solutions in methanol (1 mg/ml) were mixed with each solid sample (indicator concentration 0.4 mg/g) and dried. The ratios of the Kubelka–Munk functions, F(R), at the peaks corresponding to the ionized and unionized forms of each

indicator (peak height ratios) were determined, enabling the calculation of pHeq. The complete details were described earlier.[43,46,68]

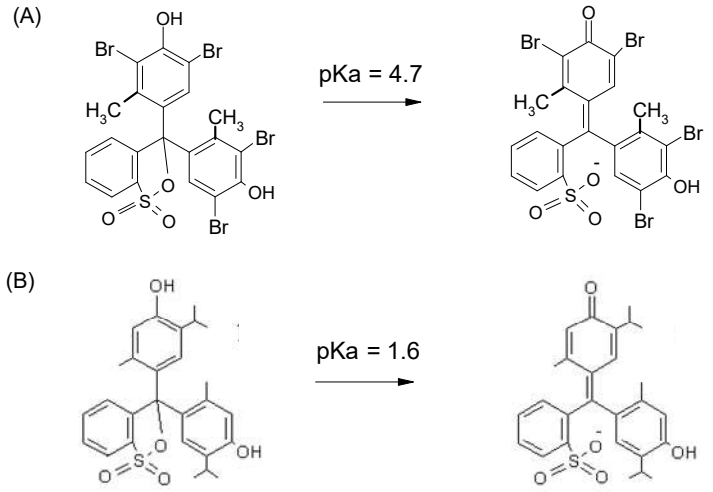

Figure 4.3. Ionization of indicator dyes (A) bromocresol green (BG) and, (B) thymol blue (TB).

4.4 Results and Discussion

4.4.1 Characterization of Pure Excipients and Placebo Blends

A tablet formulation intended for oral administration typically contains, in addition to the API, excipients with specific functionalities. Commonly used excipients are diluents (also referred to as fillers), binders, lubricants, and disintegrants. The excipients were subjected to powder X-ray diffractometry (XRD) and thermal analyses [differential scanning calorimetry (DSC) and thermogravimetric analysis (TGA)]. In addition, the interaction with water of each excipient was comprehensively investigated using an automated water sorption analyzer.

The powder XRD patterns of lactose monohydrate (LM), dibasic calcium phosphate anhydrate (DCPA) and magnesium stearate (MgSt) were in excellent agreement with the reported data in the Powder Diffraction Files of the International Centre for Diffraction

Data. LM was identified as the α-lactose monohydrate (card # 00-027-1947) while, MgSt was found to be a mixture of dihydrate [$Mg(C_{18}H_{35}O_2)_2 \cdot 2H_2O$; card #00-054-1973] and trihydrate [$Mg(C_{18}H_{35}O_2)_2 \cdot 3H_2O$; card #00-054-1974] forms. Our DSC results of the excipients agreed with that reported by Gombaz et al. (LM)[156], Delaney et al. (MgSt)[157] and Miyazaki et al. (DCPA)[158] and confirmed that the lactose was a monohydrate, MgSt was a mixture of hydrates and DCPA was in the anhydrous form.

All the crystalline excipients (LM, DCPA, MgSt) sorbed a limited amount of water (< 2%) when exposed to progressively increasing RH values up to 80% (25 °C). On the other hand, the partially crystalline (MCC) and the amorphous excipients (SSG, CCS) sorbed much higher amounts of water (Figure 4.11; Supplementary Information). The water sorption-desorption properties of the excipients were in good agreement with literature.[159]

The pH of a suspension or a saturated solution of an excipient can provide a measure of its microenvironmental acidity in a solid dosage form. A second approach, measurement of surface acidity using an indicator probe, has also found extensive use.[43,44,46,48] We used both the measurements to evaluate the effect of each excipient. These results are summarized in Table 4.2. The solution (or suspension) pH measurements of the excipients were performed in 10% w/v aqueous solutions (or slurries). The samples, in sealed vials, were shaken intermittently for 24 h before pH measurements (Table 4.2; second column). The surface acidity (pHeq) values of the excipients were determined using one of the three probe molecules (Table 4.2): bromophenol blue ($pK_a = 4.0$), bromocresol green ($pK_a = 4.7$) or phenol red ($pK_a = 7.9$).[160] When the excipients were rank-ordered, based on these two approaches, there was a broad agreement.

Table 4.2. Surface acidity of excipients (expressed as pHeq) based on indicator probe ionization. The aqueous solution/suspension pH values of the excipients are also provided.

Pure excipients	Solution/suspension pH (10% w/v) [#]	Surface acidity		
		Probe	pHeq	
			0 h	24 h[*]
Microcrystalline cellulose NF (MCC; Avicel® PH102)	5.8 ± 0.5	BG	4.3	3.6
Lactose monohydrate NF (LM; Fast Flo® 316)	6.3 ± 0.1	BG	4.1	4.1
Sodium starch glycolate NF (SSG; Explotab®)	5.7	BG	5.2	5.8
Magnesium stearate NF (MgSt)	10.3 ± 0.3	PR	6.8	7.3
Dibasic calcium phosphate anhydrous USP (DCPA; A-TAB®)	5.6 ± 0.1	BB	3.2	3.3
Croscarmellose sodium NF (CCS; Ac-Di-Sol®)	4.5 ± 0.3	-	NR	NR

[#]Determined 24 h after preparation
*pHeq determined after 24 h storage at 40 °C/75% RH
NR - Not recorded, BG - bromocresol green, PR - phenol red, BB - bromophenol blue.

Four model multi-component blends were prepared using the excipients listed in Table 4.2 and their compositions can be discerned from Table 4.1. The cocrystal (TG) and excipient blends were dry mixed and then compressed. During compression, brittle fracture, deformation or a combination of the two can occur. The deformation may be elastic or plastic. Successful tablet production will depend upon achieving the right balance of brittle fracture and plastic behavior within the compression mix.[161] Upon compression, MCC is known to undergo plastic deformation while DCPA and LM undergo brittle fracture.[162–164]

Therefore, in the multi-component excipient blends, a combination of MCC with either LM or DCPA was used. Combining MCC with either LM or DCPA has been reported to also result in good flow.[161] All the compressed placebo blend were characterized by XRD (Figure 4.4A) and the water sorption and surface acidity results are summarized in Table 4.3.

Irrespective of composition, the blends sorbed ~ 5.5% water when stored at 40 °C/75% RH. The initial pHeq of DCPA containing formulations (F2, F3) was lower than that of lactose containing formulations (F1, F4). This might be due to the more acidic nature of DCPA (pHeq = 3.2) compared to lactose (pHeq = 4.1). Earlier, the pHeq of a DCPA containing excipient blend of a substantially similar composition was reported to be 3.6, while for a lactose containing blend, the pHeq was 4.6.[43] When we stored the placebo blends at 40 °C/75% RH for 24 h, irrespective of the composition, the pHeq value was ~5.0.

Table 4.3. Water sorption behavior and surface acidity of placebo blends.

Placebo blends[#]	Water sorption analysis (Weight gain, %)	Surface acidity (pHeq)	
	40 °C/75% RH	0 h	24 h[*]
Placebo F1	~5.6	4.6 ± 0.01	5.0 ± 0.05
Placebo F2	~5.5	3.6 ± 0.04	4.9 ± 0.06
Placebo F3	~5.7	3.7 ± 0.06	4.9 ± 0.08
Placebo F4	~5.3	4.6 ± 0.07	4.8 ± 0.03
*pHeq determined after 24 h storage at 40 °C/75% RH			

4.4.2 Quantification of Cocrystal Dissociation in Tablet Formulations

Figure 4.4 is an overlay of the XRD patterns of intact cocrystal and the corresponding placebo tablet formulations. The dotted vertical lines in Figure 4.4B point the positions of

several peaks unique to TG cocrystal. At these angular values, none of the crystalline excipients exhibited diffraction peaks. As expected, the XRD patterns of F1 and F4 formulations are substantially similar as are those of F2 and F3.

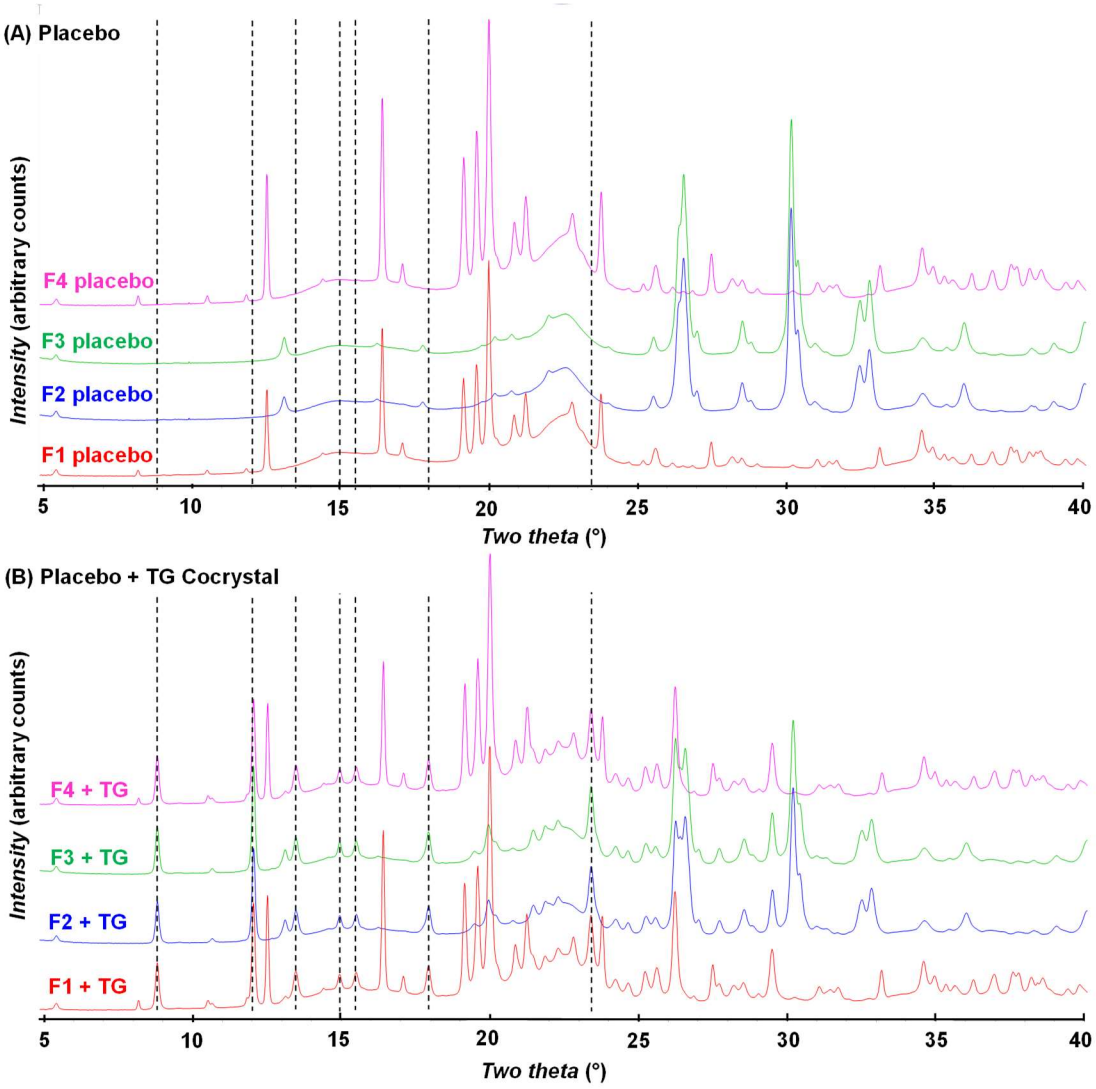

Figure 4.4. Overlay of XRD patterns of (A) placebo and (B) cocrystal tablet formulations. The dotted vertical lines point the angular values of several unique peaks of TG cocrystal.

Initially, control tablets of TG cocrystal alone (no excipient) and the formulated tablets (composition in Table 4.1) were stored at 40 °C/75% RH for two weeks and analysed in the laboratory diffractometer. In the control tablets, there was no decrease in the intensities of characteristic peaks of TG cocrystal. Moreover, there was no evidence of anhydrous theophylline formation (Figure 4.5). Therefore, it was concluded that the TG cocrystal by itself was robust under the conditions examined.

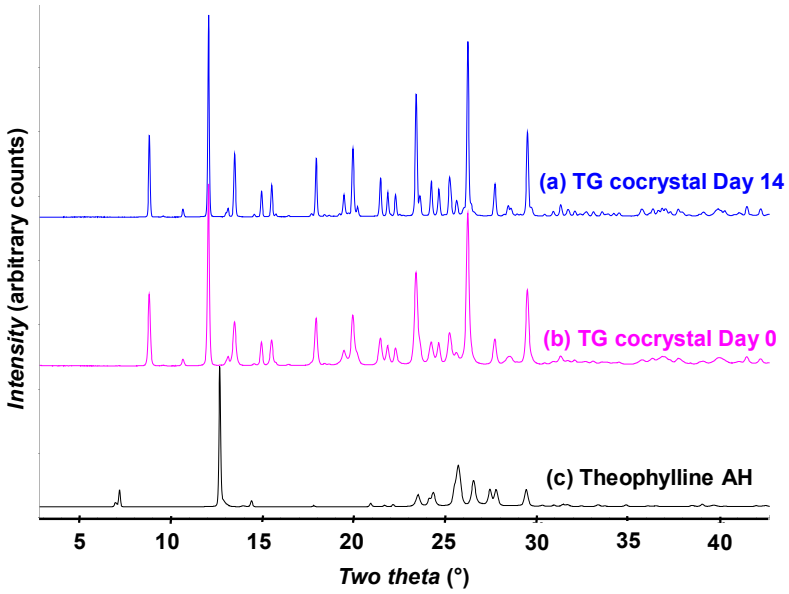

Figure 4.5. Overlay of XRD patterns of freshly prepared TG cocrystal tablet (control; no excipients), and after storage at 40°C/75% RH for 14 days are shown in (b) and (a) respectively. The XRD pattern of anhydrous theophylline tablet is shown in (c).

In contrast, in all the formulated tablets, peaks attributable to anhydrous theophylline (TH) appeared after two weeks of storage suggesting dissociation of the TG cocrystal. As a representative example, cocrystal dissociation in F1 tablet formulation is shown in Figure 4.6. While the TH peak at 14.3° 2θ could be readily discerned, the peak at 12.7° 2θ overlapped with the peak of LM at 12.5° 2θ. In light of its high intensity, the 12.7° 2θ peak was ideally suited for quantitative analyses.

The same problem was encountered in F4 formulation. To overcome this problem of overlapping Bragg peaks and to monitor dissociation kinetics in the formulations, quantitative studies were performed using high-intensity synchrotron radiation (Advanced Photon Source).

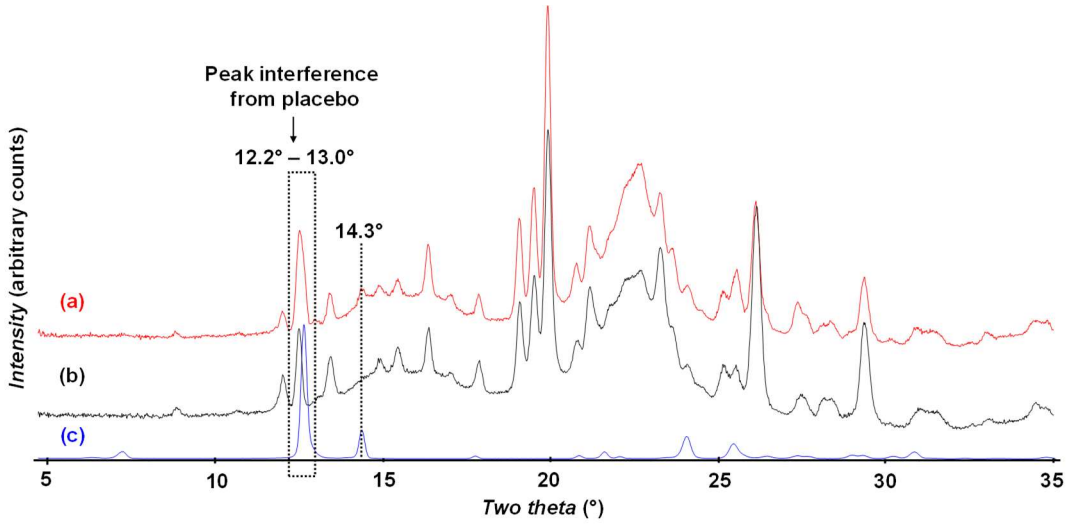

Figure 4.6. Overlay of one-dimensional XRD patterns of (a) F1 tablet formulation after 14 days of storage at 40 °C/ 75% RH, (b) F1 tablet formulation, freshly prepared, and (c) reference pattern of anhydrous theophylline (TH). The appreance of a new peak in (a) at 14.3° 2θ, attributed to formation of anhydrous theophylline, is pointed out by dotted vertical line. This peak is absent in the freshly prepared tablet formulation (b). The rectangular dotted region between 12.2° - 13.0° 2θ, highlights the overlap of the 12.5° 2θ peak of LM with the most intense peak of TH at 12.7° 2θ. The XRD patterns were collected in the laboratory diffractometer.

The diffraction patterns of F1 tablet formulation, collected at the synchrotron beamline and using a laboratory diffractometer, are compared in Figure 4.7. Synchrotron XRD offered improved peak resolution in the region of interest (12.3° –12.9° 2θ), minimized interference due to excipients, and thereby enabled quantification of the TH (one of the reaction products) formed in formulations. The concentration of crystalline TH is used as a measure of the extent of dissociation.

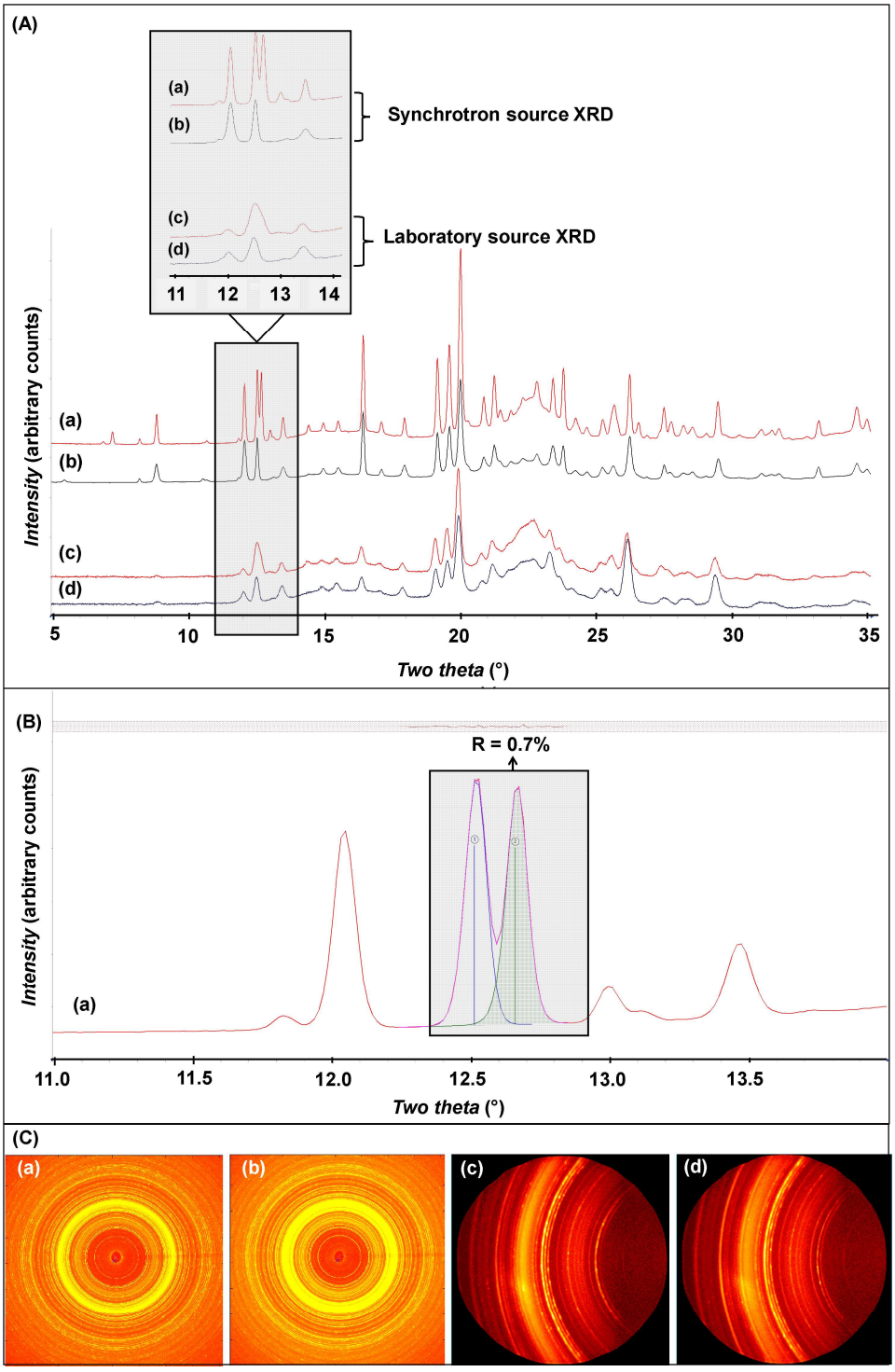

Figure 4.7. A) Overlay of the one-dimensional XRD patterns of F1 tablet formulation at day 0 (b, d) and after 14 days of storage at 40 °C/ 75% RH (a, c). The patterns (a), (b) were collected using synchrotron radiation and (c), (d) in the laboratory diffractometer. The inset is a magnified view of the 11.0 – 14.0° 2θ region. Using synchrotron radiation, it was possible to separate the

12.5° 2θ peak of LM from the 12.7° 2θ peak of TH (analyte). To enable ready comparison, both the laboratory and synchrotron data were converted for Cu Kα radiation (λ = 1.54 Å). (B) Profile fitting (Pearson-VII function; least-squares fitting residual R < 1%) of the overlapping peaks (12.3 to 12.9° 2θ) enabled the determination of integrated intensity of the 12.7° 2θ peak of the analyte. (C) Two-dimensional XRD images of tablet formulations obtained using synchrotron (a, b; λ= 0.45212 Å) and laboratory diffractometer (c, d; Co Kα radiation λ = 1.79 Å).

4.4.3 Cocrystal Dissociation in Prototype Formulations

Surprisingly, in all the prototype formulations, TH formation was very rapid and appeared to have almost plateaued within one day (Figure 4.8). The TH concentration varied considerably between the formulations, from a minimum of ~20% to a maximum of ~30%. The dissociation kinetics in F1 and F4 as well as in F2 and F3 were virtually identical to each other. MCC is the major excipient (weight fraction of 0.49) in all the formulations F1 and F4 contain LM (weight fraction 0.24) while F2 and F3 contain the same weight fraction of DCPA (Table 4.1). MgSt was the lubricant in all the formulations, while the disintegrant was either CCS (F3 & F4) or SSG (F1 & F2). Since MgSt and the disintegrant (SSG or CCS) together constitute a low weight fraction (<0.04) of the dosage form, they are unlikely to be responsible for the pronounced and rapid dissociation. MCC, a major excipient common to all the formulations can be a potential source of the problem. Interestingly, none of the formulations showed cocrystal dissociation when stored at 40 °C/0% RH for two weeks. This provides further evidence that the dissociation reaction is water mediated. Thus, the formulation microenvironment "experienced" by the cocrystal particles appears to dictate its stability and multiple excipients could be responsible for the dissociation.

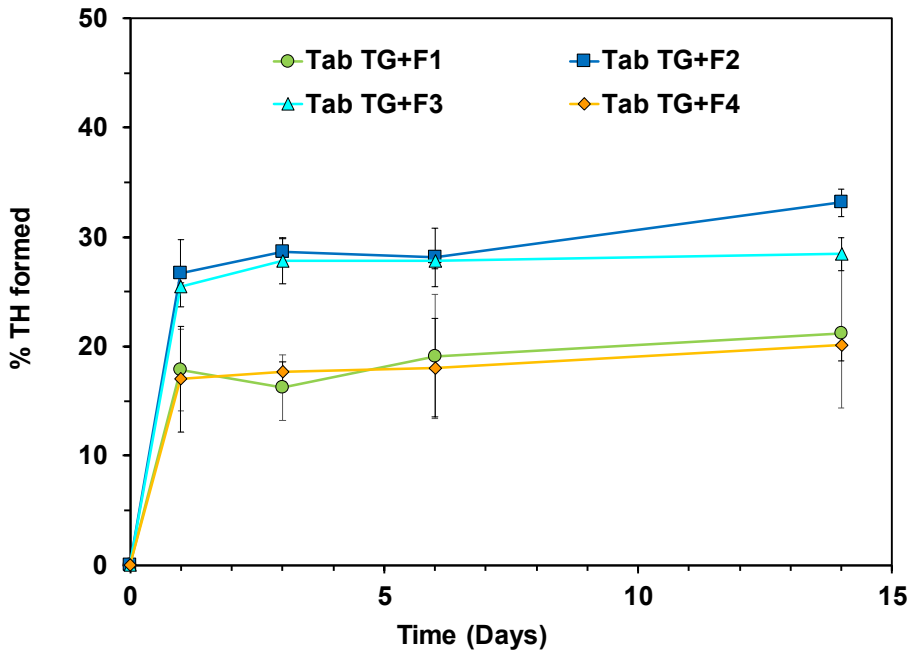

Figure 4.8. Percent TH crystallized as a function of time in four tablet formulations stored at 40 °C/75% RH for up to 14 days (n = 3, each time point).

The formulation excipients, depending on their nature and concentration, can influence the local microenvironmental acidity, and thereby coformer ionization. Since we are dealing with the cocrystal of a neutral API with a weak acid (GA), only the ionization of the coformer will be pH dependent. To identify "problem" excipients and to gain mechanistic insights, we studied the dissociation behaviour of binary compacts of TG cocrystal with each excipient.

4.4.4 Cocrystal Dissociation in Binary Compacts

Compacts containing TG cocrystal and each excipient were prepared in a 1:1 weight ratio and stored at 40 °C/75% RH for one week. A second set of binary compacts stored at 40 °C/0% RH for one week, served as controls. The compacts were

monitored periodically by XRD. When stored at 75% RH, all the excipients (except lactose) caused rapid cocrystal dissociation, based on the appearance of peaks (12.7°, 14.3° 2θ) attributable to TH (Figure 4.9). The extent of cocrystal dissociation also appeared to be excipient dependent. The excipients inducing dissociation exhibit a range of properties -MCC is neutral and hydrophilic, MgSt is ionizable and hydrophobic, DCPA is ionizable and non-hygroscopic while CCS and SSG are ionizable and hydrophilic. The extent of water sorption in the binary compacts followed the order: CCS ~ SSG > MgSt > MCC > DCPA > LM. Rapid and pronounced dissociation was observed in presence of hydrophilic excipients with a strong tendency to sorb water.

While tablets of TG cocrystal (no excipients) were stable following storage at 40 °C/75% RH for 2 weeks, rapid dissociation in presence of MCC was surprising (Figure 4.9A). MCC is a neutral (no ionizable groups) and partially crystalline excipient. Its hygroscopic nature is attributed to abundant hydroxyl groups on cellulose chains and to the relatively large surface to volume ratio of microfibrils.[165] MCC exhibited type II water sorption isotherm with a characteristic hysteresis between the sorption and desorption isotherms (Figure 4.11; Supplementary Information). The water in MCC is considered to exist in at least three states – tightly bound to anhydroglucose units, followed by a second less tightly bound layer, and finally, bulk ("free") water.[166] The tightly bound and subsequent less tightly bound water is "unavailable" to act as a solvent for any potential solution-mediated transformations of an API. Only the free water is highly reactive and mobile[167] and has been implicated in the instability of moisture-sensitive drugs such as aspirin[168]

and cephalothin.[169] In binary tablets containing (TG + MCC), dissociation of TG cocrystal was observed following storage for one day at 40 °C/75% RH. In binary tablets containing (TG + MCC), dissociation of TG cocrystal was observed following storage for one day at 40 °C/75% RH. In contrast, when stored at 40 °C/0% RH, dissociation was not detected even after one week. This suggests that excipient induced dissociation of TG cocrystal was water mediated. At 40 °C/75% RH conditions, while the TG cocrystal alone sorbed ~0.13% water, its binary compact with MCC revealed a water uptake of 1.6%. The additional water sorbed by MCC can provide a medium to facilitate cocrystal dissolution and enable solution-mediated transformation resulting in precipitation of the less soluble theophylline from solution. The crystallization of theophylline is confirmed by the appearance of characteristic peaks, for example at 12.6° and 14.3° 2θ, in the XRD pattern (Figure 4.9A). The characteristic peaks of the second reaction product, glutaric acid, for example at 13.8° and 24.6° 2θ, were not detected. This is not surprising in light of its high aqueous solubility.

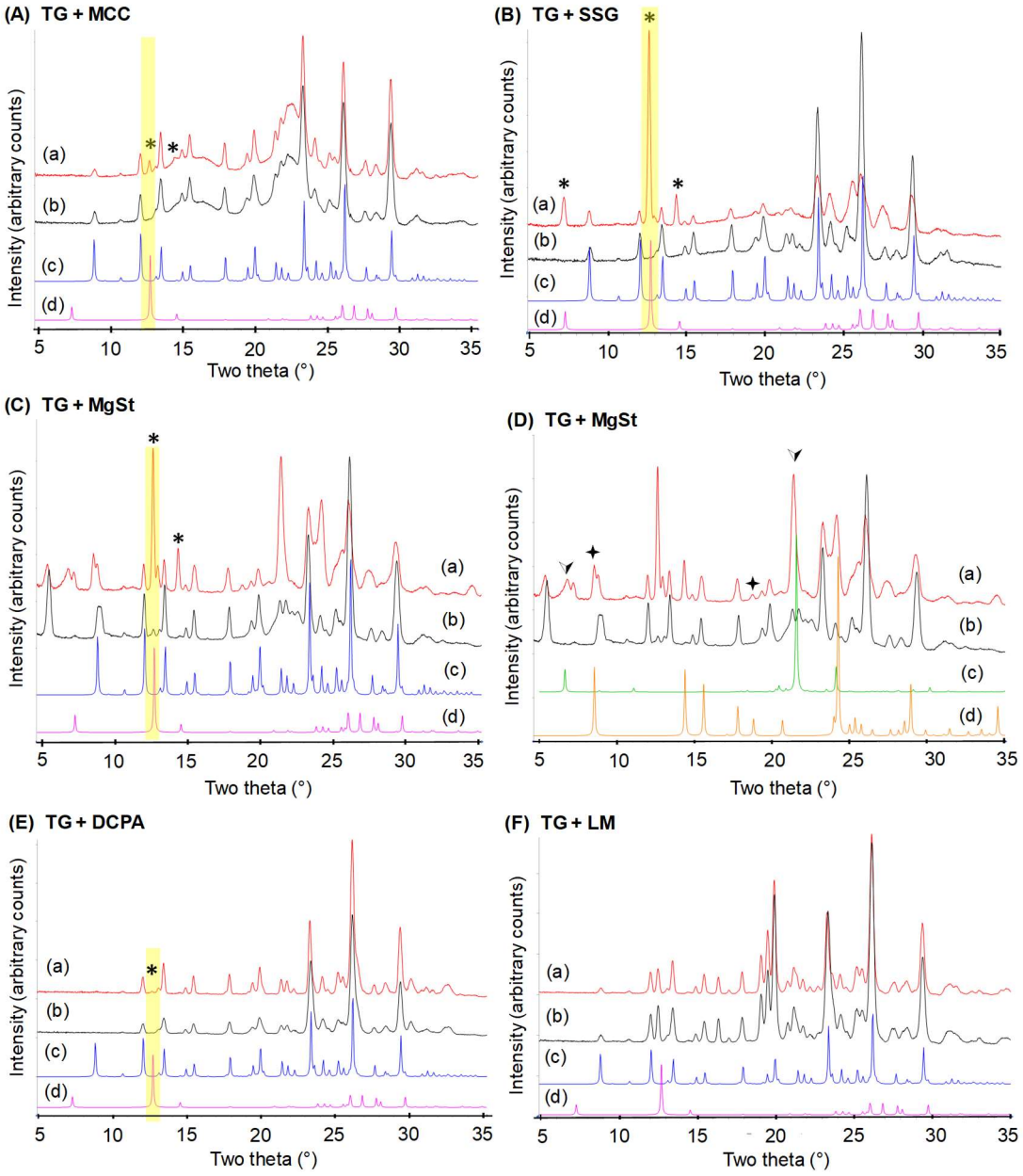

Figure 4.9. Overlay of XRD patterns of binary compacts of TG prepared with (A) MCC, (B) SSG, (C) & (D) MgSt, (E) DCPA, and (F) LM. Each panel contains the XRD patterns of freshly prepared compacts (b) and after storage at 40 °C/75% RH for 1 day (a). The reference patterns of TG cocrystal and theophylline are presented in (c) and (d), respectively (except in panel D). In panel D, (c) and (d) are the reference patterns of stearic acid (CSD ref code STARAC01) and glutaric acid-magnesium $(H_2O)_4$ complex (CSD ref code NOKFOI), respectively. One characteristic peak for theophylline (*) observed as a consequence of cocrystal dissociation is highlighted. Two peaks matching with each stearic acid (⩛) and glutaric acid-magnesium $(H_2O)_4$ complex (✦) are pointed out in panel D.

Dissociation of TG cocrystal in binary compacts with SSG and CCS, stored at 40 °C/75% RH, was evident in one day, with the appearance of characteristic peaks of TH. (SSG compacts in Figure 4.9B; CCS compacts in Figure 4.12; Supplementary Information). The high water uptake of ~10% in both the compacts is attributed to the hydrophilic nature of CCS and SSG (Figure 4.11, Supplementary Information panels B and C reveal the water sorption profiles of SSG and CCS). The pHeq of both the disintegrants is ~5.0, creating a microenvironment favourable for the pronounced (>50%) ionization of GA. The consequent enhancement in solubility difference between GA and TH will favour cocrystal dissociation. This was further supported by the absence of dissociation when tablets of TG cocrystal with either CCS or SSG were stored at 40 °C/0% RH for a week.

Dissociation was also observed in compacts of TG cocrystal with both MgSt (Figure 4.9, panels C and D) and DCPA (Figure 4.9E), after one day of storage at 40 °C/75% RH. This is interesting since both MgSt and DCPA do not exhibit a tendency to sorb water. MgSt caused dissociation of caffeine-oxalic acid cocrystal at high RH conditions resulting in the formation of caffeine hydrate, magnesium oxalate and stearic acid.[82] Interestingly, a similar water-mediated reaction between MgSt and pioglitazone HCl salt was reported to be the mechanism of the salt disproportionation reaction resulting in formation of pioglitazone free base, stearic acid and magnesium chloride.[35,68] The TG-MgSt compact, when stored at 40 °C/75% RH, sorbed ~ 3% water. Surprisingly, the amount sorbed was much higher than in the MCC compact (1.6%). Considering the hydrophobic nature of MgSt and the low water sorption tendency of TG cocrystal, a 3% water uptake was unexpected.

This unusual water sorption behaviour was explained from our XRD results which revealed the formation of a new hygroscopic species, the product of an interaction between MgSt and TG cocrystal. Following storage for 24 hours, there was a pronounced decrease in the intensity of the 5.5° 2θ MgSt peak as well as the appearance of the characteristic 12.7° 2θ peak of TH (Figure 4.9C) and 6.6° and 21.6° 2θ peaks of stearic acid (Figure 4.9D). Interestingly, the position of two additional peaks, observed at 8.5° and 18.8° 2θ (Figure 4.9D), matched with glutaric acid-magnesium-$(H_2O)_4$ complex reported in the literature (CSD ref code NOKFOI). The formation of this complex resulting from the reaction between GA and MgSt was independently confirmed. (Figure 4.13; Supplementary Information). From a mechanistic point of view, we postulate that the dissociation of TG cocrystal is initiated at the cocrystal-MgSt particle interface. The intrinsic lubricant nature of MgSt will cause pronounced surface coverage of the cocrystal particles. In addition, compression will facilitate intimate contact between MgSt and cocrystal particles. Pronounced lattice disorder at the interface, resulting from compression, facilitates water sorption. The water sorption can cause pronounced plasticization, resulting in increased molecular mobility, and enhanced reaction rate. The formation of a hygroscopic reaction product can cause additional water uptake, thereby progressively plasticizing the system. With increased water content, the aqueous phase would serve as a medium, facilitate dissolution of the crystalline phases, and enable solution-mediated transformation.

In compacts of TG cocrystal with DCPA, water mediated proton transfer from glutaric acid to hydrogen phosphate anion (HPO_4^{2-}) resulting in the formation of

metal salt, will drive cocrystal dissociation. A similar mechanism has been proposed for the dissociation of caffeine - oxalic acid cocrystal with DCPA.[82] In contrast, in compacts containing lactose monohydrate (LM), there was no evidence of dissociation (Figure 4.9F). LM is a non-ionizable excipient with little tendency to sorb water even at 75% RH (40 °C). The absence of "bulk water" (unlike MCC) and proton accepting groups (unlike MgSt, DCPA), makes lactose monohydrate a "safe" excipient with respect to solid-state stability of TG.

4.5 Significance

One of the key goals in drug development is to identify optimal dosage form compositions that can ensure the stability of API throughout its shelf-life. Comprehensive information on dosage form development for conventional small molecules is readily available in the literature. Currently, for cocrystal APIs, there is limited information on dosage form stability.[82] Specifically, the influence of excipients and processing on cocrystal stability has not been adequately investigated. Our studies in prototype tablet formulations of cocrystals have demonstrated that the formulation composition strongly influences cocrystal stability. In general, solid state dissociation reaction is expected to be "slow". However, using synchrotron radiation it was possible to monitor dissociation kinetics over short timescales (2 weeks). Surprisingly, at realistic concentration of formulation excipients, water mediated dissociation of theophylline-glutaric acid occurred very rapidly, in timescales of days. Excipient hygroscopicity and ionizability were identified to be critical attributes in the water mediated dissociation reaction in intact tablets. Cocrystal – excipient compatibility studies, coupled with the effects of unit operations (milling,

compression), can provide insights into the combined effects of formulation and processing on cocrystal stability.

In order to mitigate the risk of unintended cocrystal dissociation, it may be prudent to avoid unit operations that involve bulk water such as wet granulation. Furthermore, using a combination of formulation approaches (such as film coating, the use of colloidal hydrophobic silica for particle coating, incorporation of hydrophilic silica as water scavenger)[96] and packaging design (such as a unit dose blister pack), may be considered to reduce the likelihood of water mediated cocrystal dissociation during storage.

In addition to excipients, the nature of coformer and the intrinsic properties of the cocrystal such as its solubility are also important considerations. A pronounced solubility enhancement due to cocrystal formation can facilitate solution mediated transformation resulting in cocrystal dissociation. A detailed understanding of the role of coformer in the context of cocrystal dissociation in a formulation environment is the subject of Chapter 5.

While this is not the subject of our current investigation, it is important to recognize that potential interactions between excipient and coformer can also compromise excipient functionality and thereby affect product performance.

4.6 Conclusions

Theophylline-glutaric acid (TG) cocrystal (in the absence of excipients) was found to be robust when stored at 40 °C/75% RH for 2 weeks. However, in prototype tablet formulations, TG cocrystal disproportionated, resulting in the formation of anhydrous theophylline (TH). The dissociation reaction was water mediated, occurred very rapidly (timescale of days), and was influenced by the formulation composition. Neutral crystalline excipients, with little or no propensity for water sorption (e.g. lactose monohydrate), are

not likely to induce cocrystal dissociation. In addition to excipients, the formation of hygroscopic reaction products (as in the case of MgSt) can further render the cocrystal instable.

4.7 Supplementary Information

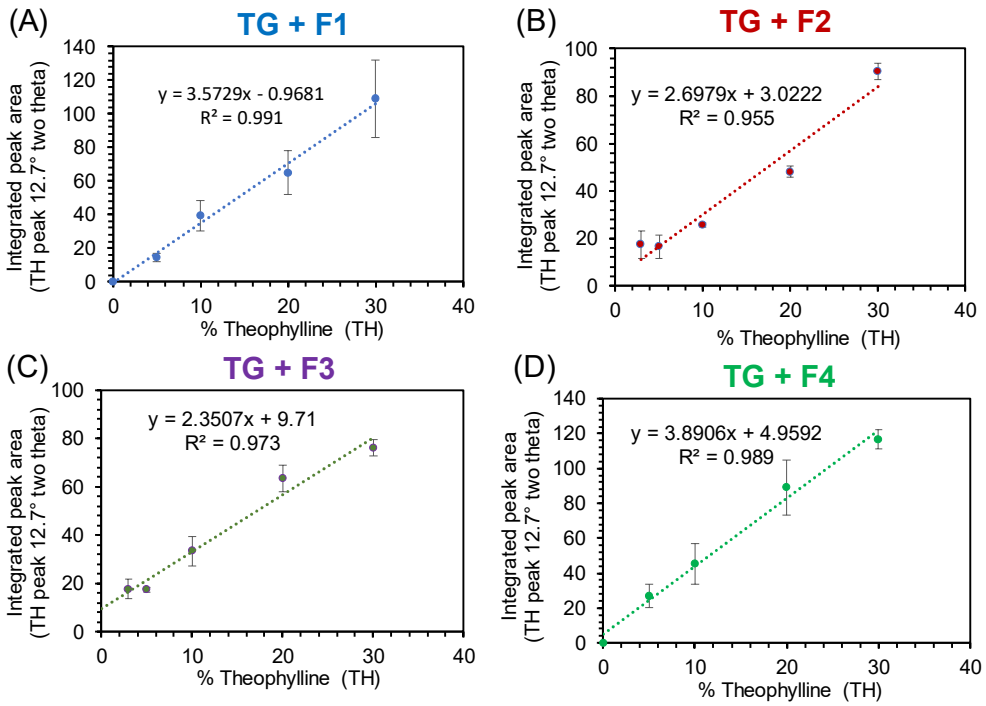

Figure 4.10. Plot of the intensity of the 12.7° 2θ peak of TH as a function of TH concentration in calibration tablets of (A) TG + F1, (B) TG + F2, (C) TG + F3, and (D) TG + F4.

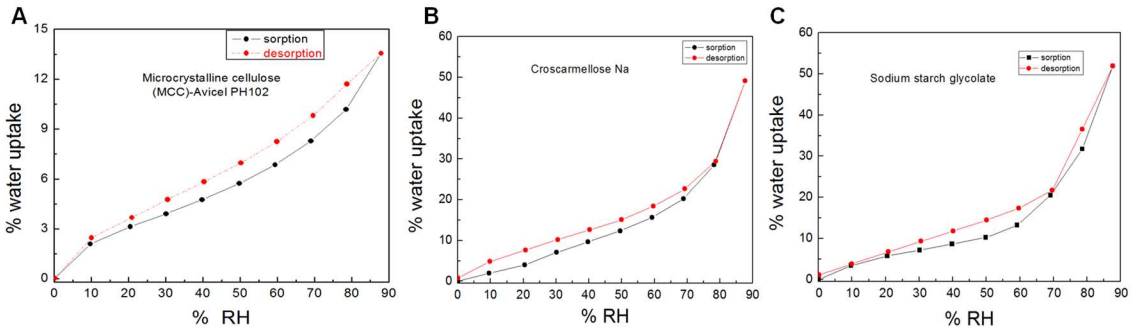

Figure 4.11. Water sorption-desorption isotherms of (A) microcrystalline cellulose, (B) croscarmellose sodium and, (C) sodium starch glycolate at 25 °C.

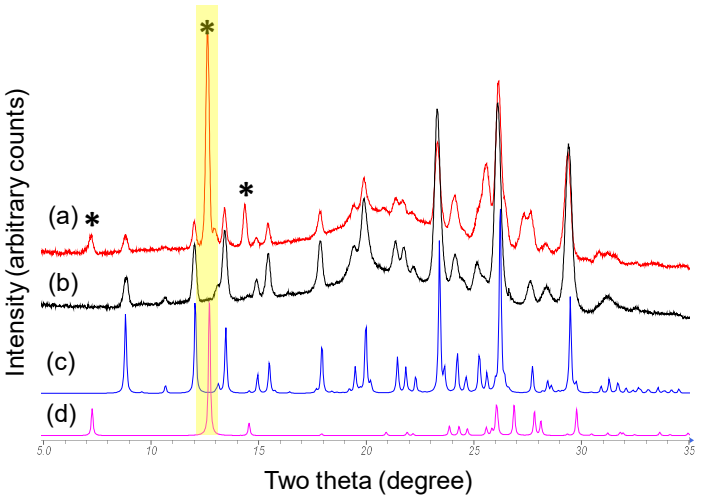

Figure 4.12. Overlay of XRD patterns of binary compacts of TG prepared with CCS. The XRD patterns of freshly prepared compacts and after storage at 40 °C/75% RH for 1 day are presented in (b) and (a) respectively. The reference patterns of TG cocrystal and theophylline are presented in (c) and (d), respectively.

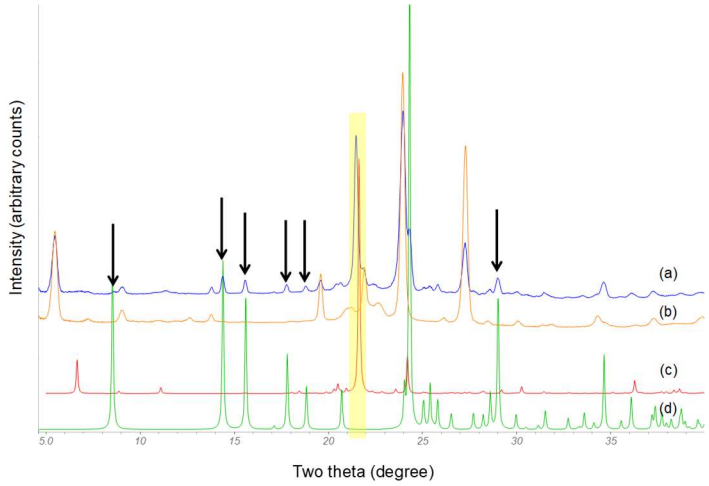

Figure 4.13. Overlay of XRD patterns of binary compacts of GA (21.15 mg) prepared with MgSt (50.00 mg). The XRD patterns of freshly prepared compacts and after storage at 40 °C/75% RH for two days are presented in (b) and (a) respectively. The reference patterns of stearic acid (CSD ref code STARAC01) and glutaric acid-magnesium-$(H_2O)_4$ complex (CSD ref code NOKFOI), are presented in (c) and (d), respectively. The arrows point several peaks matching with glutaric acid-magnesium $(H_2O)_4$ complex. One characteristic peak for stearic acid observed as a consequence of the reaction is highlighted.

Chapter 5 : Role of Coformer and Excipient Properties on the Solid-State Stability of Theophylline Cocrystals

5.1 Synopsis

The stability of theophylline cocrystals comprised of acidic (glutaric acid), basic (isonicotinamide) or neutral (benzamide) coformers, was evaluated in the presence of several excipients. Tablets of theophylline-glutaric acid (TG) and theophylline-isonicotinamide (TINT) cocrystal were stable 'as is' (no excipient) after storage at 40 °C/75% RH for one week. However, TG and TINT cocrystals dissociated rapidly in the presence of basic and acidic excipients, respectively. The dissociation reaction was water mediated and theophylline, the reaction product was identified by powder X-ray diffractometry. In case of theophylline-benzamide (TBZ) cocrystal, storage of tablets with and without excipients at 40 °C/75% RH for one week, resulted in a cocrystal polymorphic transformation. Thus, the potential for excipient-induced cocrystal dissociation exists for cocrystals comprised of acidic and basic coformers. If the coformer renders the cocrystal highly water soluble, even in the presence of neutral excipients, there is a propensity for dissociation.

5.2 Introduction

Cocrystals are multi-component systems usually containing the active pharmaceutical ingredient (API) and a coformer held together in a crystal lattice by nonionic/noncovalent interactions. In the past two decades, pharmaceutical cocrystals have emerged as new solid forms, providing opportunities to tailor the physicochemical and mechanical properties of drugs. Using a suitable coformer, properties of an API including solubility[49–51], dissolution

rate[52–54], permeability[55–57], stability[58–60] and manufacturability[61–63] can be optimized. The coformer must be non-toxic, with GRAS (generally regarded as safe) status. Cocrystal design and coformer selection is guided by a detailed understanding of the supramolecular chemistry of relevant functional groups and the synthon hierarchy.[64–66]

Although cocrystals offer many potential benefits, their propensity to undergo unintended dissociation, resulting in reversion to the corresponding free API and coformer, poses a major formulation challenge. Dissociation of the cocrystal can negate the advantages of cocrystal formation and can have undesirable consequences on product performance such as alterations in dissolution rate and bioavailability. In the solid-state, cocrystal dissociation occurred at elevated temperatures and under high relative humidity (RH) conditions.[58,59,78,80,81] Eddleston et al. reported that the rate and extent of caffeine-glutaric acid cocrystal dissociation increased as a function of RH.[78] Following storage at RT and 98% RH for one week, dicarboxylic acid (maleic, malonic, glutaric) cocrystals of caffeine and theophylline dissociated, resulting in the crystallization of caffeine/theophylline hydrate.[58,59] In another example, salicylic acid–urea and aspirin–acetamide cocrystals dissociated at high RH resulting in the formation of salicylic acid and aspirin, respectively.[78] The instability was attributed to the large aqueous solubility difference between the two cocrystal components. The driving force for dissociation of caffeine-theophylline cocrystal, when heated to a temperature substantially below the melting points of caffeine and theophylline, was explained by the entropically favorable conformation of caffeine. The combined effects of temperature and water vapor pressure were comprehensively investigated in pyrazine−phthalic acid cocrystal.[81] An elevation in temperature or water vapor pressure accelerated cocrystal dissociation. The dissociation

mechanism was postulated to be dissolution of the cocrystal in sorbed water followed by crystallization of the individual components.

To develop robust formulations of cocrystal APIs, it is essential to develop an understanding of the physical stability of cocrystals in presence of excipients, i.e., in a formulation environment. Since tablets are the most widely used dosage forms, from a practical viewpoint, it is important and relevant to develop an understanding of cocrystal dissociation in multicomponent solid matrices. A tablet formulation intended for oral administration typically contains, in addition to the API, excipients with specific functionalities such as diluents (also referred to as fillers), binders, lubricants, and disintegrants. Once the 'as is' API cocrystal is determined to be stable, the next step is to evaluate its stability in presence of excipients.

Caffeine-oxalic acid cocrystal was widely reported to be stable when stored at RT and 98% RH for seven weeks. However, when stored at 75% RH (RT) as a binary mixture with ionizable excipients (1:1 w/w ratio), it dissociated in a week.[82] An investigational cocrystal API dissociated to its free form, when binary blends with commonly used tablet excipients were stored at 40 °C/75% RH.[151] Using synchrotron radiation, we investigated the excipient induced dissociation of theophylline-glutaric acid (TG) cocrystal in prototype tablet formulations stored at 40 °C/75% RH (details in Chapter 4). The water-mediated reaction occurred rapidly and was strongly influenced by formulation composition. Dissociation was pronounced in the presence of hydrophilic excipients with a strong tendency to sorb water. In contrast, the cocrystal was stable in presence of a neutral excipient with no tendency to sorb water. Microcrystalline cellulose (MCC), while a

neutral but hydrophilic excipient, caused dissociation – an effect attributed to the pronounced aqueous solubility difference between TG cocrystal and theophylline.

In order to prevent excipient induced dissociation in theophylline cocrystals, we attempted to gain insight into the role of coformer properties on cocrystal stability. Therefore, building upon our earlier findings in TG cocrystal, two other coformers were investigated. Isonicotinamide (INT) and benzamide (BZ) were selected as the basic and neutral coformer, respectively (Figure 5.1). The water-mediated dissociation in theophylline cocrystals is hypothesized to occur under the following conditions.

(a) Cocrystals with a weakly basic coformer will dissociate in the presence of acidic excipients.

(b) Cocrystals with a weakly acidic coformer will dissociate the in presence of basic excipients.

(c) Cocrystals with a neutral coformer will be stable in the presence of acidic and basic excipients.

Ionizable (weak acid/weak base) coformers confer pH dependent solubility to theophylline cocrystals. The pH "experienced" by the cocrystal particles in the formulation microenvironment will be dictated by the excipients, and by extension, will influence the coformer ionization. Therefore, acidic excipients can cause dissociation of theophylline cocrystal with a weakly basic coformer, while basic excipients can cause dissociation of theophylline cocrystal with a weakly acidic coformer. In contrast, a cocrystal with a neutral coformer will be unaffected by the "pH" in the microenvironment and therefore, will be resistant to dissociation caused by ionizable excipients.

As discussed in Chapter 4, in case of TG cocrystal, all the basic excipients caused cocrystal dissociation. On the other hand, in the presence of lactose which is a neutral excipient, as expected, TG cocrystal was stable. Surprisingly, dissociation was observed in the presence of microcrystalline cellulose (MCC), also a neutral excipient. This was attributed to: (i) the hydrophilic nature of MCC resulting in pronounced water sorption and (ii) and the pronounced solubility difference between the TG cocrystal and theophylline. Upon storage at high RH, there can be surface dissolution of cocrystal in the sorbed water. There is ample evidence that such dissolution can occur at RH << RH_0 (critical relative humidity).[39,170–172] Lattice disorder is known to facilitate water-solid interactions.[172] Cocrystal dissociation in solution will result in supersaturation of theophylline followed by its crystallization. Thus, in addition to the microenvironmental pH and its influence on coformer ionization, the relative solubilities of the cocrystal and its constituents are important determinants of solid-state cocrystal stability.

In this study, several excipients used in tablet formulations, with wide structural diversity and functionalities, were selected. These were diluents (MCC, lactose monohydrate and dicalcium phosphate anhydrate), disintegrants (sodium starch glycolate, croscarmellose sodium), buffer/pH modifiers (adipic and itaconic acid) and a lubricant (magnesium stearate). The ability of each of these excipients to cause dissociation of theophylline cocrystals (TG, TINT and, TBZ) was determined by preparing binary tablets of cocrystal with each excipient in a 1:1 w/w ratio.

Our overall goal is to develop a basis for the rational selection of coformers and excipients which will yield stable solid dosage forms of cocrystals. Storage of tablets under elevated temperature and water vapor pressure (40 °C/75% RH) provides an avenue to study these

solution-mediated cocrystal dissociation reactions. We had three specific objectives. (i) Determine the influence of coformer on solid-state cocrystal stability. (ii) Gain a mechanistic understanding of the cocrystal dissociation brought about by excipients. (iii) Delineate the roles of coformer and excipient on solid-state cocrystal stability.

5.3 Experimental

5.3.1 Materials

Theophylline anhydrate (TH), glutaric acid (GA), isonicotinamide (INT) and benzamide (BZ); minimum 99% chemical purity, were obtained from Sigma–Aldrich Co. Ltd. Powder XRD analysis of TH, GA, INT and BZ starting materials agreed with the powder XRD pattern simulated from the known crystal structure of theophylline anhydrate (CSD reference code BAPLOT01), glutaric acid (β- polymorph; CSD ref code: GLURAC13), isonicotinamide (form I; CSD ref code: EHOWIH01) and benzamide (BZAMID01), respectively.

Microcrystalline cellulose (MCC; Avicel PH 101; NF grade), lactose monohydrate (LM; FastFlo 316, Foremost Farms; NF grade), dibasic calcium phosphate, anhydrous (DCPA; A-TAB Rhodia Pharma Solutions; USP grade), magnesium stearate (MgSt; Mallinckrodt Laboratory Chemicals; NF grade), sodium starch glycolate (SSG; Explotab, Edward Mendell; NF grade), croscarmellose sodium (CCS; Ac-di-sol, FMC BioPolymer), adipic acid (Sigma–Aldrich) and itaconic acid (Sigma–Aldrich) were used as received.

5.3.2 Preparation of Theophylline Cocrystals

Theophylline-glutaric acid (TG; 1:1) cocrystal – TG cocrystal was prepared in bulk by the isothermal slurry conversion crystallization method using chloroform as solvent.[155] Details of the preparation method are described in Chapter 4.

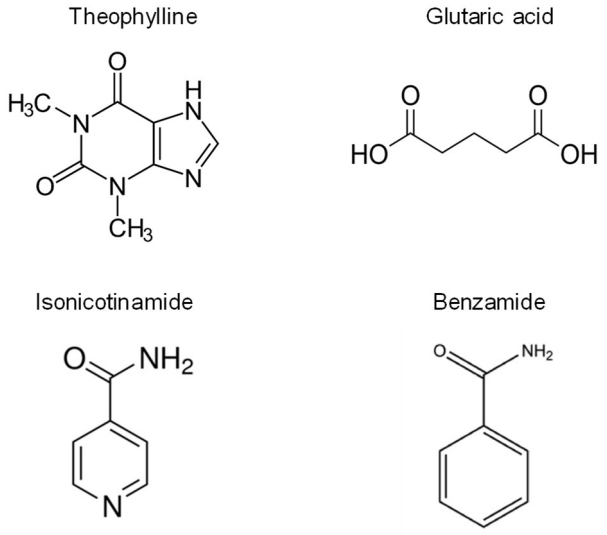

Figure 5.1. Chemical structure of anhydrous theophylline and coformers.

Theophylline-isonicotinamide (TINT; 1:1) cocrystal – TINT cocrystal was synthesized by neat grinding in a ball mill (SPEX 8000M Mixer/Mill, NJ). Theophylline (596.0 mg) and isonicotinamide (404.1 mg) were weighed into a grinding jar, and the reaction mixture was ground for 25 min at 60 Hz using two steel balls (8 mm diameter). Afterward the solid sample was characterized using powder X-ray diffractometry (XRD), differential scanning calorimetry (DSC) and, thermogravimetric analysis (TGA).

Theophylline-benzamide (TBZ; 1:1) cocrystal – TBZ cocrystal was synthesized by neat grinding in a ball mill (SPEX 8000M Mixer/Mill, NJ). Theophylline (597.9 mg) and benzamide (402.1 mg) were weighed into a grinding jar, and the reaction mixture was ground for 25 min at 60 Hz using two steel balls (8 mm diameter). Afterward the solid sample was characterized using powder XRD, DSC and TGA.

5.3.3 Tablet Preparation

Cocrystal tablets for stability study. For each of the three theophylline cocrystals (TG, TINT and TBZ), binary physical mixtures (100 mg) containing cocrystal and individual excipient were prepared in a 1:1 w/w ratio by geometric mixing. Each mixture was filled into a tablet die, held in place with a flat-faced lower punch, and compressed in a hydraulic press (Carver model C laboratory press, Menomonee Falls, WI) to a compression pressure of 177 MPa. The tablet diameter was 8 mm and the thickness was less than 2 mm. The formulated tablets were subjected to stability studies at 40 °C/75% RH chambers in open dish conditions. Control tablets (100 mg each) of pure cocrystals (TG, TINT, TBZ) were also prepared using similar method and stored at 40 °C/75% RH chambers in open dish conditions. Cocrystal dissociation in tablets containing excipients and the control tablets was monitored at select time points using laboratory source XRD.

5.3.4 Two-Dimensional X-ray Diffractometry (2D-XRD)

Intact tablet samples were mounted on an xyz stage and exposed, at room temperature, to Co Kα radiation (1.79 Å; 40 kV × 35 mA) in a two-dimensional X-ray diffractometer (D8 Discover 2D, Bruker with a 140 mm diameter window VÅNTEC-500 detector). The sample-to-detector distance was set at 20 cm and XRD patterns were collected using a 0.8 mm collimator. Two measurement frames were scanned at 10° angle of incidence with detector positioned first at 20° and then at 40° 2θ. In order to facilitate visualization, the two-dimensional XRD patterns were integrated to generate the corresponding one-dimensional patterns. Data analyses were performed using commercially available software (JADE 2010, Materials Data, Inc., Livermore, CA)

5.3.5 Thermogravimetric Analysis (TGA)

In a thermogravimetric analyzer (model Q50 TGA, TA Instruments), 5−10 mg of sample was heated in an aluminum pan from RT to 300 °C at 10 °C/min under dry nitrogen purge (75 mL/min). The TGA data were analyzed using Universal Analysis software.

5.3.6 Differential Scanning Calorimetry (DSC)

A differential scanning calorimeter (model Q2000, TA Instruments) equipped with a refrigerated cooling accessory was used. The instrument was calibrated with indium. Between 5 and 10 mg of sample was hermetically sealed in an aluminum pan. All measurements were performed at a heating rate of 10 °C/min under nitrogen purge (50 mL/min). The DSC data were analyzed using Universal Analysis software.

5.3.7 Water Sorption Analysis

Powder blends, both cocrystal alone and cocrystal-excipient binary blends, were exposed to 40 °C/75% RH in an automated vapor sorption system (Q5000 SA TA Instruments). The weight gain in the powder samples was monitored over 24 hours. All the water sorption data were analyzed using Universal Analysis software.

5.4 Results and Discussion

Baseline characterization of the three theophylline cocrystals, carried out by powder X-ray diffractometry (XRD), differential scanning calorimetry (DSC) and, thermogravimetric analysis (TGA) yielded results that were in excellent agreement with earlier findings.[155,173] The powder XRD patterns of theophylline-glutaric acid (TG), theophylline-isonicotinamide (INT) and theophylline-benzamide (TBZ) cocrystals were virtually superimposable on the calculated powder patterns published in the Cambridge Structural Database with reference codes XEJXIU[58], EVEYAH[173] and, RABXIE02[174] respectively.

Figure 5.2 is an overlay of the XRD patterns of theophylline and its cocrystals. Two unique peaks of TH (7.2° and 12.7° 2θ) are pointed out. At these angular values, none of the cocrystals exhibited diffraction peaks. Cocrystal dissociation, resulting in the formation of TH, can be readily discerned from the appearance of peaks at these angular values. The cocrystal dissociation results have been summarized in Table 5.1.

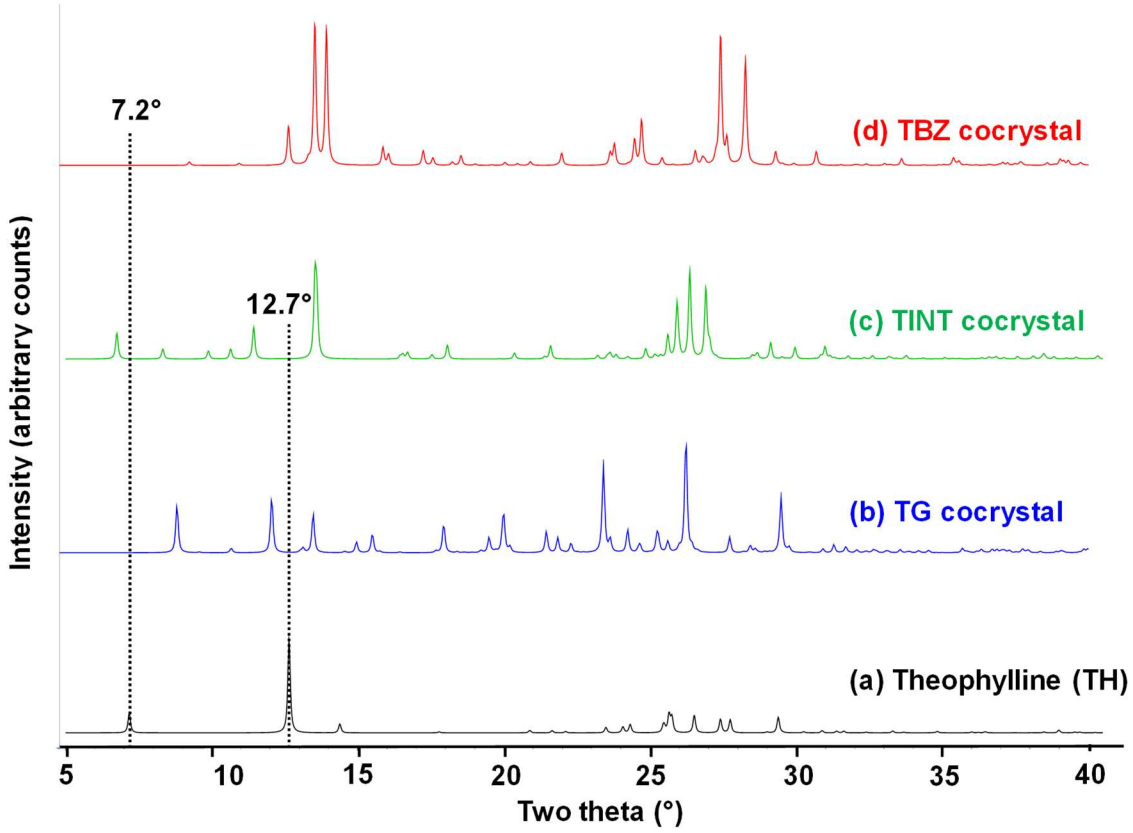

Figure 5.2. Overlay of powder XRD patterns of (a) theophylline and (b) theophylline-glutaric acid (TG), (c) theophylline-isonicotinamide (TINT) and (d) theophylline-benzamide (TBZ) cocrystals. The unique peak positions at 2θ values 7.2° and 12.7° that can be used for identification of theophylline are pointed out by dotted vertical lines.

Table 5.1. Summary of excipient induced dissociation in theophylline cocrystals.

Theophylline Cocrystal	Cocrystal Dissociation in presence of excipients (storage at 40 °C/75% RH for 7 days)				No excipients (Control) Storage at 40 °C/75% RH for 7 days
	Basic	Acidic	Neutral		
	MgSt, CCS, SSG, DCPA	ADP, ITA	MCC	LM	
Acidic coformer Theophylline-glutaric acid (TG)	D	ND	D	ND	ND
Basic coformer Theophylline-isonicotinamide (TINT)	ND	D	ND	ND	ND
Neutral coformer Theophylline-Benzamide (TBZ)	ND*	ND*	ND*	ND*	ND*

D – Dissociation, ND – No dissociation, ND* – No dissociation, cocrystal polymorphic transformation

In Chapter 4, the dissociation propensity of TG cocrystal was investigated in presence of several excipients (except adipic and itaconic acids). Both hygroscopic and basic excipients induced dissociation though the extent of the transformation was excipient dependent. For cocrystal of theophylline with GA, an acidic coformer, dissociation may be avoided by incorporating neutral or acidic excipients in the formulation. As pointed out earlier, this approach was effective with lactose, a neutral excipient with limited tendency to sorb water. However, dissociation was observed in presence of MCC, also a neutral

excipient but with a pronounced tendency to sorb water. To confirm the effectiveness of acidic excipients, the stability of TG cocrystal was investigated in presence of adipic (ADP) and itaconic (ITA) acids. Following storage of binary compacts (1:1 w/w) of TG cocrystal with each ADP and ITA acids at 40 °C/75% RH for 1 week, there was no appearance of the characteristic peaks of TH, suggesting that TG cocrystal was stable in the presence of acidic excipients (Figure 5.3).

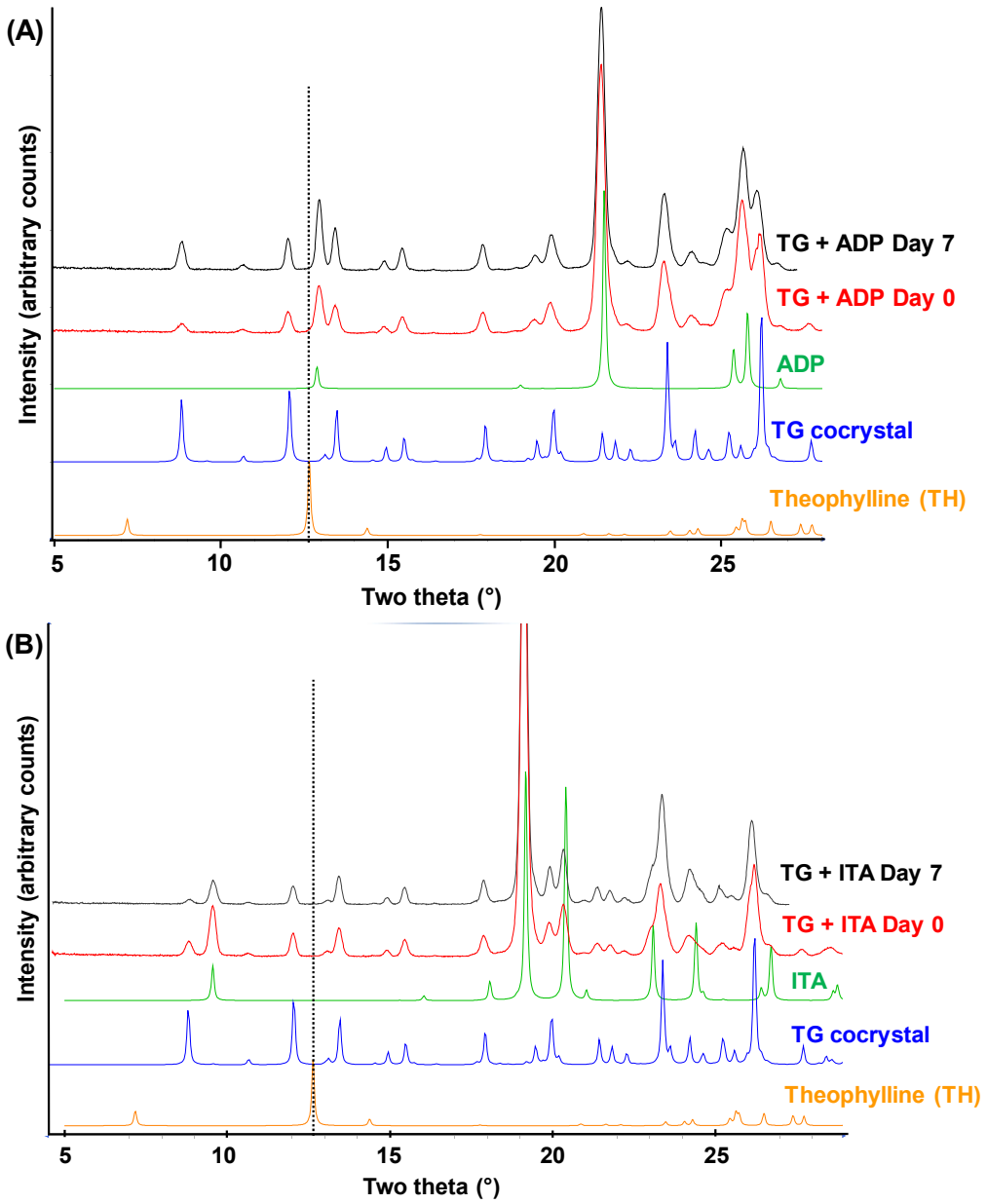

Figure 5.3. Overlay of XRD patterns of TG binary tablets (1:1 w/w) with: (A) adipic acid (ADP) and, (B) itaconic acid (ITA). The diffractograms of the freshly prepared (day 0) and the stored (40 °C/75% RH for 7 days) tablets are presented. Reference patterns of TH, TG cocrystal, adipic acid and itaconic acid are also provided. The dotted line points the highest intensity peak unique to TH.

The stability of TG cocrystal in the presence of acidic excipients can be explained from our earlier observations (Chapter 4). We had observed dissociation of TG cocrystal in presence of DCPA, a crystalline basic excipient. Pronounced lattice disorder at the

cocrystal-excipient interface, resulting from compression, facilitated water sorption. The sorbed water can serve as a medium for the proton transfer from glutaric acid to hydrogen phosphate anion (HPO_4^{2-}), driving cocrystal dissociation. However, in the presence of adipic and itaconic acids, ionization of glutaric acid in solution is not favored thereby retaining the cocrystal stable.

Thus, cocrystal stability in the presence of excipients is dictated by two factors: (i) ability of the coformer to ionize in response to the microenvironment created by the excipient, and (ii) the solubility difference between cocrystal and the parent drug.

Building upon our findings in the TG cocrystal, we investigated the propensity of TINT and TBZ cocrystals to undergo excipient induced dissociation. These results are discussed in the subsequent sections.

Theophylline-Isonicotinamide cocrystal (TINT; 1:1). A cocrystal of theophylline with isonicotinamide, a basic coformer (pKa 3.61)[175], contains the amide-pseudo amide hydrogen bonding motif between the two coformers. Details of the crystal structure are reported by Fischer et al.[173] The TINT cocrystal has three different types of hydrogen bonds: (i) between the acidic imidazole nitrogen atom from a theophylline molecule and the oxygen atom from the amide group of the isonicotinamide molecule, (ii) between the amide group of an isonicotinamide molecule and the carbonyl group of a theophylline molecule, and (iii) between the amide group of an isonicotinamide molecule and the second carbonyl group of a theophylline molecule, resulting in a chain-structure motif.

Control tablets of TINT (no excipients), when stored at 40 °C/75% RH, were stable for a week, with no appearance of the characteristic peaks of TH (Figure 5.4). Moreover, the

TINT peak intensities did not decrease as a function of time. We therefore concluded that, in the absence of excipients, the TINT cocrystal was robust. In order to determine the stability of TINT cocrystal in presence of excipients, binary tablets of TINT with each excipient, prepared in a 1:1 w/w ratio, were stored at 40 °C/75% RH for one week. Cocrystal dissociation in each of the binary tablets was monitored by powder XRD.

Among the excipients investigated, dissociation of the TINT cocrystal occurred rapidly in tablets containing each, itaconic acid (ITA; Figure 5.5A) and, adipic acid (ADP; Figure 5.5B). In these tablets, following storage at 40 °C/75% RH for 1 day, the formation of crystalline TH (dissociation product), was readily evident from the appearance of its characteristic peak at 12.7° 2θ in the XRD pattern (Figure 5.5). In contrast, in binary tablets of TINT with basic (CCS, SSG, MgSt, DCPA) or neutral (MCC, LM) excipients, there was no evidence of TH formation following storage at 40 °C/75% RH for one week (data not shown).

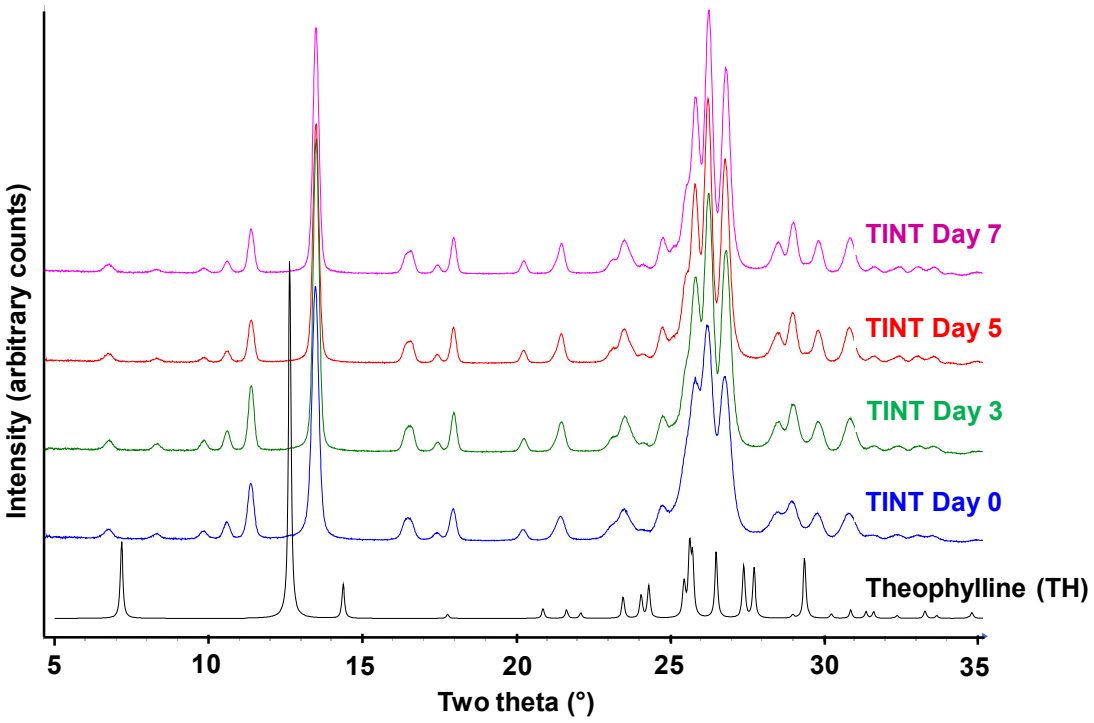

Figure 5.4. Overlay of XRD patterns of control tablets of TINT (no excipient) following storage at 40 °C/75% RH for one week. The XRD pattern of TH is also included.

These results complement our findings of excipient induced dissociation in TG cocrystal (Table 5.1). The stability of theophylline cocrystal with ionizable (acidic or basic) coformers appears to be strongly influenced by the formulation excipients. Following water sorption, the ionizable excipients, depending on their nature and concentration, can influence the local microenvironmental pH, and thereby facilitate coformer ionization. Thus, acidic excipients (ITA, ADP) were detrimental to the stability of cocrystal of theophylline with a basic coformer, isonicotinamide. Similarly, basic excipients (MgSt, CCS, SSG, DCPA) caused the dissociation of a cocrystal of theophylline with an acidic coformer, glutaric acid (Table 5.1).

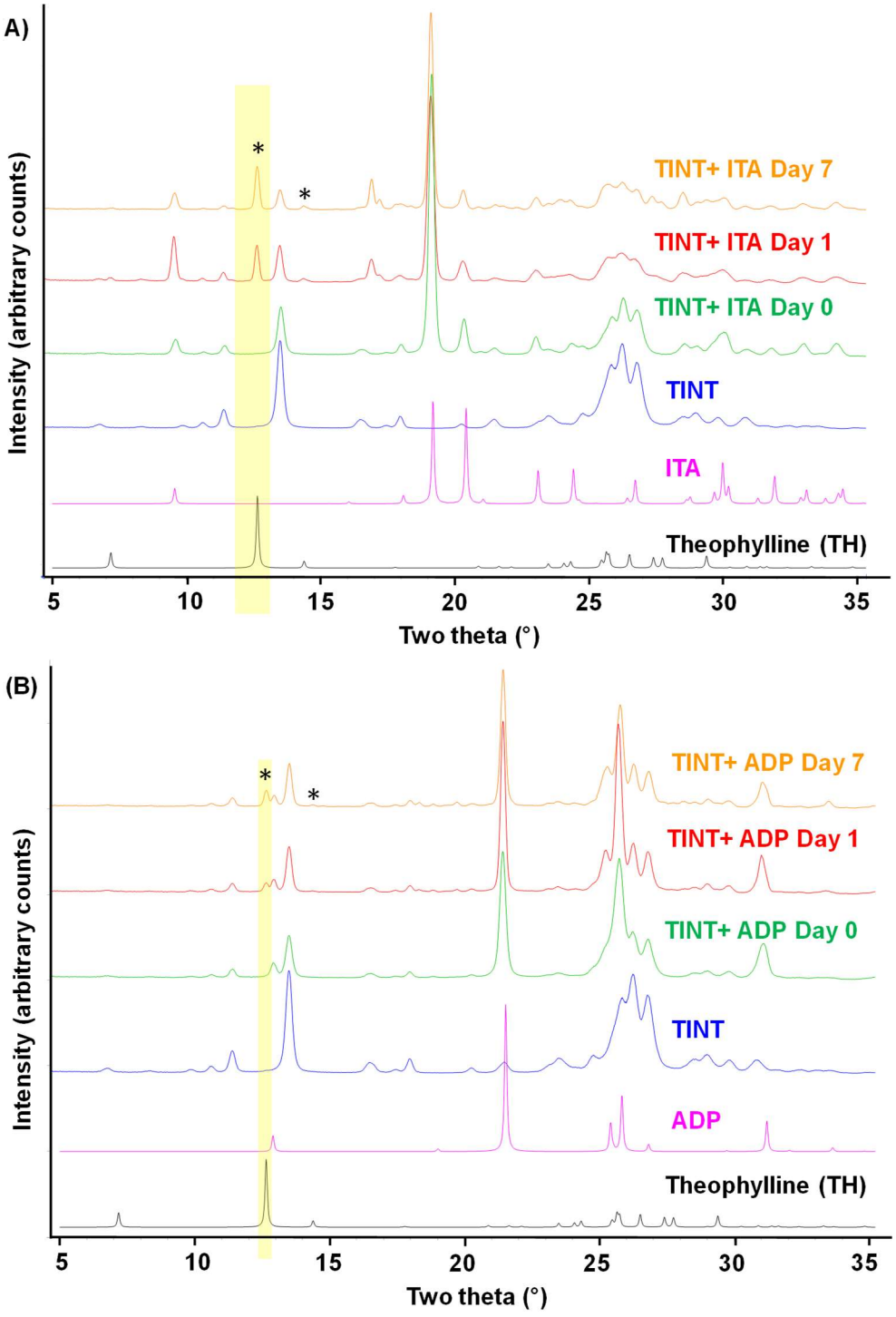

Figure 5.5. XRD patterns of TINT binary tablets (1:1 w/w) with (A) itaconic acid (ITA) and (B) adipic acid (ADA). In each panel, the XRD patterns of the fresh tablets (day 0) and following storage at 40°C/75% RH (days 1 and 7) are presented. The reference patterns of TH, ITA, ADP, and TINT cocrystal are also shown. One characteristic TH peak (*), observed as a consequence of TINT cocrystal dissociation, is highlighted.

Interestingly, unlike the TG cocrystal, the TINT cocrystal did not dissociate in the presence of MCC (neutral and hydrophilic excipient). The TG and TINT cocrystals, by themselves, sorb < 0.5% water at 40 °C/75% RH. However, binary blends of each cocrystal with MCC revealed a water uptake of ~2.5%, attributable to the hydrophilic nature of MCC. A fraction of the water sorbed by MCC is expected to have properties of "bulk" (i.e. "free") water and can potentially serve as a medium for solution-mediated transformations.[176]

The difference in the dissociation propensity of TG and TINT cocrystals in the presence of MCC can be explained by the relative aqueous solubilities of the two cocrystals. The cocrystal to parent drug solubility ratio (in this case, solubility of TINT/solubility of TH), appears to be the driving force for cocrystal dissociation in solution. Generally, cocrystal solubility increases as a function of coformer solubility.[148,177,178] For theophylline, carbamazepine, and caffeine cocrystals, a direct correlation between cocrystal and coformer solubilities was evident.[177] When cocrystals of carbamazepine were slurried in water, dissociation was observed selectively in cases where the coformers had a "relatively" high aqueous solubility.[179] In our case, since the molar solubility of GA is approximately 8-fold that of INT, it is expected that the solubility of TG cocrystal >> TINT cocrystal. As a result, the driving force for dissociation of TG cocrystal is expected to be much higher.

Theophylline-Benzamide cocrystal (TBZ; 1:1). Cocrystal of theophylline with benzamide, a neutral coformer, is reported to exist as two polymorphic forms. The crystal structures of the two TBZ cocrystal polymorphs were reported by Fischer et al.[174,180] The metastable TBZ form I was generated when an equimolar ratio of theophylline to benzamide was subjected to neat or liquid-assisted grinding in the presence of a non-polar

solvent (e.g. cyclohexane). The thermodynamically stable TBZ form II resulted from grinding the coformers (or TBZ form I) in the presence of a polar solvent (e.g. water, acetone, ethanol or acetonitrile). Belenguer et al. studied the conversions between the two polymorphic forms as a function of solvent concentration and established a relationship between water concentration and weight fraction of form II.[181] Both polymorphs have the amide-pseudo amide hydrogen bonding motif between the two coformers.

In this work, consistent with previous reports, TBZ cocrystal form I resulted from neat grinding of theophylline and benzamide in a ball mill.[173] The form I cocrystal was compressed (without excipients) to form control tablets. Additionally, binary tablets of form I cocrystal with each excipient in a 1:1 w/w were prepared. To evaluate the dissociation propensity of TBZ cocrystal, the tablets (excipient containing and control), were stored at 40 °C/75% RH for 1 week and were monitored periodically.

The powder XRD pattern of the control tablets stored at 40 °C/75% RH for a day, revealed the appearance of several new peaks, and their positions matched with that of stable TBZ form II polymorph (Figure 5.6). There was no evidence of TH formation. The polymorphic transformation appears to be complete after 7 days of storage at 40 °C/75% RH (Figure 5.6). The 2D XRD image of the freshly prepared control tablet revealed smooth and continuous Debye rings. However, just after a day of storage at 40 °C/75% RH, the rings exhibited a spotty character, revealing the formation of large crystallites of form II.

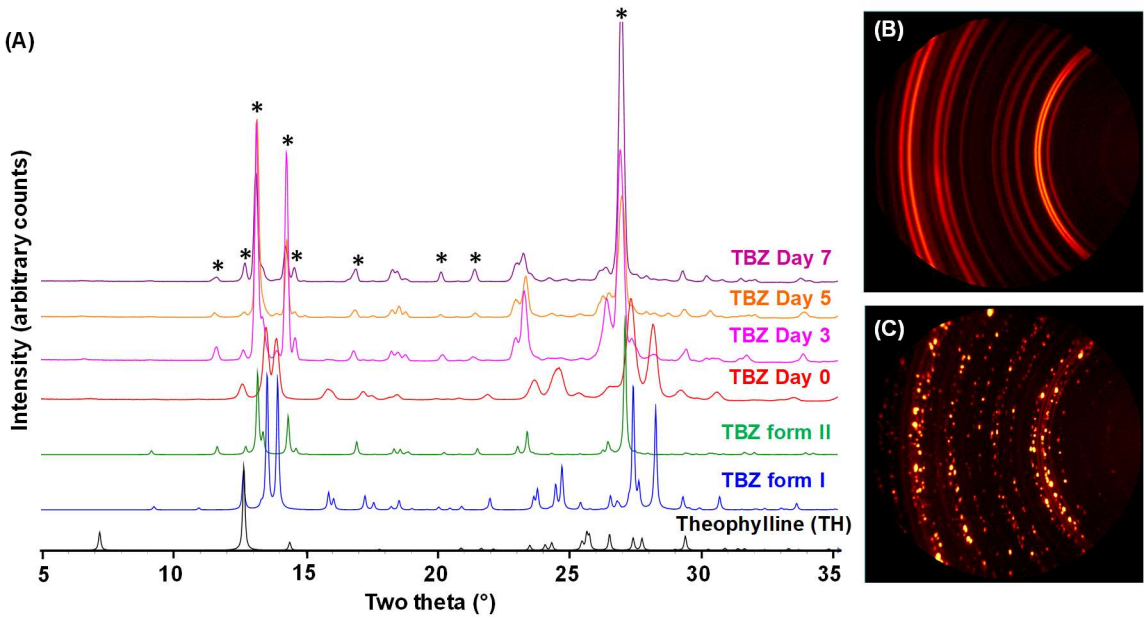

Figure 5.6. A) Overlay of one-dimensional XRD patterns of TBZ cocrystal tablets at day 0 and following storage at 40 °C/75% RH for up to 7 days. To enable comparison, the reported XRD patterns of theophylline and the TBZ cocrystal polymorphs (forms I and II) are also presented. (B) and (C) are respectively the two-dimensional images of the fresh TBZ tablet (at day 0) and after storage for 7 days (40 °C/75% RH). The several unique peaks of TBZ cocrystal form II are pointed out (*).

While direct addition of bulk water is known to facilitate crystallization of the stable TBZ form II polymorph,[180] our results indicate that exposure to elevated temperature (40 °C) and water vapor pressure (75%) can also bring about polymorphic transformation in TBZ cocrystal system. A similar example demonstrating differences in stability of cocrystal polymorphs has been reported for form I and form II cocrystals of caffeine-glutaric acid.[59,182]

In binary tablets of TBZ with each excipient (1:1 w/w ratio), the appearance of several characteristic peaks of TBZ form II was readily discernable in the powder XRD patterns of the tablets collected after 1 week of storage at 40 °C/75% RH. As representative examples, the XRD patterns of binary compacts of TBZ with MgSt (Figure 5.7A), SSG

(Figure 5.7B), MCC (Figure 5.7C), and DCPA (Figure 5.7D) are shown. The highlighted region in Figure 5.7, between 12.0° and 15.0° 2θ, reveals the appearance of form II TBZ cocrystal. There was no evidence of TH formation. Thus, while the TBZ cocrystal underwent a polymorphic transformation, both in the presence and absence of excipients, there was no evidence of cocrystal dissociation.

.

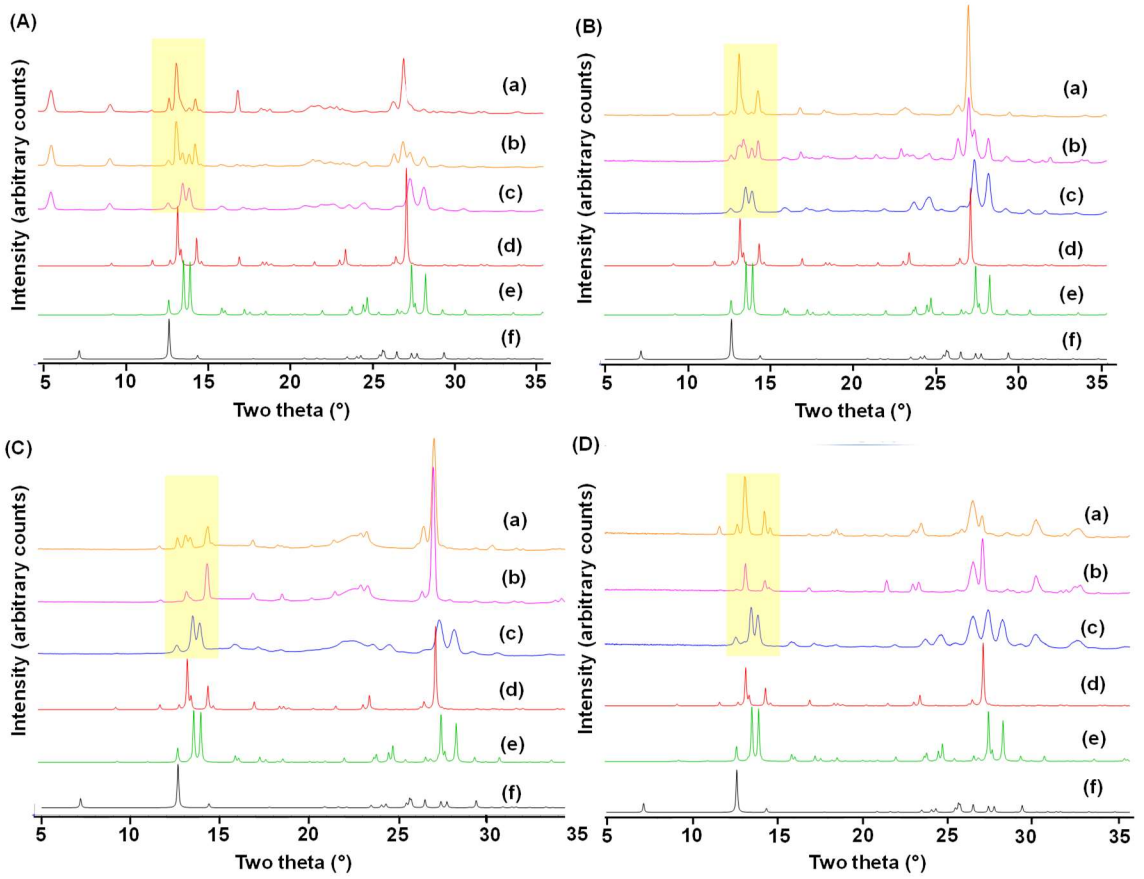

Figure 5.7. Overlay of XRD patterns of binary compacts of TBZ prepared with (A) MgSt, (B) SSG, (C) MCC, and (D) DCPA. Each panel contains the XRD patterns of freshly prepared compacts (c) and after storage at 40 °C/75% RH for 3 days (b) and 7 days (a). The reference patterns of TBZ cocrystal form II, form I, and TH are presented in (d), (e) and (f), respectively. A select portion of the 2θ range wherein peaks for TBZ form II were observed, as a consequence of cocrystal polymorphic transformation is highlighted.

5.5 Significance

The coformer provides an avenue to modulate cocrystal stability when formulated into a solid dosage form, i.e. in the presence of excipients. We observed that acidic excipients (ITA, ADP) were detrimental to the stability of theophylline when cocrystallized with a basic coformer (isonicotinamide). Similarly, basic excipients (MgSt, CCS, SSG, DCPA) destabilized cocrystal of theophylline with an acidic coformer (glutaric acid). Thus, a potential for excipient-induced cocrystal dissociation exists for cocrystals comprising of acidic and basic coformers. If there is limited flexibility with respect to excipient selection, the use of a neutral coformer can provide an avenue to minimize the risk of cocrystal dissociation. Furthermore, the solubility difference between the cocrystal and the parent drug is the driving force for cocrystal dissociation. In this context, it is instructive to see the parallel between salt and cocrystal disproportionation. As pointed out by Stephenson et al., the objective of salt selection is to enhance solubility but only to the desired extent.[27] Pronounced solubility enhancement, with respect to the free acid (or base) can lead to physical and chemical instability.[27] A similar conundrum may be faced with cocrystal systems.

5.6 Conclusions

Basic and hygroscopic excipients induced dissociation of the TG cocrystal, while acidic excipients rendered the cocrystal stable. In contrast, the presence of acidic excipients was detrimental to the stability of the TINT cocrystal, whereas the cocrystal was intact in presence of basic and neutral excipients. In case of the TBZ cocrystal, although cocrystal dissociation was not observed, a polymorphic transformation occurred.

Chapter 6 : Summary

When dealing with drugs having sub-optimal physicochemical and/or biopharmaceutical properties - for example low aqueous solubility, poor processability, or low bioavailability, formation of salts and cocrystals provides an avenue to modify the drug properties. However, the success of this approach hinges on retaining the intact salt and cocrystal, both during processing and storage. The overall goal of this thesis was to develop mechanistic insights into solid-state stability of pharmaceutical salts and cocrystals in drug product environment. The role of drug-excipient interactions, impact of processing and storage conditions, on salt and cocrystal disproportionation reactions in formulations (tablets and lyophilized systems) were investigated. The use of several complementary analytical techniques such as powder X-ray diffractometry (laboratory and synchrotron source), spectroscopy and thermo-analytical methods, enabled us to develop an in-depth understanding of the disproportionation mechanism. One important theme that emerged for both salts and cocrystals APIs, was the critical role of excipients, sorbed water and microenvironmental acidity on disproportionation in multi-component pharmaceutical formulations.

The first part of the thesis (Chapters 2 and 3), focused on the effect of excipients and processing conditions on salt disproportionation in tablet and lyophilized formulations. The research overview for these chapters is presented in Figure 6.1 and a summary of the findings from the individual chapters is given below.

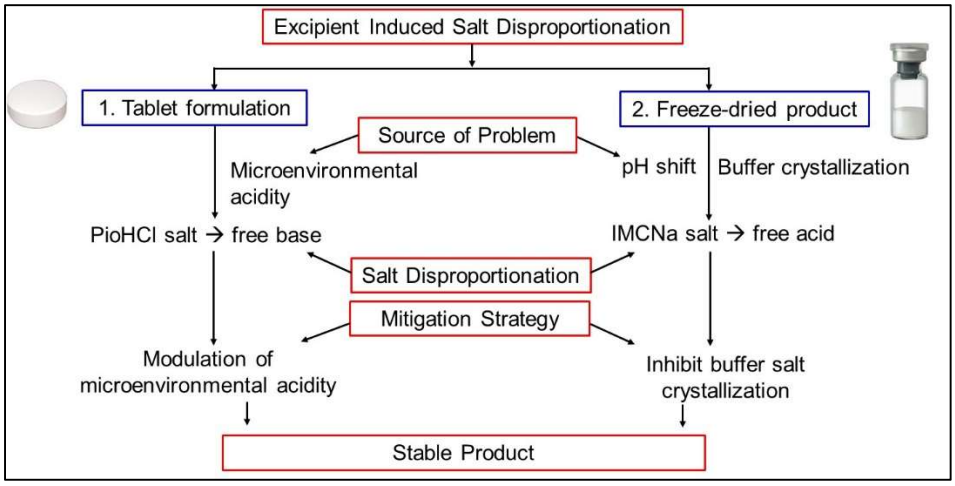

Figure 6.1. Flowchart describing the overview of salt disproportionation research discussed in Chapters 2 and 3.

Chapter 2. In tablet formulations of pioglitazone hydrochloride (PioHCl), the presence of basic excipients (magnesium stearate or croscarmellose sodium) caused disproportionation, yielding the crystalline free base. Salt disproportionation occurred via a solution-mediated transformation, wherein water (i) causes solution formation at the excipient-drug interface, (ii) affects the microenvironmental acidity "experienced" by the salt and (iii) serves as a medium for proton transfer. Synchrotron XRD enabled the simultaneous quantification of PioHCl (reactant) remaining and free base (product) formed in the tablets. The *in situ,* real time tablet "mapping" experiments revealed first evidence of disproportionation in intact tablets. The disproportionation reaction was initiated on the tablet surface and progressed towards the tablet core. The transformation was solution-mediated and the spatial heterogeneity in disproportionation could be explained by the migration of sorbed water (Figure 6.2). This finding represented the first known example of spatial heterogeneity of salt disproportionation in intact tablets. A good correlation

between microenvironmental acidity and extent of PioHCl disproportionation was demonstrated.

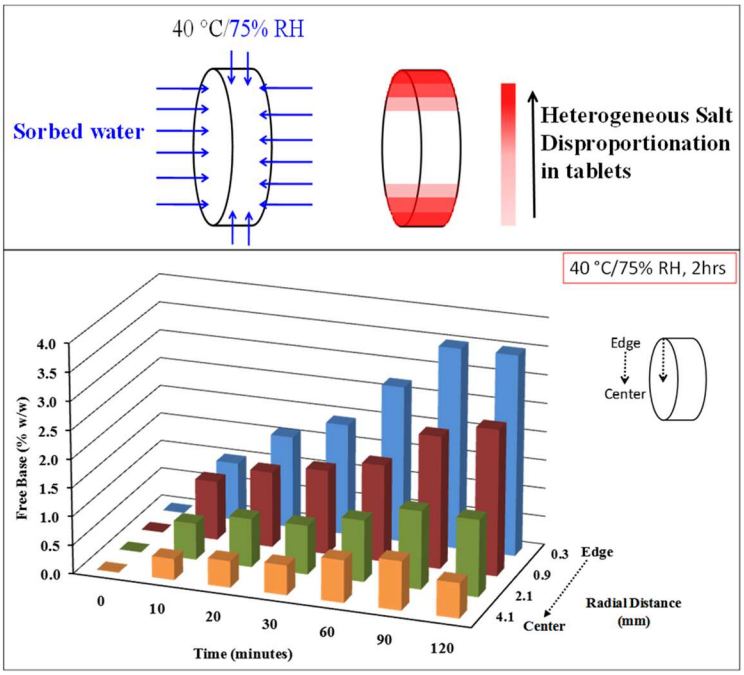

Figure 6.2. Schematic representation of the spatial heterogeneity in salt disproportionation in intact tablets.

Chapter 3. Salt disproportionation in lyophilized formulations, while posing a challenging problem, has not been extensively investigated. In lyophilized formulations of indomethacin sodium (IMCNa), selective crystallization of the buffer component ($Na_2HPO_4 \cdot 12H_2O$) during freezing and the consequent pH lowering, resulted in disproportionation of a soluble salt (IMCNa) to an insoluble (IMC) free acid (Figure 6.3). Low temperature pH measurements served as an effective tool to identify salt disproportionation during freeze-drying. The concentration of the IMCNa influenced the crystallization behavior of the buffer and thereby the salt ➔ free acid conversion. Thus, a complex interplay of the API and excipient concentrations dictated the API stability.

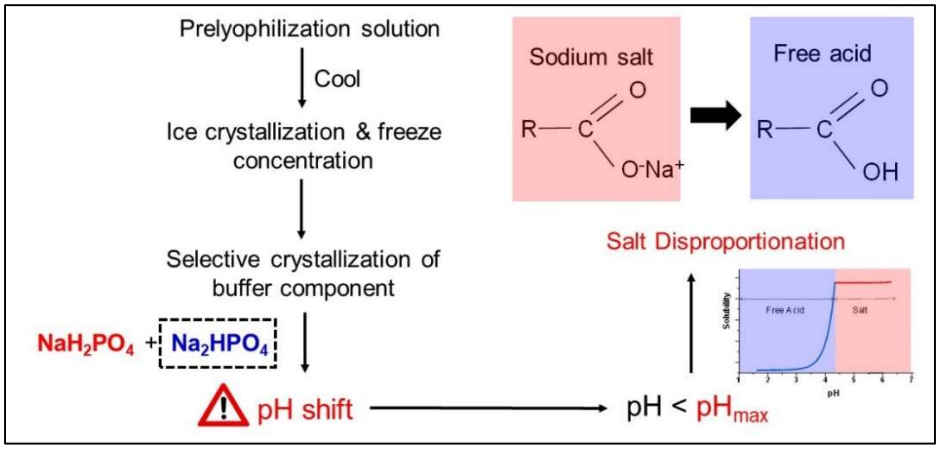

Figure 6.3. Schematic representation of salt disproportionation during lyophilization.

Thus, the salt disproportionation investigations carried out in model tablet and lyophilized formulations, enabled an in-depth understanding of the disproportionation mechanism. This can aid in the development of strategies for preventing, or at least controlling, disproportionation. Salt disproportionation mitigation strategies are discussed in the future work (Chapter 7) of this thesis.

The second part of the thesis (Chapters 4 and 5), demonstrated the potential risk of excipient-induced cocrystal dissociation in tablet formulations and highlights the critical role of coformer properties on cocrystal stability. A summary of the findings in these chapters is given below.

Chapter 4. Tablets of theophylline-glutaric acid (TG) cocrystal (without excipient) were stable at 40 °C/75% RH for 2 weeks. However, in prototype tablet formulations, the cocrystal rapidly dissociated, forming crystalline theophylline, at 40 °C/75% RH (Figure 6.4). Utilizing two-dimensional XRD (laboratory and synchrotron source), a nondestructive technique, cocrystal dissociation kinetics in intact tablets formulations were monitored. The water-mediated dissociation reaction occurred rapidly and was strongly

influenced by formulation composition. Several excipients, widely used in manufacture of tablets (e.g. microcrystalline cellulose, sodium starch glycolate), caused cocrystal dissociation. Dissociation was pronounced in the presence of hydrophilic excipients with a strong tendency to sorb water. In contrast, the cocrystal was stable in the presence of a neutral excipient with no tendency to sorb water. Microcrystalline cellulose, while a neutral but hydrophilic excipient, caused dissociation, an effect attributed the pronounced aqueous solubility difference between theophylline and TG cocrystal. The reaction between magnesium stearate and theophylline-glutaric acid cocrystals resulted in a coordination complex (Figure 6.4). Thus, in intact tablets, a chemical reaction between excipient and cocrystal components was observed.

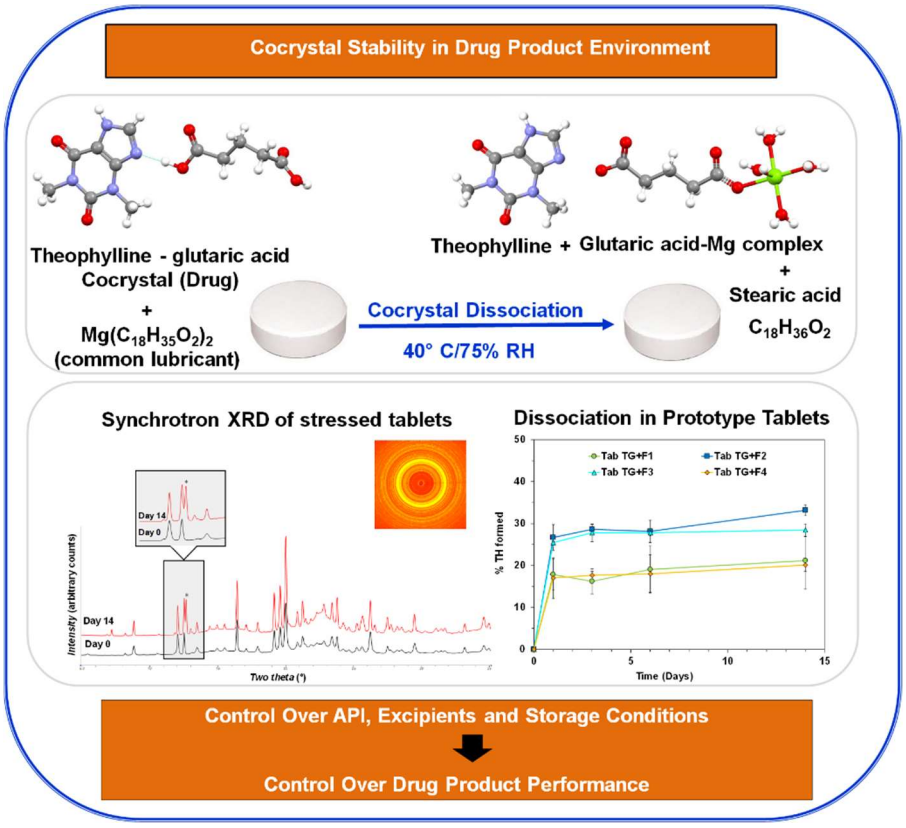

Figure 6.4. Schematic illustration of excipient-induced dissociation in tablet formulations of theophylline-glutaric acid cocrystal.

Chapter 5. In this Chapter, we attempted to gain insights into the role of coformer properties on cocrystal stability. Therefore, building upon our findings in the TG cocrystal, discussed in Chapter 4, two other coformers were investigated. Isonicotinamide (INT) and benzamide (BZ) were selected as the basic and neutral coformer, respectively. The stability of the three theophylline cocrystals (TG, TINT and TBZ) was investigated in the presence of several excipients following storage at 40 °C/75% RH for one week. In case of TG and TINT cocrystals, while the 'as is' (no excipient) cocrystals were stable at 40 °C/75% RH for one week, they rapidly dissociated in the presence of selective excipients. A cocrystal of theophylline with isonicotinamide, a basic coformer, dissociated in presence of acidic coformers. Complementarily, a cocrystal of theophylline with glutaric acid, an acidic coformer, dissociated in the presence of basic excipients. In case of the theophylline cocrystal with benzamide, a neutral coformer, although cocrystal dissociation was not observed, a polymorphic transformation occurred with and without excipients. Thus, a potential for excipient-induced cocrystal dissociation exists for cocrystals comprised of acidic and basic coformers. Furthermore, if a chosen coformer renders a highly soluble cocrystal, even in presence of a neutral excipient, the cocrystal can have a high propensity to undergo dissociation.

Chapter 7 : Future Work

This thesis focused on understanding the fundamental mechanisms underlying the physical instability of salts and cocrystals in drug product environment. The ultimate goal is to develop solid-state formulations of salts and cocrystals having reproducible and predictable performance, with minimum batch-to-batch variation and an optimum shelf-life. The future work arising from these studies is discussed in the following sections.

In Chapter 2, it was demonstrated that salt disproportionation reaction, mediated by water, is attributed to the microenvironmental acidity "experienced" by the salt particles in the formulation. This can form the basis for the development of a rational and systematic approach to prevent salt disproportionation by modulation of microenvironmental acidity of the solid formulation. Future studies need to examine the effect of adding pH modifiers to modulate the acidity in the solid formulation and thereby influence the extent of disproportionation. Based on the assumption that microenvironmental acidity is reflective of the pH in the adsorbed water layer, it can be hypothesized that the water-soluble pH modifier dissolves in the water layer to form a saturated solution. Therefore, the effect of a pH modifier on the microenvironmental acidity will be dependent on both its ionization constant (pKa) as well as its aqueous solubility. Furthermore, it would be interesting to assess the effect of mode of incorporation of the pH modifier on the extent of disproportionation. If the incorporation is not uniform, there can still be "exposed" reactive surfaces. Approaches that favor a more homogenous distribution of the pH modifier can potentially be successful in preventing disproportionation completely.

In Chapter 3, using indomethacin sodium (IMCNa) as a model compound, we have documented its disproportionation propensity during lyophilization in the presence of

sodium phosphate buffer. During freeze drying, the selective crystallization of buffer component (dibasic sodium phosphate) and the consequent pH shift resulted in disproportionation of a soluble salt (IMCNa) to an insoluble free acid. Future studies examining the effect of adding cosolutes, such as sucrose or trehalose, that modulate the crystallization behavior of buffer components and thereby prevent pH shifts, need to be tested so as to mitigate salt disproportionation in lyophilized formulations.

In Chapters 4 and 5, we demonstrated the dissociation propensity of theophylline cocrystals in the presence of several excipients. The dissociation reaction was water mediated and occurred very rapidly (timescale of days) even in prototype formulations containing realistic concentration of excipients. The ionizable nature of the coformer and the aqueous solubility of the cocrystal appeared to dictate cocrystal stability in presence of excipients. Based on a mechanistic understanding of cocrystal dissociation, the next step would be to develop strategies to prevent dissociation. Since cocrystal dissociation is a water-mediated reaction, formulation approaches that limit the entry of water such as film coating of tablets, use of colloidal hydrophobic silica for coating cocrystal particles combined with the incorporation of hydrophilic silica that can serve as water scavenger in the formulation, need to be investigated in detail. Moreover, as the water-mediated dissociation is expected to initiate at the poorly crystalline regions of cocrystal-excipient particle interface, approaches such as annealing that can lead to an increased crystallinity and thereby decreased water uptake, should be examined. For cocrystals that exhibit a pH_{max}, formulation strategies to control the local pH of the solid dosage forms should be explored. Furthermore, formulation approaches that can minimize the contact area between cocrystal and excipients would be interesting to evaluate.

Bibliography

(1) Broach, J. R.; Thorner, J. High-Throughput Screening for Drug Discovery. *Nature* **1996**, *384* (6604), 14–16.

(2) Teague; Davis; Leeson; Oprea. The Design of Leadlike Combinatorial Libraries. *Angew. Chem. Int. Ed. Engl.* **1999**, *38* (24), 3743–3748.

(3) Dressman, J. B.; Amidon, G. L.; Reppas, C.; Shah, V. P. Dissolution Testing as a Prognostic Tool for Oral Drug Absorption: Immediate Release Dosage Forms. *Pharm. Res.* 1998, pp 11–22.

(4) Yu, L. X. An Integrated Model for Determining Causes of Poor Oral Drug Absorption. *Pharm. Res.* **1999**, *16* (12), 1883–1887.

(5) Zhang, Y.; Benet, L. Z. The Gut as a Barrier to Drug Absorption: Combined Role of Cytochrome P450 3A and P-Glycoprotein. *Clin. Pharmacokinet.* **2001**, *40* (3), 159–168.

(6) Amidon, G. L.; Lennernäs, H.; Shah, V. P.; Crison, J. R. A Theoretical Basis for a Biopharmaceutic Drug Classification: The Correlation of in Vitro Drug Product Dissolution and in Vivo Bioavailability. *Pharm. Res.* 1995, pp 413–420.

(7) Butler, J. M.; Dressman, J. B. The Developability Classification System: Application of Biopharmaceutics Concepts to Formulation Development. *J. Pharm. Sci.* **2010**, *99* (12), 4940–4954.

(8) Childs, S. L.; Stahly, G. P.; Park, A. The Salt-Cocrystal Continuum: The Influence of Crystal Structure on Ionization State. *Mol. Pharm.* **2007**, *4* (3), 323–338.

(9) Aitipamula, S.; Banerjee, R.; Bansal, A. K.; Biradha, K.; Cheney, M. L.; Choudhury, A. R.; Desiraju, G. R.; Dikundwar, A. G.; Dubey, R.; Duggirala, N.; Ghogale, P. P.; Ghosh, S.; Goswami, P. K.; Goud, N. R.; Jetti, R. R. K. R.; Karpinski, P.; Kaushik, P.; Kumar, D.; Kumar, V.; Moulton, B.; Mukherjee, A.; Mukherjee, G.; Myerson, A. S.; Puri, V.; Ramanan, A.; Rajamannar, T.; Reddy, C. M.; Rodriguez-Hornedo, N.; Rogers, R. D.; Row, T. N. G.; Sanphui, P.; Shan, N.; Shete, G.; Singh, A.; Sun, C. C.; Swift, J. A.; Thaimattam, R.; Thakur, T. S.; Kumar Thaper, R.; Thomas, S. P.; Tothadi, S.; Vangala, V. R.; Variankaval, N.; Vishweshwar, P.; Weyna, D. R.; Zaworotko, M. J. Polymorphs, Salts, and Cocrystals: What's in a Name? *Cryst. Growth Des.* **2012**, *12* (5), 2147–2152.

(10) Duggirala, N. K.; Perry, M. L.; Almarsson, Ö.; Zaworotko, M. J. Pharmaceutical Cocrystals: Along the Path to Improved Medicines. *Chem. Commun.* **2016**, *52* (4), 640–655.

(11) Stahl, P.H., Wermuth, C. G. *Handbook of Pharmaceutical Salts Properties, Selection, and Use.*, Second, re.; Wiley-VCH, New York., 2011.

(12) O'Connor, K. M.; Corrigan, O. I. Preparation and Characterisation of a Range of Diclofenac Salts. *Int. J. Pharm.* **2001**, *226* (1–2), 163–179.

(13) David, S. E.; Timmins, P.; Conway, B. R. Impact of the Counterion on the Solubility and Physicochemical Properties of Salts of Carboxylic Acid Drugs. *Drug Dev. Ind. Pharm.* **2012**, *38* (1), 93–103.

(14) Kumar, L.; Amin, A.; Bansal, A. K. Preparation and Characterization of Salt Forms of Enalapril. *Pharm. Dev. Technol.* **2008**, *13* (5), 345–357.

(15) Paulekuhn, G. S.; Dressman, J. B.; Saal, C. Trends in Active Pharmaceutical Ingredient Salt Selection Based on Analysis of the Orange Book Database. *J. Med. Chem.* **2007**, *50* (26), 6665–6672.

(16) Corrigan, O. I. *Salt Forms : Pharmaceutical Aspects*, Fourth.; Informa Healthcare, New York, 2013; Vol. 4.

(17) Gould, P. L. Salt Selection for Basic Drugs. *Int. J. Pharm.* **1986**, *33* (1–3), 201–217.

(18) Berge, S.; Bighley, L.; Monkhouse, D. Pharmaceutical Salts. *J. Pharm. Sci* **1977**, *66* (1), 1–19.

(19) Bastin, R. J.; Bowker, M. J.; Slater, B. J. Salt Selection and Optimisation Procedures for Pharmaceutical New Chemical Entities. *Org. Process Res. Dev.* **2000**, *4* (5), 427–435.

(20) Thakral, N. K.; Behme, R. J.; Aburub, A.; Peterson, J. A.; Woods, T. A.; Diseroad, B. A.; Suryanarayanan, R.; Stephenson, G. A. Salt Disproportionation in the Solid State: Role of Solubility and Counterion Volatility. *Mol. Pharm.* **2016**, *13* (12), 4141–4151.

(21) Thakral, N. K.; Kelly, R. C. Salt Disproportionation : A Material Science Perspective. *Int. J. Pharm.* **2017**, *520* (1–2), 228–240.

(22) Nie, H.; Byrn, S. R.; Zhou, Q. (Tony). Stability of Pharmaceutical Salts in Solid Oral Dosage Forms. *Drug Dev. Ind. Pharm.* **2017**, *43* (8), 1215–1228.

(23) Rohrs, B.; Thamann, T.; Ping, G.; Stelzer, D.; Bergren, M.; Chao, R. Tablet Dissolution Affected by a Moisture Mediated Solid-State Interaction Between Drug and Disintegrant. *Pharm. Res.* **1999**, *16* (12), 1850–1856.

(24) Zannou, E. a.; Ji, Q.; Joshi, Y. M.; Serajuddin, A. T. M. Stabilization of the Maleate Salt of a Basic Drug by Adjustment of Microenvironmental pH in Solid Dosage Form. *Int. J. Pharm.* **2007**, *337* (1), 210–218.

(25) Unger, E. F. Weighing Benefits and Risks — The FDA ' S Review of Prasugrel. *N. Engl. J. Med.* **2009**, *361* (10), 942–945.

(26) Williams, A. C.; Cooper, V. B.; Thomas, L.; Griffith, L. J.; Petts, C. R.; Booth, S. W. Evaluation of Drug Physical Form during Granulation , Tabletting and Storage. *Int. J. Pharm.* **2004**, *275*, 29–39.

(27) Stephenson, G. A.; Aburub, A.; Woods, T. A. Physical Stability of Salts of Weak Bases in the Solid-State. *J. Pharm. Sci.* **2011**, *100* (5), 1607–1617.

(28) Guerrieri, P.; Taylor, L. S. Role of Salt and Excipient Properties on

Disproportionation in the Solid-State. *Pharm. Res.* **2009**, *26* (8), 2015–2026.

(29) Bogardus, J. B.; Blackwood, R. K. Solubility of Doxycycline in Aqueous Solution. *J. Pharm. Sci.* **1979**, *68* (2), 188–194.

(30) Serajuddin, A. T. M. Salt Formation to Improve Drug Solubility. *Adv. Drug Deliv. Rev.* **2007**, *59* (7), 603–616.

(31) Hsieh, Y.-L.; Taylor, L. S. Salt Stability - Effect of Particle Size, Relative Humidity, Temperature and Composition on Salt to Free Base Conversion. *Pharm. Res.* **2014**, *32* (2), 549–561.

(32) Christensen, N. P. A.; Rantanen, J.; Cornett, C.; Taylor, L. S. Disproportionation of the Calcium Salt of Atorvastatin in the Presence of Acidic Excipients. *Eur. J. Pharm. Biopharm.* **2012**, *82* (2), 410–416.

(33) Hsieh, Y.-L.; Merritt, J. M.; Yu, W.; Taylor, L. S. Salt Stability – The Effect of pHmax on Salt to Free Base Conversion. *Pharm. Res.* **2015**, *32* (9), 3110–3118.

(34) Merritt, J. M.; Viswanath, S. K.; Stephenson, G. a. Implementing Quality by Design in Pharmaceutical Salt Selection: A Modeling Approach to Understanding Disproportionation. *Pharm. Res.* **2012**, *30* (1), 1–15.

(35) John, C. T.; Xu, W.; Lupton, L. K.; Harmon, P. A. Formulating Weakly Basic HCl Salts: Relative Ability of Common Excipients to Induce Disproportionation and the Unique Deleterious Effects of Magnesium Stearate. *Pharm. Res.* **2013**, *30* (6), 1628–1641.

(36) Ahlneck, C.; Zografi, G. The Molecular Basis of Moisture Effects on the Physical and Chemical Stability of Drugs in the Solid State. *Int. J. Pharm.* **1990**, *62* (2–3), 87–95.

(37) Peters, S. J.; Ewing, G. E. Thin Film Water on NaCl(100) under Ambient Conditions: An Infrared Study. *Langmuir* **1997**, *13* (24), 6345–6348.

(38) Peters, S. J.; Ewing, G. E. Water on Salt : An Infrared Study of Adsorbed H 2 O on NaCl (100) under Ambient Conditions. **1997**, *5647* (100), 10880–10886.

(39) Luna, M.; Rieutord, F.; Melman, N.; Dai, Q.; Salmeron, M. Adsorption of Water on Alkali Halide Surfaces Studied by Scanning Polarization Force Microscopy. *J. Phys. Chem. A* **1998**, *5639* (98), 6793–6800.

(40) Narang, A. S.; Desai, D.; Badawy, S. Impact of Excipient Interactions on Solid Dosage Form Stability. *Pharm. Res.* **2012**, *29* (10), 2660–2683.

(41) Wu, Y.; Levons, J.; Narang, A. S.; Raghavan, K.; Rao, V. M. Reactive Impurities in Excipients: Profiling, Identification and Mitigation of Drug–Excipient Incompatibility. *AAPS PharmSciTech* **2011**, *12* (4), 1248–1263.

(42) Serajuddin, A. T. M.; Jarowski, C. I. Effect of Diffusion Layer pH and Solubility on the Dissolution Rate of Pharmaceutical Acids and Their Sodium Salts II: Salicylic Acid, Theophylline, and Benzoic Acid. *J. Pharm. Sci.* **1985**, *74* (2), 148–154.

(43) Govindarajan, R.; Zinchuk, A.; Hancock, B.; Shalaev, E.; Suryanarayanan, R. Ionization States in the Microenvironment of Solid Dosage Forms: Effect of Formulation Variables and Processing. *Pharm. Res.* **2006**, *23* (10), 2454–2468.

(44) Hailu, S. A.; Bogner, R. H. Solid-State Surface Acidity and pH-Stability Profiles of Amorphous Quinapril Hydrochloride and Silicate Formulations. *J. Pharm. Sci.* **2010**, *99* (6), 2786–2799.

(45) Scheef, C. A.; Oelkrug, D.; Schmidt, P. C. Surface Acidity of Solid Pharmaceutical Excipients III. Excipients for Solid Dosage Forms. *Eur. J. Pharm. Biopharm.* **1998**, *46* (2), 209–213.

(46) Govindarajan, R.; Landis, M.; Hancock, B.; Gatlin, L. a.; Suryanarayanan, R.; Shalaev, E. Y. Surface Acidity and Solid-State Compatibility of Excipients with an Acid-Sensitive API: Case Study of Atorvastatin Calcium. *AAPS PharmSciTech* **2015**, *16* (2), 354–363.

(47) Govindarajan, R.; Chatterjee, K.; Gatlin, L.; Suryanarayanan, R.; Shalaev, E. Y. Impact of Freeze-Drying on Ionization of Sulfonephthalein Probe Molecules in Trehalose–Citrate Systems. *J. Pharm. Sci.* **2006**, *95* (7), 1498–1510.

(48) Chatterjee, K.; Shalaev, E. Y.; Suryanarayanan, R.; Govindarajan, R. Correlation between Chemical Reactivity and the Hammett Acidity Function in Amorphous Solids Using Inversion of Sucrose as a Model Reaction. *J. Pharm. Sci.* **2008**, *97* (1), 274–286.

(49) Remenar, J. F.; Morissette, S. L.; Peterson, M. L.; Moulton, B.; MacPhee, J. M.; Guzmán, H. R.; Almarsson, Ö. Crystal Engineering of Novel Cocrystals of a Triazole Drug with 1, 4-Dicarboxylic Acids. *J. Am. Chem. Soc.* **2003**, *125* (28), 8456–8457.

(50) Childs, S. L.; Chyall, L. J.; Dunlap, J. T.; Smolenskaya, V. N.; Stahly, B. C.; Stahly, G. P. Crystal Engineering Approach to Forming Cocrystals of Amine Hydrochlorides with Organic Acids. Molecular Complexes of Fluoxetine Hydrochloride with Benzoic, Succinic, and Fumaric Acids. *J. Am. Chem. Soc.* **2004**, *126* (41), 13335–13342.

(51) Bolla, G.; Sanphui, P.; Nangia, A. Solubility Advantage of Tenoxicam Phenolic Cocrystals Compared to Salts. *Cryst. Growth Des.* **2013**, *13* (5), 1988–2003.

(52) Shiraki, K.; Takata, N.; Takano, R.; Hayashi, Y.; Terada, K. Dissolution Improvement and the Mechanism of the Improvement from Cocrystallization of Poorly Water-Soluble Compounds. *Pharm. Res.* **2008**, *25* (11), 2581–2592.

(53) Sanphui, P.; Goud, N. R.; Khandavilli, U. B. R.; Nangia, A. Fast Dissolving Curcumin Cocrystals. *Cryst. Growth Des.* **2011**, *11* (9), 4135–4145.

(54) Goud, N. R.; Gangavaram, S.; Suresh, K.; Pal, S.; Manjunatha, S. G.; Nambiar, S.; Nangia, A. Novel Furosemide Cocrystals and Selection of High Solubility Drug Forms. *J. Pharm. Sci.* **2012**, *101* (2), 664–680.

(55) Sanphui, P.; Devi, V. K.; Clara, D.; Malviya, N.; Ganguly, S.; Desiraju, G. R.

Cocrystals of Hydrochlorothiazide: Solubility and Diffusion/permeability Enhancements through Drug-Coformer Interactions. *Mol. Pharm.* **2015**, *12* (5), 1615–1622.

(56) Yan, Y.; Chen, J.-M.; Lu, T.-B. Simultaneously Enhancing the Solubility and Permeability of Acyclovir by Crystal Engineering Approach. *CrystEngComm* **2013**, *15* (33), 6457.

(57) Saikia, B.; Bora, P.; Khatioda, R.; Sarma, B. Hydrogen Bond Synthons in the Interplay of Solubility and Membrane Permeability/Diffusion in Variable Stoichiometry Drug Cocrystals. *Cryst. Growth Des.* **2015**, *15* (11), 5593–5603.

(58) Trask, A. V.; Motherwell, W. D. S.; Jones, W. Physical Stability Enhancement of Theophylline via Cocrystallization. *Int. J. Pharm.* **2006**, *320* (1–2), 114–123.

(59) Trask, A. V.; Samuel Motherwell, W. D.; Jones, W. Pharmaceutical Cocrystallization: Engineering a Remedy for Caffeine Hydration. *Cryst. Growth Des.* **2005**, *5* (3), 1013–1021.

(60) Wang, J.-R.; Zhou, C.; Yu, X.; Mei, X. Stabilizing Vitamin D $_3$ by Conformationally Selective Co-Crystallization. *Chem. Commun.* **2014**, *50* (7), 855–858.

(61) Sayantan Chattoraj, L. S. and C. C. S. Understanding the Relationship between Crystal Structure, Plasticity and Compaction Behaviour of Theophylline, Methyl Gallate, and Their 1 : 1 Co-Crystal. *CrystEngComm* **2010**, *12* (8), 2466–2472.

(62) Chattoraj, S.; Shi, L.; Chen, M.; Alhalaweh, A.; Velaga, S.; Sun, C. C. Origin of Deteriorated Crystal Plasticity and Compaction Properties of a 1:1 Cocrystal between Piroxicam and Saccharin. *Cryst. Growth Des.* **2014**, *14* (8), 3864–3874.

(63) Sun, C. C.; Hou, H. Improving Mechanical Properties of Caffeine and Methyl Gallate Crystals by Cocrystallization Improving Mechanical Properties of Caffeine and Methyl Gallate Crystals by Cocrystallization. *Cryst. Growth Des.* **2008**, *8* (5), 1575–1579.

(64) Aakeröy, C. B. Crystal Engineering: Strategies and Architectures. *Acta Crystallogr. Sect. B Struct. Sci.* **1997**, *53* (4), 569–586.

(65) Vishweshwar, P.; McMahon, J. A.; Peterson, M. L.; Hickey, M. B.; Shattock, T. R.; Zaworotko, M. J. Crystal Engineering of Pharmaceutical Co-Crystals from Polymorphic Active Pharmaceutical Ingredients. *Chem. Commun.* **2005**, *10* (36), 4601.

(66) Desiraju, G. R. Supramolecular Synthons in Crystal Engineering—A New Organic Synthesis. *Angew. Chemie Int. Ed. English* **1995**, *34* (21), 2311–2327.

(67) Bethune, S. Thermodynamic and Kinetic Parameters That Explain Crystallization and Solubility of Pharmaceutical Cocrystals, Ph.D. Thesis, University of Michigan., 2009.

(68) Koranne, S.; Govindarajan, R.; Suryanarayanan, R. Investigation of Spatial Heterogeneity of Salt Disproportionation in Tablets by Synchrotron X-Ray

Diffractometry. *Mol. Pharm.* **2017**, *14* (4), 1133–1144.

(69) Nie, H.; Xu, W.; Ren, J.; Taylor, L. S.; Marsac, P. J.; John, C. T.; Byrn, S. R. Impact of Metallic Stearates on Disproportionation of Hydrochloride Salts of Weak Bases in Solid-State Formulations. *Mol. Pharm.* **2016**, *13* (10), 3541–3552.

(70) McNamara, D. P.; Childs, S. L.; Giordano, J.; Iarriccio, A.; Cassidy, J.; Shet, M. S.; Mannion, R.; O'Donnell, E.; Park, A. Use of a Glutaric Acid Cocrystal to Improve Oral Bioavailability of a Low Solubility API. *Pharm. Res.* **2006**, *23* (8), 1888–1897.

(71) Stanton, M. K.; Bak, A. Physicochemical Properties of Pharmaceutical Co-Crystals: A Case Study of Ten AMG 517 Co-Crystals. *Cryst. Growth Des.* **2008**, *8* (10), 3856–3862.

(72) Stanton, M. K.; Tufekcic, S.; Morgan, C.; Bak, A. Drug Substance and Former Structure Property Relationships in 15 Diverse Pharmaceutical Co-Crystals. *Cryst. Growth Des.* **2009**, *9* (3), 1344–1352.

(73) Sanphui, P.; Rajput, L. Tuning Solubility and Stability of Hydrochloro-Thiazide Co-Crystals. *Acta Crystallogr. Sect. B Struct. Sci. Cryst. Eng. Mater.* **2014**, *70* (1), 81–90.

(74) Yamashita, H.; Sun, C. C. Improving Dissolution Rate of Carbamazepine-Glutaric Acid Cocrystal Through Solubilization by Excess Coformer. *Pharm. Res.* **2018**, *35*.

(75) Suryanarayan Cherukvada, N. Jagadeesh Babu, A. N. Nitrofurantoin–p-Aminobenzoic Acid Cocrystal: Hydration Stability and Dissolution Rate Studies. *J Pharm Sci* **2011**, *100* (8), 3233–3244.

(76) Lohani, S.; Cooper, H.; Jin, X.; Nissley, B. P.; Manser, K.; Rakes, L. H.; Cummings, J. J.; Fauty, S. E.; Bak, A. Physicochemical Properties, Form, and Formulation Selection Strategy for a Biopharmaceutical Classification System Class II Preclinical Drug Candidate. *J. Pharm. Sci.* **2014**, *103* (10), 3007–3021.

(77) Bhardwaj, S.; Lipert, M.; Bak, A. Mitigating Cocrystal Physical Stability Liabilities in Preclinical Formulations. *J. Pharm. Sci.* **2017**, *106* (1), 31–38.

(78) Eddleston, M. D.; Thakuria, R.; Aldous, B. J.; Jones, W. An Investigation of the Causes of Cocrystal Dissociation at High Humidity. *J Pharm Sci* **2014**, *103* (9), 2859–2864.

(79) Arhangelskis, M.; Lloyd, G. O.; Jones, W. Mechanochemical Synthesis of Pyrazine : Dicarboxylic Acid Cocrystals and a Study of Dissociation by Quantitative Phase Analysis. *Cryst. Eng. Comm.* **2012**, *14*, 5203–5208.

(80) Eddleston, M. D.; Lloyd, G. O.; Jones, W. Cocrystal Dissociation and Molecular Demixing in the Solid State. *Chem. Commun.* **2012**, *48*, 8075–8077.

(81) Arhangelskis, M.; Lloyd, G. O.; Jones, W. Mechanochemical Synthesis of Pyrazine: Dicarboxylic Acid Cocrystals and a Study of Dissociation by Quantitative Phase Analysis. *CrystEngComm* **2012**, *14* (16), 5203–5208.

(82) Duggirala, N. K.; Vyas, A.; Krzyzaniak, J. F.; Arora, K. K.; Suryanarayanan, R. Mechanistic Insight into Caffeine–Oxalic Cocrystal Dissociation in Formulations: Role of Excipients. *Mol. Pharm.* **2017**, *14* (11), 3879–3887.

(83) Bethune, S. J.; Huang, N.; Jayasankar, A.; Rodríguez-Hornedo, N. Understanding and Predicting the Effect of Cocrystal Components and pH on Cocrystal Solubility. *Cryst. Growth Des.* **2009**, *9* (9), 3976–3988.

(84) Huang, N. C. Engineering Cocrystal Solubility and Stability via Ionization and Micellar Solubilization, PhD Thesis, University of Michigan, 2011.

(85) Sreenivas Reddy, L.; Bethune, S. J.; Kampf, J. W.; Rodríguez-Hornedo, N. Cocrystals and Salts of Gabapentin: pH Dependent Cocrystal Stability and Solubility. *Cryst. Growth Des.* **2009**, *9* (1), 378–385.

(86) Eddleston, M. D.; Madusanka, N.; Jones, W. Cocrystal Dissociation in the Presence of Water : A General Approach for Identifying Stable Cocrystal Forms. *J Pharm Sci* **2014**, *103*, 2865–2870.

(87) Oswald, I. D. H.; Allan, D. R.; McGregor, P. A.; Motherwell, W. D. S.; Parsons, S.; Pulham, C. R. The Formation of Paracetamol (Acetaminophen) Adducts with Hydrogen-Bond Acceptors. *Acta Crystallogr. Sect. B Struct. Sci.* **2002**, *58* (6), 1057–1066.

(88) Arenas-García, J. I.; Herrera-Ruiz, D.; Morales-Rojas, H.; Höpfl, H. Interrelation of the Dissolution Behavior and Solid-State Features of Acetazolamide Cocrystals. *Eur. J. Pharm. Sci.* **2017**, *96*, 299–308.

(89) Nie, H.; Liu, Z.; Marks, B. C.; Taylor, L. S.; Byrn, S. R.; Marsac, P. J. Analytical Approaches to Investigate Salt Disproportionation in Tablet Matrices by Raman Spectroscopy and Raman Mapping. *J. Pharm. Biomed. Anal.* **2016**, *118*, 328–337.

(90) Skrdla, P. J.; Zhang, D. Disproportionation of a Crystalline Citrate Salt of a Developmental Pharmaceutical Compound: Characterization of the Kinetics Using pH Monitoring and Online Raman Spectroscopy plus Quantitation of the Crystalline Free Base Form in Binary Physical Mixtures. *J. Pharm. Biomed. Anal.* **2014**, *90*, 186–191.

(91) Usui, F.; Carstensen, J. T. Interactions in the Solid State I: Interactions of Sodium Bicarbonate and Tartaric Acid Under Compressed Conditions. *J. Pharm. Sci.* **1985**, *74* (12), 1293–1297.

(92) Carstensen, J. T.; Kothari, R. C. Solid-State Decomposition of Alkoxyfuroic Acids in the Presence of Microcrystalline Cellulose. *J. Pharm. Sci.* **1983**, *72* (10), 1149–1154.

(93) Marshall, K.; Macleod, H. The Determination of Density Distribution in Ceramic Compacts Using Autoradiography. *Powder Technol.* **1977**, *16*, 107–122.

(94) Thakral, N. K.; Yamada, H.; Stephenson, G. A.; Suryanarayanan, R. Spatial Distribution of Trehalose Dihydrate Crystallization in Tablets by X-Ray Diffractometry. *Mol. Pharm.* **2015**, *12* (10), 3766–3775.

(95) Toby, B. H.; Von Dreele, R. B. GSAS-II: The Genesis of a Modern Open-Source All Purpose Crystallography Software Package. *J. Appl. Crystallogr.* **2013**, *46* (2), 544–549.

(96) Thakral, N. K.; Ragoonanan, V.; Suryanarayanan, R. Quantification, Mechanism, and Mitigation of Active Ingredient Phase Transformation in Tablets. *Mol. Pharm.* **2013**, *10* (8), 3128–3136.

(97) Zinchuk, A. V.; Hancock, B. C.; Shalaev, E. Y.; Reddy, R. D.; Govindarajan, R.; Novak, E. The Influence of Measurement Conditions on the Hammett Acidity Function of Solid Pharmaceutical Excipients. *Eur. J. Pharm. Biopharm.* **2005**, *61* (3), 158–170.

(98) Yathirajan, H. S.; Nagaraj, B.; Nagaraja, P.; Michael, B. Pioglitazone Hydrochloride. *Acta Crystallogr. Sect. E* **2005**, *61* (1), 154–155.

(99) Malta, V.; Celotti, G.; Zannetti, R.; Martelli, A. F. Crystal Structure of the C Form of Stearic Acid. *J. Chem. Soc. B* **1971**, 548.

(100) Goto, M.; Asada, E. The Crystal Structure of the B-Form of Stearic Acid. *Bull.Chem.Soc.Jpn.* **1978**, *51* (9), 2456–2459.

(101) Rao, K. P.; Chawla, G.; Kaushal, A. M.; Bansal, A. K. Impact of Solid-State Properties on Lubrication Efficacy of Magnesium Stearate. *Pharm. Dev. Technol.* **2005**, *10* (3), 423–437.

(102) Li, J.; Wu, Y. Lubricants in Pharmaceutical Solid Dosage Forms. *Lubricants* **2014**, *2* (1), 21–43.

(103) Koradia, V.; Tenho, M.; Lopez De Diego, H.; Ringkjøbing-Elema, M.; Møller-Sonnergaard, J.; Salonen, J.; Lehto, V. P.; Rantanen, J. Investigation of Solid Phase Composition on Tablet Surfaces by Grazing Incidence X-Ray Diffraction. *Pharm. Res.* **2012**, *29* (1), 134–144.

(104) Koivisto, M.; Heinänen, P.; Tanninen, V. P.; Lehto, V. P. Depth Profiling of Compression-Induced Disorders and Polymorphic Transition on Tablet Surfaces with Grazing Incidence X-Ray Diffraction. *Pharm. Res.* **2006**, *23* (4), 813–820.

(105) Zografi, G.; Newman, A. Interrelationships Between Structure and the Properties of Amorphous Solids of Pharmaceutical Interest. *J. Pharm. Sci* **2017**, *106* (1), 5–27.

(106) Adams, M. L.; Sharma, V.; Gokhale, M.; Huang, Y.; Stefanski, K.; Su, C.; Hussain, M. a. Dehydration and Stabilization of a Reactive Tertiary Hydroxyl Group in Solid Oral Dosage Forms of BMS-779788. *J. Pharm. Sci.* **2016**, *105* (4), 1478–1488.

(107) Ahlneck C, Waltersson J-O, L. P. Difference in Effect of Powdered and Granular Magnesium Stearate on the Solid State Stability of Acetylsalicylic Acid. *Acta Pharm. Technol.* **1987**, *33*, 21–26.

(108) Tantry, J. S.; Tank, J.; Suryanarayanan, R. A. J. Processing-Induced Phase Transitions of Theophylline — Implications on the Dissolution of Theophylline Tablets. *J. Pharm. Sci.* **2007**, *96* (5), 1434–1444.

(109) Bross, P. F.; Kane, R.; Farrell, A. T.; Bross, P. F.; Kane, R.; Farrell, A. T.; Abraham, S.; Benson, K.; Brower, M. E.; Bradley, S.; Gobburu, J. V; Goheer, A.; Lee, S.; Leighton, J.; Liang, C. Y.; Lostritto, R. T.; Mcguinn, W. D.; Morse, D. E.; Rahman, A.; Rosario, L. A.; Verbois, S. L.; Williams, G.; Wang, Y.; Pazdur, R. Approval Summary for Bortezomib for Injection in the Treatment of Multiple Myeloma. *Clin. Cancer Res.* **2004**, *10* (12), 3954–3964.

(110) Thakral, S.; Suryanarayanan, R. Salt Formation during Freeze-Drying - an Approach to Enhance Indomethacin Dissolution. *Pharm. Res.* **2015**, *32* (11), 3722–3731.

(111) van den Berg, L.; Rose, D. Effect of Freezing on the pH and Composition of Sodium and Potassium Phosphate Solutions: The Reciprocal System KH2PO4-Na2HPO4-H2O. *Arch. Biochem. Biophys.* **1959**, *81* (2), 319–329.

(112) Gomez, G.; Pikal, M. J.; Rodriguez-Hornedo, N. Effect of Initial Buffer Composition on pH Changes during Far-from-Equilibrium Freezing of Sodium Phoaphate Buffer Solutions. *Pharm. Res.* **2001**, *18* (1), 90–97.

(113) Szkudlarek, B. A. Selective Crystallization of Phosphate Buffer Components and pH Changes during Freezing: Implication to Protein Stability, Ph.D. Thesis, University of Michigan., 1997.

(114) Sundaramurthi, P.; Shalaev, E.; Suryanarayanan, R. "pH Swing" in Frozen Solutions—Consequence of Sequential Crystallization of Buffer Components. *J. Phys. Chem. Lett.* **2010**, *1* (1), 265–268.

(115) Sundaramurthi, P.; Shalaev, E.; Suryanarayanan, R. Calorimetric and Diffractometric Evidence for the Sequential Crystallization of Buffer Components and the Consequential pH Swing in Frozen Solutions. *J. Phys. Chem. B* **2010**, *114* (14), 4915–4923.

(116) Pikal-Cleland, K. A.; Carpenter, J. F. Lyophilization-Induced Protein Denaturation in Phosphate Buffer Systems: Monomeric and Tetrameric β-Galactosidase. *J. Pharm. Sci.* **2001**, *90* (9), 1255–1268.

(117) Hora, M. S.; Rana, R. K.; Smith, F. W. Lyophilized Formulations of Recombinant Tumor Necrosis Factor. *Pharm. Res.* **1992**, *9* (1), 33–36.

(118) Hill, J. P.; Dickinson, M. F. Enzyme Storage—to Freeze or Not to Freeze? *Biochem. Soc. Trans.* **1989**, *17* (6), 1079–1080.

(119) Lam, X. M.; Costantino, H. R.; Overcashier, D. E.; Nguyen, T. H.; Hsu, C. C. Replacing Succinate with Glycolate Buffer Improves the Stability of Lyophilized Interferon-Gamma. *Int. J. Pharm.* **1996**, *142* (1), 85–95.

(120) Larsen, S. S. Studies on Stability of Drugs in Frozen Systems. IV. The Stability of Benzylpenicillin Sodium in Frozen Aqueous Solutions. *Dan. Tidsskr. Farm.* **1971**, *45* (9), 307–316.

(121) te Booy, M. P. W. M.; de Ruiter, R. A.; de Meere, A. L. J. Evaluation of the Physical Stability of Freeze-Dried Sucrose-Containing Formulations by Differential Scanning Calorimetry. *Pharm. Res.* **1992**, *9* (1), 109–114.

(122) Williams, A. C.; Cooper, V. B.; Thomas, L.; Griffith, L. J.; Petts, C. R.; Booth, S. W. Evaluation of Drug Physical Form during Granulation, Tabletting and Storage. *Int. J. Pharm.* **2004**, *275* (1), 29–39.

(123) Guo, Y.; Byrn, S. R.; Zografi, G. Effects of Lyophilization on the Physical Characteristics and Chemical Stability of Amorphous Quinapril Hydrochloride. *Pharm Res* **2000**, *17* (8), 930–935.

(124) Brien, M. O.; Mccauley, J.; Cohen, E. *Indomethacin. In:Analytical Profiles of Drug Substances*; Florey K, Ed.; New York: Academic Press, 1984; Vol. 13.

(125) James Arthur, R. Crystalline Sodium and Potassium Indomethacin and Their Trihydrates, Process for Preparing and Pharmaceutical Compositions Containing the Same. EP 0006223 A1, 1980.

(126) De Marzi, S.; Morini, V. Use of Meglumine Indomethacin in the Treatment of Pain due to Neoplastic Disease. *Clin. Ter.* **1972**, *62* (2), 175–180.

(127) *Indocin IV. Product Information, Merck*; Whitehouse Station, NJ, 2002.

(128) Siddiqui, A.; Rahman, Z.; Khan, S. R.; Awotwe-otoo, D.; Khan, M. A. Root Cause Evaluation of Particulates in the Lyophilized Indomethacin Sodium Trihydrate Plug for Parenteral Administration. *Int. J. Pharm.* **2014**, *473* (1), 545–551.

(129) Jain, A. K. Solubilization of Indomethacin Using Hydrotropes for Aqueous Injection. *Eur. J. Pharm. Biopharm.* **2008**, *68* (3), 701–714.

(130) Taylor, L. S.; Zografi, G. Spectroscopic Characterization of Interactions between PVP and Indomethacin in Amorphous Molecular Dispersions. *Pharm. Res.* **1997**, *14* (12), 1691–1698.

(131) Tong, P.; Zografi, G. Solid-State Characteristics of Amorphous Sodium Indomethacin Relative to Its Free Acid. *Pharm. Res.* **1999**, *16* (8), 1186–1192.

(132) Savolainen, M.; Heinz, A.; Strachan, C.; Gordon, K. C.; Yliruusi, J.; Rades, T.; Sandler, N. Screening for Differences in the Amorphous State of Indomethacin Using Multivariate Visualization. *Eur. J. Pharm. Sci.* **2007**, *30* (2), 113–123.

(133) Surwase, S. A.; Boetker, J. P.; Saville, D.; Boyd, B. J.; Gordon, K. C.; Peltonen, L.; Strachan, C. J. Indomethacin: New Polymorphs of an Old Drug. *Mol. Pharm.* **2013**, *10* (12), 4472–4480.

(134) Gomez, G. Crystallization-Related pH Changes during Freezing of Sodium Phosphate Buffer Solutions., Ph.D. Thesis, University of Michigan., 1995.

(135) Lin, S.-Y. Isolation and Solid-State Characteristics of a New Crystal Form of Lndomet Haci N. *J. Pharm. Sci.* **1991**, *81* (6), 572–576.

(136) Borka, L. The Polymorphism of Indomethacine. New Modifications, Their Melting Behavior and Solubility. *Acta Pharm. Suec.* **1974**, *11* (3), 295–303.

(137) Tong, P.; Zografi, G. A Study of Amorphous Molecular Dispersions of Indomethacin and Its Sodium Salt. *J. Pharm. Sci.* **2001**, *90* (12), 1991–2004.

(138) Varshney, D. B.; Kumar, S.; Shalaev, E. Y.; Kang, S. W.; Gatlin, L. A.; Suryanarayanan, R. Solute Crystallization in Frozen Systems-Use of Synchrotron Radiation to Improve Sensitivity. *Pharm. Res.* **2006**, *23* (10), 2368–2374.

(139) Tong, P.; Zografi, G. Effects of Water Vapor Absorption on the Physical and Chemical Stability of Amorphous Sodium Indomethacin. *AAPS PharmSciTech* **2004**, *5* (2), 1–8.

(140) Sundaramurthi, P.; Suryanarayanan, R. The Effect of Crystallizing and Non-Crystallizing Cosolutes on Succinate Buffer Crystallization and the Consequent pH Shift in Frozen Solutions. *Pharm. Res.* **2011**, *28* (2), 374–385.

(141) Trissel, L. A. *Handbook on Injectable Drugs*, 11th ed.; American Society of Health-System Pharmacists, 2001.

(142) Nail, S. L.; Jiang, S.; Chongprasert, S.; Knopp, S. A. *Fundamentals of Freeze-Drying. In: Development and Manufacture of Protein Pharmaceuticals*; Nail, S., Akers, M., Eds.; Springer, Boston MA, 2002.

(143) Kumar, L.; Baheti, A.; Mokashi, A.; Bansal, A. K. Effect of Counterion on the Phase Behaviour during Lyophilization of Indomethacin Salt Forms. *Eur. J. Pharm. Sci.* **2011**, *44* (1), 136–141.

(144) Cavatur, R. K.; Suryanarayanan, R. Characterization of Frozen Aqueous Solutions by Low Temperature X-Ray Powder Diffractometry. *Pharm. Res.* **1998**, *15* (2), 194–199.

(145) Suzuki, T.; Franks, F. Solid–liquid Phase Transitions and Amorphous States in Ternary Sucrose–glycine–water Systems. *J. Chem. Soc., Faraday Trans.* **1993**, *89* (17), 3283–3288.

(146) Pikal-Cleland, K. A.; Cleland, J. L.; Anchordoquy, T. J.; Carpenter, J. F. Effect of Glycine on pH Changes and Protein Stability during Freeze-Thawing in Phosphate Buffer Systems. *J. Pharm. Sci.* **2002**, *91* (9), 1969–1979.

(147) Wu, C.; Shamblin, S.; Varshney, D.; Shalaev, E. Advance Understanding of Buffer Behavior during Lyophilization. **2015**, 25–41.

(148) Schultheiss, N.; Newman, A. Pharmaceutical Cocrystals and Their Physicochemical Properties. *Cryst. Growth Des.* **2009**, *9* (6), 2950–2967.

(149) Hickey, M. B.; Peterson, M. L.; Scoppettuolo, L. A.; Morrisette, S. L.; Vetter, A.; Guzmán, H.; Remenar, J. F.; Zhang, Z.; Tawa, M. D.; Haley, S.; Zaworotko, M. J.; Almarsson, Ö. Performance Comparison of a Co-Crystal of Carbamazepine with Marketed Product. *Eur. J. Pharm. Biopharm.* **2007**, *67* (1), 112–119.

(150) Lu, J.; Rohani, S. Preparation and Characterization of Theophylline - Nicotinamide Cocrystal. *Org. Process Res. Dev.* **2009**, *13* (2), 1269–1275.

(151) Kong, A.; Arora, K.; Mehrens, S.; Nickerson, B.; Alstine, L. Van; Daddario, P.; Zhou, Y.; Gerst, P.; Schmidt, H. F. Impact of Excipients on the Disproportionation of a Cocrystal API in Drug Product. *AAPS. 2014*.

(152) Wray, P. S.; Sinclair, W.; Jones, J.; Clarke, G.; Both, D. The Use of In Situ Near Infrared Imaging and Raman Mapping to Study the Disproportionation of a Drug HCl Salt During Dissolution. *Int. J. Pharm.* **2015**, *493* (1–2), 198–207.

(153) Ebisuzaki, Y.; Boyle, P. D.; Smith, J. A. Methylxanthines. I. Anhydrous Theophylline. *Acta Crystallogr. Sect. C Cryst. Struct. Commun.* **1997**, *53* (6), 777–779.

(154) Mishra, M. K.; Ramamurty, U.; Desiraju, G. R. Hardness Alternation in A,ω-Alkanedicarboxylic Acids. *Chem. - An Asian J.* **2015**, *10* (10), 2176–2181.

(155) Zhang, S.; Rasmuson, Å. C. Thermodynamics and Crystallization of the Theophylline-Glutaric Acid Cocrystal. *Cryst. Growth Des.* **2013**, *13* (3), 1153–1161.

(156) Á. Gombás, P. Szabó-Révész, M. Kata, G. R. J. and I. E. Quantitative Determination of Crystallinity of α-Lactose Monohydrate by DSC. *J. Therm. Anal. Calorim.* **2002**, *68* (2), 503–510.

(157) Delaney, S. P.; Nethercott, M. J.; Mays, C. J.; Winquist, N. T.; Arthur, D.; Calahan, J. L.; Sethi, M.; Pardue, D. S.; Kim, J.; Amidon, G.; Munson, E. J. Characterization of Synthesized and Commercial Forms of Magnesium Stearate Using Differential Scanning Calorimetry , Thermogravimetric Analysis , Powder X-Ray Diffraction , and Solid-State NMR Spectroscopy. *J. Pharm. Sci.* **2017**, *106* (1), 338–347.

(158) Miyazaki, T.; Sivaprakasam, K.; Tantry, J.; Suryanarayanan, R. Physical Characterization of Dibasic Calcium Phosphate Dihydrate and Anhydrate. *J. Pharm. Sci.* **2009**, *98* (3), 905–916.

(159) Rowe RC, Sheskey PJ, Weller PJ, Rowe R, Sheskey P, W. P. *Handbook of Pharmaceutical Excipients.*, 4th edn.; APhA Publications, Pharmaceutical Press, London, UK, 2003.

(160) *The Merck Index.*, 12th Editi.; S.Budavari, Ed.; Merck Research Labs, Merck & Co, 1996.

(161) Jivraj, M.; Martini, L. G.; Thomson, C. M. An Overview of the Different Excipients Useful for the Direct Compression of Tablets. *Pharm. Sci. Technolo. Today* **2000**, *3* (2), 58–63.

(162) Patel, S.; Kaushal, A. M.; Bansal, A. K. Compression Physics in the Formulation Development of Tablets. *Crit. Rev. Ther. Drug Carrier Syst.* **2006**, *23* (1), 1–65.

(163) Riepma, K. A.; Vromans, H.; Zuurman, K.; Lerk, C. F. The Effect of Dry Granulation on the Consolidation and Compaction of Crystalline Lactose. *Int. J. Pharm.* **1993**, *97* (1–3), 29–38.

(164) David, S. T.; Augsburger, L. L. Plastic Flow during Compression of Directly Compressible Fillers and Its Effect on Tablet Strength. *J. Pharm. Sci.* **1977**, *66* (2), 155–159.

(165) Sun, C. C. Mechanism of Moisture Induced Variations in True Density and

Compaction Properties of Microcrystalline Cellulose. *Int. J. Pharm.* **2008**, *346* (1–2), 93–101.

(166) Zografi, G.; Kontny, M. J.; Yang, A. Y. S.; Brenner, G. S. Surface Area and Water Vapor Sorption of Microcrystalline Cellulose. *Int. J. Pharm.* **1984**, *18* (1–2), 99–116.

(167) Narang, A. S.; Rao, V. M.; Raghavan, K. S. *Excipient Compatibility. In: Developing Solid Oral Dosage Forms*; Elsevier Inc., 2009.

(168) Ahlneck , C. & Alderborn, G. Solid State Stability of Acetylsalicylic Acid in Binary Mixtures with Microcrystalline and Microfine Cellulose. *Acta Pharm. Suec.* **1988**, *25* (1), 41 – 52.

(169) Aso , Y. , Sufang , T. , Yoshioka , S. & Kojima, S. Amount of Mobile Water Estimated from 2H Spin-Lattice Relaxation Time, and Its Effects on the Stability of Cephalothin in Mixtures with Pharmaceutical Excipients . *Drug Stab.* **1997**, *1* (4), 237–242.

(170) Verdaguer, A.; Sacha, G. M.; Luna, M.; Frank Ogletree, D.; Salmeron, M. Initial Stages of Water Adsorption on NaCl (100) Studied by Scanning Polarization Force Microscopy. *J. Chem. Phys.* **2005**, *123* (12), 124703.

(171) Dai, D. J.; Peters, S. J.; Ewing, G. E. Water Adsorption and Dissociation on NaCl Surfaces. *J. Phys. Chem.* **1995**, *99* (25), 10299–10304.

(172) Kontny, Mark J., George P. Grandolfi., G. Z. Water Vapor Sorption of Water-Soluble Substances: Studies of Crystalline Solids below Their Critical Relative Humidities. *Pharm. Res.* **1987**, *4* (2), 104–112.

(173) Fischer, F.; Lubjuhn, D.; Greiser, S.; Rademann, K.; Emmerling, F. Supply and Demand in the Ball Mill: Competitive Cocrystal Reactions. *Cryst. Growth Des.* **2016**, *16* (10), 5843–5851.

(174) Fischer, F.; Schmidt, M. U.; Greiser, S.; Emmerling, F. The Challenging Case of the Theophylline-Benzamide Cocrystal. *Acta Crystallogr. Sect. C Struct. Chem.* **2016**, *72* (3), 217–224.

(175) Bhogala, B. R.; Basavoju, S.; Nangia, A. Tape and Layer Structures in Cocrystals of Some Di- and Tricarboxylic Acids with 4,4′-Bipyridines and Isonicotinamide. From Binary to Ternary Cocrystals. *CrystEngComm* **2005**, *7* (90), 551.

(176) Zografi, G.; Kontny, M. J. The Interactions of Water with Cellulose- and Starch-Derived Pharmaceutical Excipients. *Pharmaceutical Research: An Official Journal of the American Association of Pharmaceutical Scientists*. 1986, pp 187–194.

(177) Good, D. J.; Nair Rodrıguez-Hornedo. Solubility Advantage of Pharmaceutical Crystals.pdf. *Cryst. Growth Des.* **2009**, *9* (5), 2252–2264.

(178) Kale, D. P.; Zode, S. S.; Bansal, A. K. Challenges in Translational Development of Pharmaceutical Cocrystals. *J. Pharm. Sci.* **2017**, *106* (2), 457–470.

(179) Childs, S. L.; Rodríguez-Hornedo, N.; Reddy, L. S.; Jayasankar, A.; Maheshwari, C.; McCausland, L.; Shipplett, R.; Stahly, B. C. Screening Strategies Based on Solubility and Solution Composition Generate Pharmaceutically Acceptable Cocrystals of Carbamazepine. *CrystEngComm* **2008**, *10* (7), 856.

(180) Fischer, F.; Heidrich, A.; Greiser, S.; Benemann, S.; Rademann, K.; Emmerling, F. Polymorphism of Mechanochemically Synthesized Cocrystals: A Case Study. *Cryst. Growth Des.* **2016**, *16* (3), 1701–1707.

(181) Belenguer, A. M.; Lampronti, G. I.; Cruz-Cabeza, A. J.; Hunter, C. A.; Sanders, J. K. M. Solvation and Surface Effects on Polymorph Stabilities at the Nanoscale. *Chem. Sci.* **2016**, *7* (11), 6617–6627.

(182) Trask, A. V.; Motherwell, W. D. S.; Jones, W. Solvent-Drop Grinding: Green Polymorph Control of Cocrystallisation. *Chem. Commun.* **2004**, No. 7, 890.